



UNIVERSITÀ DI PISA

School of graduate studies

“Scienza del farmaco e delle sostanze bioattive”

**“DESIGN AND SYNTHESIS OF NOVEL ZINC-DEPENDENT
METALLOENZYMES
INHIBITORS AS ANTI-TUMORAL DRUG CANDIDATES.”**

Tutor:

Prof. Concettina La Motta

PhD Student:

Matteo Morelli

XXIV Cycle

2012

Index

CHAPTER 1

Cancer the never ending night mare	pg. 1
Bibliography	pg. 7

CHAPTER 2

Matrix Metalloproteinases: An introduction	pg. 8
Bibliography	Pg. 31

CHAPTER 3

Developmental of matrix metalloproteinases inhibitors	pg. 33
- Benzo[d]isothiazol-3(2H)-one-1,1-dioxide Derivatives	pg. 35
- Isoindoline-1,3-dione Derivatives	pg. 42
- Thiazolidinedionic and thiohydantoinic core-based MMPs inhibitors	pg. 46
- Pyridopyrimidinone derivatives	pg. 58
Bibliography	pg. 60

CHAPTER 4

Esperimental section	pg. 63
Bibliography	pg. 89

CHAPTER 5

The ubiquitin–protein ligase system	pg. 92
Bibliography	pg. 107

CHAPTER 6

Inhibitors of E2, E3 enzymes	pg. 109
- Carbamo(dithioperoxo)thioates derivatives	pg. 110
- Triazinic derivatives	pg. 113
Bibliography	pg. 117

CHAPTER 7

Experimental section	pg. 118
Bibliography	pg. 130

CHAPTER 1

Cancer: the never ending nightmare

Cancer continues to be a worldwide killer, despite the enormous amount of research and rapid developments seen during the past decade. According to recent statistics, cancer accounts for about 23% of the total deaths in the USA and is the second most common cause of death after heart disease. Death rates for heart disease, however, have been steeply decreasing in both older and younger populations in the USA from 1975 through 2002. In contrast, no appreciable differences in death rates for cancer have been observed in the United States.

Cancer is caused by both internal factors (such as inherited mutations, hormones, and immune conditions) and environmental/acquired factors (such as tobacco, diet, radiation, and infectious organisms; Fig. 1.1). The link between diet and cancer is revealed by the large variation in rates of specific cancers in various countries and by the observed changes in the incidence of cancer in migrating. For example, Asians have been shown to have a 25 times lower incidence of prostate cancer and a ten times lower incidence of breast cancer than do residents of Western countries, and the rates for these cancers increase substantially after Asians migrate to the West.¹

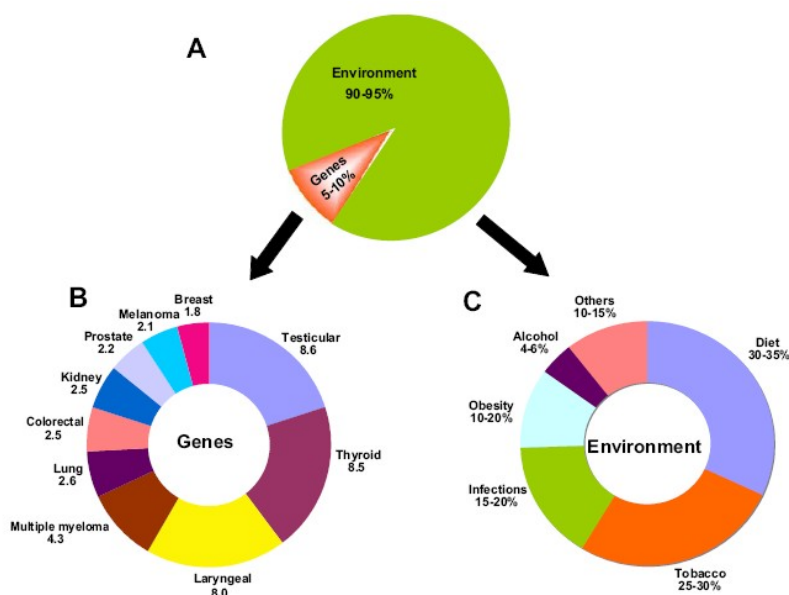


Figure 1.1 Subdivision between genetic and environmental causes.¹

Main cause of cancer insurgence and development.

Diet and Exercise.

The importance of lifestyle factors in the development of cancer was also shown in studies of monozygotic twins. Only 5–10% of all cancers are due to an inherited gene defect. Although all cancers are a result of multiple mutations, these mutations are due to interaction with the environment. These observations indicate that most cancers are not of hereditary origin and that lifestyle factors, such as dietary habits, smoking, alcohol consumption, and infections, have a profound influence on their development. Although the hereditary factors cannot be modified, the lifestyle and environmental factors are potentially modifiable. The lesser hereditary influence of cancer and the modifiable nature of the environmental factors point to the preventability of cancer. The important lifestyle factors that affect the incidence and mortality of cancer include tobacco, alcohol, diet, obesity, infectious agents, environmental pollutants, and radiation. ¹

In the United States, overweight and obesity contribute to 14% to 20% of all cancer-related mortality. Overweight and obesity are clearly associated with increased risk for developing many cancers, including cancers of the breast in postmenopausal women, colon, endometrium, adenocarcinoma of the esophagus, and kidney. Evidence is highly suggestive that obesity also increases risk for cancers of the pancreas, gallbladder, thyroid, ovary, and cervix, and for multiple myeloma, Hodgkin lymphoma, and aggressive prostate cancer.

These findings are supported by both epidemiologic studies in humans and other research.

Overweight and obesity are thought to affect risk of these cancers through a variety of mechanisms, some of which are specific to particular cancer types. These mechanisms include effects on fat and sugar metabolism; immune function; levels of several hormones, including insulin and estradiol; factors that regulate cell proliferation and growth, such as insulin-like growth factor-1; and proteins that make hormones more or less available to tissues, such as sex hormone-binding globulin.

Overweight and obesity may increase risk of adenocarcinoma of the esophagus by increasing risk of gastroesophageal reflux disease and Barrett's esophagus.

Most research on energy imbalance and cancer focuses on increased risks associated with overweight and obesity. Recently, studies exploring intentional weight loss suggest that losing weight may reduce the risk of breast cancer.

Surgery to treat morbid obesity and short-term intentional weight loss have been shown to improve insulin sensitivity and biochemical measures of hormone metabolism, which have been

postulated to contribute to the relationship between obesity and certain cancers. The surgical removal of intra-abdominal fat has also been shown to reduce the metabolic syndrome.

Even though our knowledge about the relationship between weight loss and cancer risk is incomplete, individuals who are overweight or obese should be encouraged and supported in their efforts to reduce weight. ²

Chemicals.

A very large amount of organic and inorganic compounds are deputed or suspected to provoke cancer.

It should be an infinite list.

Among the most prominent we can cite chemicals released from tobacco burning (such as nitrosamine and polycyclic aromatic hydrocarbons), asbestos, benzene, alcoholic beverage. ³

Infection.

Worldwide approximately 18% of cancers are related to infectious diseases.[1] This proportion varies in different regions of the world from a high of 25% in Africa to less than 10% in the developed world. ¹

Viruses are the usual infectious agents that cause cancer but bacteria and parasites may also have an effect.

A virus that can cause cancer (called oncovirus) include human papillomavirus (cervical carcinoma), Epstein-Barr virus (B-cell lymphoproliferative disease and nasopharyngeal carcinoma), Kaposi's sarcoma herpesvirus (Kaposi's Sarcoma and primary effusion lymphomas), hepatitis B and hepatitis C viruses (hepatocellular carcinoma), and Human T-cell leukemia virus-1 (T-cell leukemias). Bacterial infection may also increase the risk of cancer, as seen in Helicobacter pylori-induced gastric carcinoma.[23] Parasitic infections strongly associated with cancer include Schistosoma haematobium (squamous cell carcinoma of the bladder) and the liver flukes, Opisthorchis viverrini and Clonorchis sinensis (cholangiocarcinoma). ⁴

Radiation.

Principal Cellular and Tissue Effects of Radiation can be resumed in: cell killing, mutagenesis, chromosomal aberrations and neoplastic transformations.

Radiation can kill cells by two distinct mechanisms. The first is apoptosis, also called programmed cell death or interphase death. Cells undergoing apoptosis as an immediate consequence of radiation damage usually die in interphase within a few hours of irradiation, irrespective of and without intervening mitosis. The second mechanism for cell killing is radiation-induced reproductive failure. Radiation in sufficient doses can inhibit mitosis; that is, the cell's ability to divide and proliferate indefinitely. The inhibition of cellular proliferation is the mechanism by which radiation kills most cells.

The major potential consequence of radiation-induced mutations in human populations is heritable genetic effects resulting from mutations induced in germinal cells.⁵

Hormones.

Neoplasia of hormone-responsive tissues currently accounts for more than 35% of all newly diagnosed male and more than 40% of all newly diagnosed female cancers in the United States. Given that endogenous hormones apparently affect the risk of these cancers and their overall frequency, concern exists about the effects on cancer risk if the same or closely related hormones are administered for therapeutic purposes.

Oral contraceptives

The relationship of oral contraceptive (OC) use to breast cancer risk has been the topic of many review articles. A recent combined analysis of 54 studies that included over 150,000 women has provided many important answers about the risk of breast cancer among users of combination OC (COC), i.e., OCs which provide an estrogen and progestin in combination in a single pill. This analysis indicates that a modest increased risk of breast cancer is observed among current (relative risk, RR = 1.24) and recent (RR = 1.16) COC users. Age at first COC use modifies the association with recent use. For recent users, the risks are highest for those who began COC use before the age of 20 years. However, total duration of COC use was not associated with increased risk of breast cancer, once recency of use was taken into account. Although the scope of this combined analysis was broad, it still provides little information on COC effects 10 or more years after cessation of use. Moreover, most women who stopped use 10 or more years ago had used COCs for only short periods of time. Women who began use as teenagers are now becoming perimenopausal and postmenopausal. Current studies now underway will be able to examine more complex patterns of COC use, as related to breast cancer risk.

Hormone replacement therapy

Hormone replacement therapy in the form of unopposed estrogen therapy gained widespread popularity in the United States during the 1960s and 1970s. Concomitant with this increasing usage, incidence rates of endometrial cancer in postmenopausal women also increased rapidly, especially on the West Coast, where use of ERT was particularly common. By 1975, the results of epidemiologic case-control studies, demonstrating a strong overall association between ERT and risk of endometrial cancer were being published. Literally dozens of studies have now documented a high relative increase in the risk of endometrial cancer following ERT. Risk is strongly related both to dose and duration of use, but high relative increments in risk follow even moderate doses taken for moderately long periods of time. Women who use ERT for 5 years or longer have approximately a 3.5-fold increase in risk compared with that of women who have never used such therapy.⁶

A lot of therapies exist, but even if cancer treatments have lead to prolonged life-span, no one definitive treatment is yet in use.

Bibliography

1 Anand P. et al. Cancer is a preventable disease that requires major lifestyle changes. *Pharmaceutical Research*, **2008**, 25, 2097-2116.

2 L. H. Kushi et all. American Cancer Society Guidelines on Nutrition and Physical Activity for cancer prevention: reducing the risk of cancer with healthy food choices and physical activity. *CA: A Cancer Journal for Clinicians* **2006** 56, 254–281.

3 Kuper, H.; Adami, H. O.; Boffetta P.; Tobacco use, cancer causation and public health impact. *Journal of internal medicine World Health Organization* **2007** 251 455–66.

4 Vassilis, S.; Petros R., I.; Eleni G., M.; Peppas, G.; Falagas, M., E.; Chronic bacterial and parasitic infections and cancer: a review *The Journal of Infection in Developing Countries* **2010** 4 267–281.

5 Little, J., B.; "Chapter 14: Ionizing Radiation". In Bast RC, Kufe DW, Pollock RE, et al.. *Holland-Frei Cancer Medicine* (5th ed.) **2000**.

6 Henderson, B., E.; Bernstein, L.; Ross, R., K.; Chapter 13: Hormones and the Etiology of Cancer. *Cancer Medicine* (5th ed.). **2000**.

CHAPTER 2

Matrix Metalloproteinases: An introduction.

Matrix metalloproteinases (MMPs) are an important family of zinc- and calcium-dependent peptidases involved in the regulation of the cellular behavior by proteolytic processing of the pericellular environment. ¹ The founding member of the matrix metalloproteinase (MMP) family, collagenase, was identified in 1962 by Gross and Lapiere, who found that tadpole tails during metamorphosis contained an enzyme that could degrade fibrillar collagen IV. Subsequently, an interstitial collagenase, collagenase-1 or MMP1, was found in diseased skin and synovium. *In vitro*, MMP1 initiates degradation of native fibrillar collagens, crucial components of vertebrate extracellular matrix, by cleaving the peptide bond between Gly 775–Ile 776 or Gly 775–Lys 776 in native type I, II or III collagen molecules. ² Based on domain organization and substrate preference, MMPs are grouped into collagenases, gelatinases, stromelysins, matrilysins, membrane-type (MT)-MMPs and others. ³

Name	Alias	Category
MMP-1	Interstitial collagenase; fibroblast collagenase	Collagenase
MMP-2	72-kDa type IV collagenase; gelatinase A; 72-kDa gelatinase	Gelatinase
MMP-3	Stromelysin-1	Stromelysin
MMP-7	Matrilysin-1; PUMP1	Stromelysin
MMP-8	Neutrophil collagenase; PMNL collagenase	Collagenase
MMP-9	92-kDa type IV collagenase; gelatinase B; 92-kDa gelatinase	Gelatinase
MMP-10	Stromelysin-2; transin-2	Stromelysin
MMP-11	Stromelysin-3	Stromelysin
MMP-12	Macrophage proteinase; macrophage elastase; metalloelastase	Stromelysin
MMP-13	Collagenase 3	Collagenase
MMP-14	MT1-MMP; MT-MMP1	Membrane-type MMP
MMP-15	MT2-MMP; MT-MMP2	Membrane-type MMP
MMP-16	MT3-MMP; MT-MMP3	Membrane-type MMP
MMP-17	MT4-MMP; MT-MMP4	Membrane-type MMP
MMP-19	MMP-18; Matrix metalloproteinase RASI; RASI-1; stromelysin-4	Non-classified
MMP-20	Enamel metalloproteinase; enamelysin	Non-classified
MMP-21	X-MMP	Non-classified
MMP-23A	CA-MMP	Non-classified
MMP-23B	MIFR; MIFR-1	Non-classified
MMP-24	MT5-MMP; MT-MMP5	Membrane-type MMP
MMP-25	MT6-MMP; MT-MMP6	Membrane-type MMP
MMP-26	Matrilysin-2; endometase	Stromelysin
MMP-27	MMP-22; C-MMP	Non-classified
MMP-28	Epilysin	Non-classified

Table 2.1 List of MMPs. ⁴

Collagenases

Collagenases (MMP-1, MMP-8, MMP-13 and MMP-18) cleave interstitial collagens I, II and III into characteristic 3/4 and 1/4 fragments but they can digest other ECM molecules and soluble proteins. Recent studies indicated that MMP-1 activates protease activated receptor (PAR) 1 by cleaving the same Arg-Ser bond cleaved by thrombins, which promotes growth and invasion of breast carcinoma cells. Two other matrixins: MMP-2 and MMP-14 (MT1-MMP), have collagenolytic activity, but they are classified into other subgroups because of their domain compositions.

Gelatinases

Gelatinases (MMP-2 and MMP-9) readily digest gelatin with the help of their three fibronectin type II repeats that binds to gelatin/collagen. They also digest a number of ECM molecules including type IV, V and XI collagens, laminin, aggrecan core protein, etc. MMP-2, but not MMP-9, digests collagens I, II and III in a similar manner to the collagenases. The collagenolytic activity of MMP-2 is much weaker than MMP-1 in solution, but because proMMP-2 is recruited to the cell surface and activated by the membrane-bound MT-MMPs, it may express reasonable collagenolytic activity on or near the cell surface.

Stromelysins

Stromelysins (MMP-3, MMP-10 and MMP-11) have a domain arrangement similar to that of collagenases, but they do not cleave interstitial collagens. MMP-3 and MMP-10 are similar in structure and substrate specificity, but MMP-11 (stromelysin 3) is distantly related. The MMP-11 gene is located on chromosome 22, whereas MMP-3 and MMP-10 are on chromosome 11, along with MMP-1, -7, -8, -12, -20, -26 and -27. MMP-3 and MMP-10 digest a number of ECM molecules and participate in proMMP activation. MMP-11, on the other hand, has very weak activity toward ECM molecules, but cleaves serpins more readily. MMP-11 has a furin recognition motif RX[R/K]R at the C-terminal end of the propeptide and therefore it is activated intracellularly. An intracellular 40-kDa MMP-11 isoform (β -stromelysin 3) is found in cultured cells and placenta.

This transcript, resulting from alternative splicing and promoter usage, lacks the signal peptide and the pro-domain. The function of this isoenzyme is not known.

Matrilysins

Matrilysins (MMP-7 and -26) lack a hemopexin domain. MMP-7 is synthesized by epithelial cells and is secreted apically. Besides ECM components it processes cell surface molecules such as pro- α -defensin, Fas-ligand, pro-tumor necrosis factor α , and E-cadherin. MMP-26 is expressed in normal cells such as those of the endometrium and in some carcinomas. It digests several ECM molecules, and unlike most other MMPs, it is largely stored intracellularly.

MT-MMPs

MT-MMPs in mammals includes four type I transmembrane proteins (MMP-14, -15, -16, and -24) and two glycosylphosphatidylinositol-anchored proteins (MMP-17 and -25). They all have a furin recognition sequence RX[R/K]R at the C-terminus of the propeptide. They are therefore activated intracellularly and active enzymes are likely to be expressed on the cell surface. All MT-MMPs, except MT4-MMP (MMP-17) can activate proMMP-2. MT1-MMP (MMP-14) has collagenolytic activity on collagens I, II, and III. MT1-MMP null mice exhibit skeletal abnormalities during post-natal development, which is attributed to the lack of collagenolytic activity.

Seven MMPs are not grouped in the above categories although MMP-12, MMP-20 and MMP-27 have similar structures and chromosome location as stromelysins.

Metalloelastase, Enamelysin, Epilysin and other MMPs.

Metalloelastase (MMP-12) is expressed primarily in macrophages, but is also found in hypertrophic chondrocytes and osteoclasts. It digests elastin and a number of ECM molecules. It is essential in macrophage migration.

MMP-19 digests many ECM molecules including the components of basement membranes. It is also called RASI (rheumatoid arthritis synovial inflammation) as it is found in the activated lymphocytes and plasma from patients with rheumatoid arthritis and it is also recognised as an

autoantigen in patients with rheumatoid arthritis and systemic lupus erythematosus. It is, however, widely expressed in many organs including proliferating keratinocytes in healing wounds.

Enamelysin (MMP-20) is expressed in newly formed tooth enamel and digests amelogenin.

MMP-21 was originally found in *Xenopus* and more recently in mice and humans. It is expressed in various fetal and adult tissues and in basal and squamous cell carcinomas. It digests gelatin, but information about the action on ECM components is not known.

MMP-23 is a unique member as it has unique C-terminal cysteine-rich immunoglobulin-like domains instead of a hemopexin domain. The propeptide lacks a cysteine switch. It is proposed to be a type II membrane protein having a transmembrane domain at the N-terminal of the propeptide, but the enzyme is released from the cell as the membrane anchored propeptide is cleaved by a proprotein convertase.

MMP-27 was first found in chicken embryo fibroblasts. Chicken MMP-27 digests gelatin and casein and causes autolysis of the enzyme, but little information is available on the activity of mammalian enzyme.

Epilysin (MMP-28) is expressed in many tissues such as lung, placenta, heart, gastrointestinal tract and testis. The enzyme expressed in basal keratinocytes in skin is considered to function in wound repair. It is also elevated in cartilage from patients with osteoarthritis and rheumatoid arthritis.

MMP-21, MMP-23 and MMP-28 have a furin recognition sequence before the catalytic domain and therefore they are likely to be activated intracellularly and secreted as active enzymes.³

Interest in MMPs increased in the late 1960s and early 1970s following observations that MMPs are up-regulated in diverse human diseases including rheumatoid arthritis and cancer.

However, recent clinical data indicate that the relationship between MMPs and disease is not simple; for example, increased MMP activity can enhance tumour progression or inhibit it.

This complex relationship between MMP expression and cancer has increased the basic and clinical interest in understanding MMP function *in vivo*, but it has also focused attention on MMPs and pathologies.

The activity of MMPs is controlled at many levels and the regulation of their activity remains a topic of intense research.

Analysis of MMPs genetic knockouts animals have offers opportunities to identify essential functions of every single MMP and to validate candidate substrates by looking for cleavage products in the control animal and uncleaved proteins in the mutant animal.

The initial characterizations have described surprisingly subtle phenotypes, with all MMP knockout lines surviving to birth (table 2.2).⁵

MMP gene	Mutant phenotypes (mouse, unless noted)
<i>Mmp2</i>	Reduced body size ¹⁵² ; reduced neovascularization ⁵⁵ ; decreased primary ductal invasion in the mammary gland ⁵⁴ ; reduced lung saccular development ¹⁵³
<i>Mmp3</i>	Altered structure of neuromuscular junctions ¹⁵⁴ ; reduced purse stringing during wound healing ⁸⁶ ; altered secondary branching morphogenesis in the mammary gland ⁵⁴
<i>Mmp7</i>	Innate immunity defects ⁸³ ; decreased re-epithelialization after lung injury ⁸⁵
<i>Mmp8</i>	Increased skin tumours ¹⁰⁴ ; resistance to tumour necrosis factor (TNF)-induced lethal hepatitis ¹⁰³
<i>Mmp9</i>	Bone-development defects ³⁶ ; defective neuronal remyelination after nerve injury ¹⁵⁵ ; delayed healing of bone fractures ³⁹ ; impaired vascular remodelling ¹⁵⁶ ; impaired angiogenesis ³⁶
<i>Mmp10</i>	Increased inflammation and increased mortality in response to infection or wounding (W. C. Parks , personal communication)
<i>Mmp11</i>	Delayed mammary tumorigenesis ¹⁵⁷
<i>Mmp12</i>	Diminished recovery from spinal cord crush ¹⁵⁸ ; increased angiogenesis due to decreased angiostatin ¹²⁸
<i>Mmp13</i>	Bone remodelling defects ^{7,40} ; reduced hepatic fibrosis ¹⁵⁹ ; increased collagen accumulation in atherosclerotic plaques ¹⁶⁰
<i>Mmp14</i>	Skeletal remodelling defects ^{42,43,45,161} ; angiogenesis defects ⁴⁶ ; inhibition of tooth eruption and root elongation ¹⁶² ; defects in lung and submandibular gland ^{46,163}
<i>Mmp19</i>	Obesity ¹⁶⁴
<i>Mmp20</i>	Defects in tooth enamel ¹⁶⁵
<i>Mmp23</i>	No phenotype reported
<i>Mmp24</i>	Abnormal response to sciatic nerve injury ¹⁶⁶
<i>Mmp28</i>	Increased inflammatory response (W. C. Parks , personal communication)

Table 2.2. Relation between MMP-null rats and impaired functions. ⁵

Main Structure of MMPs

MMPs are members of the metzincin group of proteases, which are named after the zinc ion and the conserved Metionine residue at the active site.

The first structure of an MMP in complex with a synthetic inhibitor (MMP-1 catalytic domain) was reported by Lovejoy and co-workers. ⁶

Mammalian MMPs share a conserved domain structure (figure 2.1) that consists of a catalytic domain and an auto-inhibitory pro-domain.

The catalytic activity of MMPs is regulated at four points: gene expression, compartmentalization (i.e., pericellular accumulation of enzyme), proenzyme (or zymogen) activation, and enzyme inactivation and is further controlled by substrate availability and affinity. ⁷

Most of the matrix metalloproteinases consist of four distinct domains, which are N-terminal pro-domain, catalytic domain, hinge region, and C-terminal hemopexin-like domain.

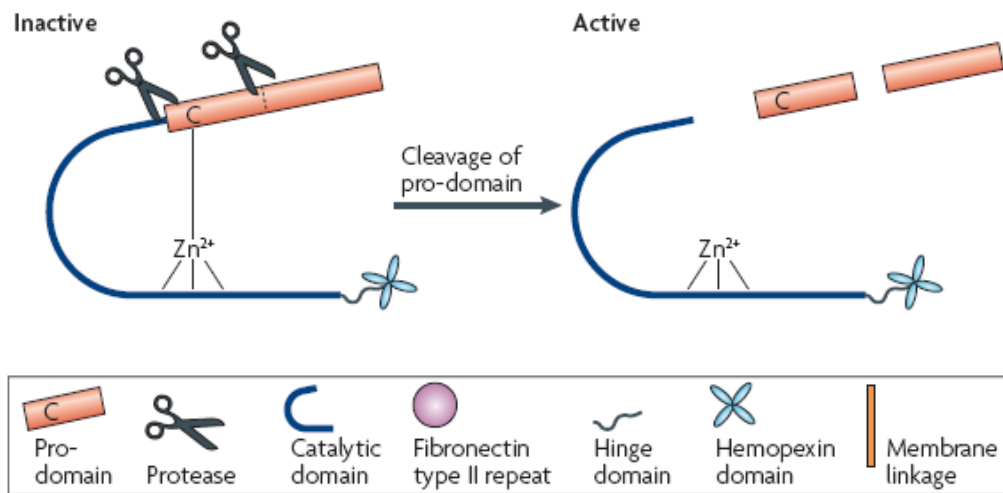


Figure 2.1. MMP domains and activation mechanism.⁵

The N-terminal prodomain.

The MMPs are initially synthesized as inactive zymogens with a pro-peptide domain that must be removed in order to activate the enzyme.

The prodomain essentially consists of three helices that are arranged nearly perpendicular to each other and connected via rather flexible and proteolysis susceptible loops. In case of MMP-1 and MMP-2, the loop between helix H1 and helix H2 contains the region of the first activation cleavage. This first cleavage is supposed to destabilize the threehelix bundle of the MMP prodomains.⁸

The catalytic domain

The catalytic power of MMPs is encoded in four essential structural elements:

1. Binding of the main chain of the substrate in the active site cleft.
2. The specificity subsite pockets that define the active site, in particular the S1' subsite.
3. The zinc ion-binding histidine triad and catalytic glutamate.
4. Binding to secondary substrate sites outside the active site.

The catalytic domain of the MMPs contains two zinc atoms. One of these atoms plays a catalytic role and the other a structural role. The thiol group of the cysteine residue within the propeptide coordinates to the catalytic zinc atom and thereby confers latency. This interaction must be broken

before the metalloproteinase can degrade matrix proteins.⁹ Main chain binding of protein or peptide substrates to the active site occurs through formation of an antiparallel β -sheet structure, with hydrogen bonds formed between the substrate and enzyme. A polarized water molecule bound to the active site Zn^{2+} ion and general base glutamate residue is essential in catalyzing peptide bond cleavage. In MMPs, the Zn^{2+} ion is coordinated by the three histidines in the HExxHxxGxxH metzincin signature motif. Mutagenesis of any one of these His residues ablates catalytic activity.

The nucleophilic attack by the catalytic water molecule in MMPs occurs on the carbonyl of the substrate scissile peptide bond to form a tetrahedral transition-state intermediate in which the negatively charged oxygen is stabilized by coordination with the catalytic Zn^{2+} ion.¹⁰

The catalytic domain of all MMPs is similar in showing a shallow active-site cleft notched into the front surface and separating the smaller 'lower subdomain' from the larger 'upper subdomain'. This cleft extends horizontally across the molecule and would bind a peptide substrate from left to right. The upper subdomain encompasses a characteristic five-stranded, highly twisted β -sheet, flanked by three surface loops on its convex side and by two long regular α -helices on its concave side. Four of the five β -strands are aligned in a parallel fashion, only the cleft-sided 'edge strand' IV runs in opposite direction.⁸

The active site is constituted by specificity subsite pockets that define it:

S1, S2, S3, S4, S1', S2', S3' and S4' and the substrate poses the corresponding portions named P1, P2, P3, P4, P1', P2', P3', P4' (figure 2.2).

The S1' specificity pocket of MMPs accommodates this side chain and so the size and chemical characteristics of the S1' subsite are important in determining peptide bond preference for cleavage. For example, the small hydrophobic S1' pocket of MMP-1 and MMP-7 restrains substrate preference to small hydrophobic residues at P1'. In contrast, other MMPs such as MMP-2, MMP-3, MMP-8, MMP-9, and MMP-13 have large S1' pockets and can accommodate a more diverse range of amino acids at P1'.^{9, 10}

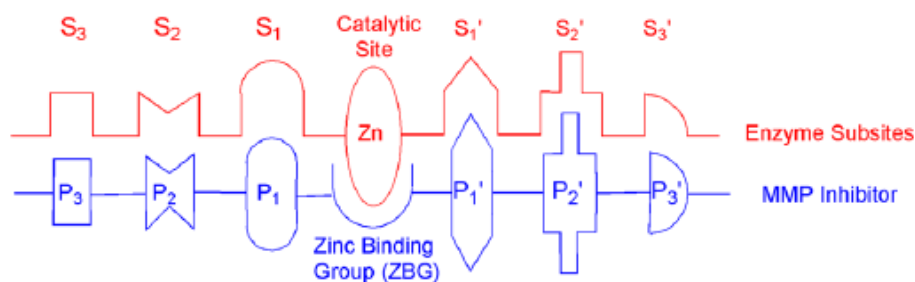


Figure 2.2. Schematic interactions between MMPs and MMP inhibitors.¹¹

The S1' pocket is relatively deep for most MMP enzymes (e.g., MMP-2, MMP-3, MMP-8, MMP-9, MMP-13, etc.), but for certain MMP enzymes (e.g., MMP-1, MMP-7, and MMP-11) it is partially or completely occluded due to an increase in the size of the side chain of the amino acid at position 193 (MMP-8 numbering) from leucine to arginine (MMP-1), tyrosine (MMP-7), glutamine (MMP-11), or one of the amino acid residues that form the pocket. It has also been shown that the mutation of S1' subunit tyrosine of MMP-7 to leucine changes the substrate specificity to be more like that of the deep pocket enzyme MMP-3. Homology models for MMP-2 and MMP-9 based on the structure of MMP-3 suggest that there may be differences in the shape of the bottom of the S1' subunit for the deep pocket enzymes. In the case of MMP-2, the S1' pocket may be a channel with no bottom, whereas that for MMP-9 is said to be a pocket-like subsite. Generally the subunit S2' is a solvent-exposed cleft and the S3' subunit is a really ill-defined solvent-exposed region.

Substrate selectivity

The preferred amino acid in substrate subunit P3 is proline for all the kinds of examined enzymes. Arginine is preferred at P2 for MMP-2 selectivity, whereas Leucine and Methionine are preferred for MMP-7. Phenylalanine is preferred over Leucine and Methionine at P2 for MMP-3. Valine at P1 results in negligible cleavage for all of the enzymes. At the P1 position, Glutamine provides significant cleavage by MMP-7 and MMP-8, and negligible by MMP-1, MMP-2, and MMP-9. At P1', the presence of a Tyrosine residue results in highly selective cleavage by MMP-8 as well as Leucine and Methionine appear to be preferred for broad-spectrum cleavage; however, on the other hand, the phage-displayed results suggest that Methionine at P1' gives minimal cleavage with MMP-7. However, the substrate specificity studies suggest that Phenylalanine at P1' is preferred for cleavage by MMP-3 over the other enzymes, whereas the phage-displayed results indicate that Phenylalanine at P1' provides negligible cleavage. It has also been shown that MMP-11 and MMP-14 cleave substrates containing unusual amino acids with extremely long side chains at their P1' position more efficiently than the corresponding substrates with natural phenylalanine or leucine amino acids. There is a very little selectivity by the various substitutions at P2' position and generally Tryptophan is preferred for efficient cleavage. The same is true for amino acid changes at P3'.

The S3–S1 subsites form a shallow region bordered on one side by the α -strand IV that features a hydrophobic proline binding cleft at S3.

It is interesting to note that the selective replacement of catalytic zinc of MMP-3 catalytic domain with other transition metals that are Co^{2+} , Mn^{2+} , Cd^{2+} , and Ni^{2+} results in the retention of protease activity. However, substitution of the catalytic metal influences the substrate specificity of enzyme, since the active-site geometry is altered and hence affects substrate binding.⁹

The hinge region.

The hinge-region in MMPs is a segment of 15–65 amino acids. It is of critical importance for the stability of the enzyme and also for the degradation of complex substrates such as fibrillar collagen by collagenases which require the concerted action of the catalytic and of the hemopexin domain. The hinge region itself contributes to the collagen binding and unwinding and its breakdown.

The structures of human and porcine MMP-1 show an elongated peptide segment which is in close contact with the catalytic and the hemopexin-like domain.

Highly conserved residues for the collagenases in this area are prolines, which are in direct contact with the catalytic and the hemopexin domain thus stabilizing the domain arrangement in MMP-1. In accordance with these structures, mutagenesis experiments showed an 98.5% drop in activity when four prolines in the hinge are replaced by alanines. A single mutation of the central glycine in the center of the hinge region of MMP-1 to aspartate also strongly reduces collagenolysis, which might be explained by reduced flexibility at this site.⁸

The C-terminal Hemopexin domain.

This domain has a beautiful common fold. The overall shape is a squat cylinder comprised of four β -sheets each representing a hemopexin module and each forming a blade of the four-bladed β -propeller structure. Each blade is a twisted four-stranded β -sheet that links to the adjacent blades by small connecting strands on the rim of the domain and from a longer loop at the center. Extensive packing faces on the blade sides between adjacent modules arrange one next to another in a stable configuration. Packing of the wedge-shaped modules also forms a central pore in the domain, in which are bound either one or two Ca^{2+} ions. The central Ca^{2+} ions in the MMP-2 hemopexin C

domain are structurally important—their chelation eliminates heparin and fibronectin interactions. Although X-ray crystallography also showed a potential Zn²⁺ ion binding site on the MMP-2 hemopexin C domain, inductive coupled plasma mass spectrometry analysis did not measure any significant zinc molar content in a recombinant human MMP-2 hemopexin C domain. The hemopexin C domain has homology to the collagen-binding domain of vitronectin (which therefore will also likely have domains with a four-bladed β-propeller structure).¹⁰

Regulation of MMP Activity

As for all secreted proteinases, the catalytic activity of MMPs is regulated at four points:

- gene expression
- compartmentalization (i.e., pericellular accumulation of enzyme)
- proenzyme (or zymogen) activation, and enzyme inactivation
- substrate availability and affinity.

Some members, such as MMP-2, MMP-19, MMP-28, and several MT-MMPs, are expressed in normal tissues, implying a role in homeostasis. However, most MMPs are not expressed in resting tissue yet are induced in repair or remodeling processes and in diseased or inflamed tissues.

The cysteine switch

Harold Van Wart and Henning Birkdahl-Hansen proposed this process as general and required step in the activation of all proMMPs (1990), and they named this mechanism the “cysteine switch”, a term that remains valid and widely accepted. In essence, the thiol-Zn²⁺ interaction can be broken - and a latent MMP can gain catalytic activity – by three mechanisms:

- direct cleavage of the pro-domain by another proteinase
- reduction of the free thiol by oxidants or by nonphysiologic reagents such as alkylating agents, heavy metal ions, and disulfides,
- allosteric perturbation of zymogen (Figure 2.5).

Thiol reduction and allosteric controls would lead to inter or intramolecular autolytic cleavage of the prodomain.

An important component of the cysteine-switch mechanism is that the prodomain does not need to be removed for a zymogen to acquire activity; only disruption of the zinc-thiol interaction is absolutely required.

Furin Activation

Furin is a type 1 membrane serine protease present in the trans-Golgi network.

About one-third of MMPs contain an RXKR or RRKR sequence between the pro and catalytic domains, which serves as a target sequence for proprotein convertases or furins. MMPs with such cleavage site are processed intracellularly before secretion (figure 2.3).

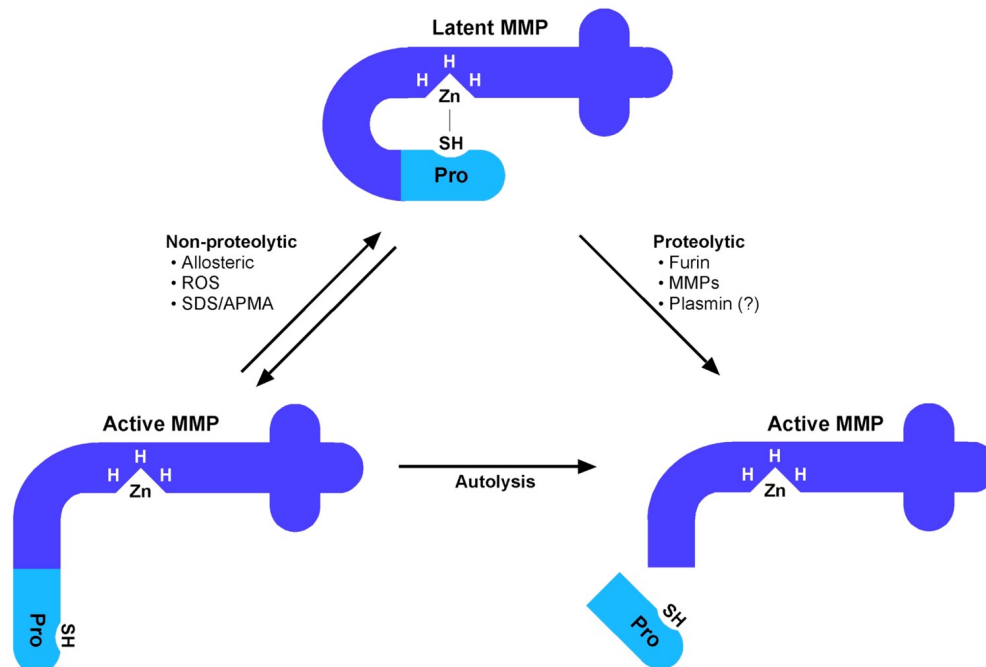


Figure 2.3. Schematic representation of MMP activation. ⁷

TIMPs: the endogenous inhibitors of MMPs.

TIMPs is an acronym that stand for tissue inhibitors of metalloproteinases.

Four TIMP family members exist: TIMP-1, -2, -3 and TIMP-4.

Each of their N- and C-terminal domains contains 6 conserved cysteine residues that form three disulfide loops. The N-terminal region binds to the MMPs' catalytic domain and inhibits MMP activity, whereas, the C-terminal region interacts with the the proforms of MMP-2 and MMP-9 C-terminal hemopexin domain to stabilize the pro-enzyme inhibitor complex. TIMP-2 is the only TIMP member that specifically interacts on the cell surface with both MT1-MMP and pro-MMP-2 in order to facilitate the activation of pro-MMP-2. Thus TIMP-2 is unique due to its functions of

MMP inhibitor and activator. TIMPs can inhibit all active MMPs, however, not with the same efficacy. TIMP-1 preferentially inhibits MMP-7, MMP-9, MMP-1 and MMP-3, whereas, TIMP-2 inhibit more effectively MMP-2. TIMP-3 can inhibits MMP-2 and MMP-9 among other enzymes (ADAMs), whereas TIMP-4 inhibits MT1-MMP and MMP-2 catalytic activity. TIMPs regulate proteolytic activity and all the MMP-mediated activities.¹²

Collagene Hydrolysis: Reaction mechanism

The reaction mechanism for the proteolysis by MMPs has been delineated on the basis of structural information and shown in Figure 2.4. It is proposed that the scissile amide carbonyl coordinates to the active-site zinc (II) ion. This carbonyl is attacked by a water molecule, which is both hydrogen bonded to a conserved glutamic acid (Glu-198 in MMP-8) and coordinated to the zinc(II) ion. The water molecule donates a proton to the Glu residue that transfers it to the nitrogen of the scissile amide, which is followed by the Glu residue shuttling the remaining proton from the water molecule to the nitrogen of the scissile amide with resultant peptide bond cleavage. In this process, the positively charged zinc(II) ion helps to stabilize a negative charge at the carbon of the scissile amide and a conserved alanine (Ala-161 in MMP-8) residue helps stabilize positive charge at the nitrogen of the scissile amide.

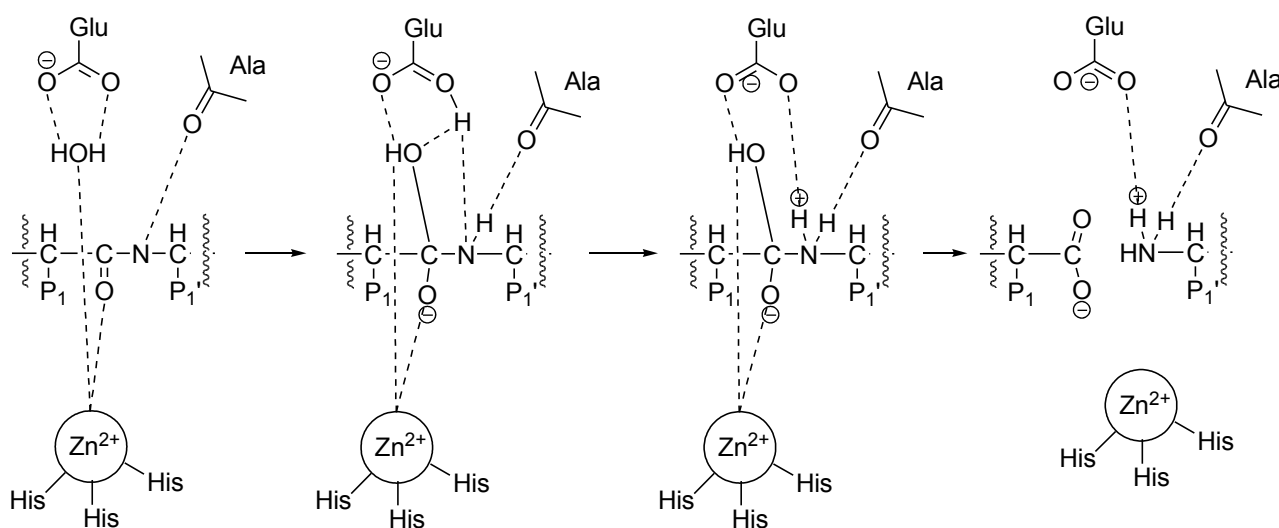


Figure 2.4. Mechanism of collagen degradation.⁹

MMP of our interest

Despite the huge amount of metalloproteinases that have been discovered, we have choose just three of them: MMP-2, MMP-9 and MMP-13.

MMP-2

MMP-2 (gelatinase A, 72-kDa type IV collagenase) is one of the two described human gelatinases in the MMP family, named for their ability to proteolytically degrade gelatine (denatured collagen). MMP-2 is ubiquitously expressed as a 72-kDa proenzyme and subject to extensive glycosylation. Expression of MMP-2 is constitutive and most proinflammatory stimuli fail to increase the expression level since the gene, in contrast to that of MMP-9, lacks binding sites for pro-inflammatory transcription factors such as activator protein-1.

The MMP-2 proenzyme is activated by forming a complex with TIMP-2 under appropriate stoichiometric conditions, which in turn is a substrate for the membrane bound membrane type-1 MMP (MMP-14) that removes the prodomain of proMMP-2 by proteolytic cleavage (aided by free active MMP-2), yielding the truncated 64-kDa active enzyme. If the concentration of TIMP-2 is too high, both MMP-14 and active MMP-2 will be inhibited and no further activation will ensue. Besides this activation pathway, proMMP-2 can also be activated by thrombin and activated protein C. MMP-2 differs from other MMPs in that the catalytic domain contains cysteine-rich inserts that resemble the collagen-binding regions of the type II repeats in fibronectin. These inserts are required for binding and cleavage of collagen and elastin. MMP-2 is capable of cleaving gelatine, type I, IV and V collagens, elastin and vitronectin.

Through their ability to degrade collagen in the vascular basal membranes, the gelatinases are involved in neovascularisation both under physiological conditions and in pathologies such as tumor metastasis.

The state of activation seems to be of crucial importance for the function of MMP-2 in angiogenesis. Recent research has demonstrated that the fully mature active form induces apoptosis in endothelial cells and inhibits neovascularization, while an intermediate activated complex with MMP-14 enhances cell survival and promotes angiogenesis. MMP-2 can also facilitate migration of cells by direct degradation of the basement membrane thus allowing infiltration of, for instance, neutrophils and lymphocytes, or liberation of chemoattractants. This latter process, named 'ectodomain shedding', is an important physiological function of the membrane-bound ADAM proteases, but has also been described for many other members of the metzincin superfamily. MMP-2 has been known to be involved in both promoting and inhibiting inflammation by liberation of pro-inflammatory mediators.

Interestingly, MMP-2 knockout mice exhibit a normal phenotype under physiological conditions, although the animals do show different response patterns upon allergen challenge, which may be attributed to disturbance of the important role of clearing immune cells.

These findings indicate that MMP-2 function may be interchangeable with other metalloproteases, an hypothesis that is supported by the observation that expression of the second gelatinase, MMP-9, is greatly increased in MMP-2 null mice.¹³

MMP-9

MMP-9 (gelatinase B, 92-kDa type IV collagenase) was first discovered in neutrophils in 1974. MMP-9 is expressed as a 92-kDa proenzyme, which can be activated to the 83-kDa mature enzyme. The larger size of MMP-9 relative to MMP-2 can be attributed to a heavily O-glycosylated collagen V-like insert that links the metalloprotease domain to the hemopexin-like domain. MMP-9 activation may be mediated by removal of the prodomain by serine proteases or other MMPs, or may be a direct response to oxidative stress that disrupts the cysteine switch (as a matter this particular MMP can be useful as a marker for acute ischemic stroke).¹⁴ While a considerable overlap exists in the substrates degraded by MMP-2 and -9, MMP-9 is incapable of direct proteolysis of collagen I.

MMP-9 has been described to release the biologically active form of vascular endothelial growth factor (VEGF), which plays an important role in angiogenesis. This process is complemented by the direct proteolytic degradation of vascular basement membrane proteins, indicating that MMP-9 (even more than MMP-2) may play a crucial role in the formation of new blood vessels.

Interestingly, the hemopexin domain of MMP-9 was reported to be an inhibiting factor in angiogenesis as demonstrated by decreased invasion of glioblastoma cells overexpressing the MMP-9 hemopexin domain in a xenograft model.

MMP-9 null mice show decreased fertility, since MMP-9 is crucial during several stages of the female reproductive cycle (implantation of the embryo and remodeling of endometrial tissue that occurs during the menstrual cycle). Absence of MMP-9 also leads to disorders in bone development, specifically delayed bone ossification due to insufficient angiogenesis in growth plates and reduced osteoclast recruitment.

Whereas MMP-2 is primarily inhibited by TIMP-2, MMP-9 is mostly inhibited by TIMP-1 and contrary to MMP-2, which is expressed ubiquitously under physiological conditions, MMP-9 is increased in malignant cell lines and correlates with their metastatic potential.

The role of gelatinases in pathology has been studied extensively, especially in lung diseases and cancer. The amount of both gelatinases in BALF and sputum of patients suffering from chronic

asthma is higher than in healthy individuals and this increase may be responsible for the characteristic tissue remodeling events observed in chronic asthma such as thickening of the basement membrane, smooth muscle tissue hypertrophy and reduced epithelial thickness. Presence and activity of gelatinases is elevated in many other pulmonary diseases, such as cystic fibrosis, bronchiectasis, acute respiratory distress syndrome (ARDS) and infections.¹³

MMP-13

MMP-13 (collagenase-3) is the latest human collagenase described in literature. This enzyme exhibits preference toward cleavage of type II collagen, effectively completing the substrate spectrum of the collagenases. Collagenase-3 was first cloned from breast cancer tissue in 1994. MMP-13 expression can be influenced by a wide range of hormones and cytokines, such as parathyroid hormone (indicative of the important role of MMP-13 in bone development), insulin-like growth factors I and II, platelet derived growth factor, basic fibroblast growth factor, transforming growth factor β 1 (interestingly both up- and downregulates MMP-13 expression depending on the tissue), interleukin-1 and -6, tumor necrosis factor α and many more. ProMMP-13 can be activated by auto-proteolysis or propeptide removal by various other MMPs like stromelysin-1 (MMP-3), yielding a mature enzyme of 48 kDa, which in turn can be inhibited by TIMP-1, -2 and -3. Active MMP-13 is a key factor in the activation pathway of several MMPs. Besides the TIMP route of inactivation, MMP-13 can bind to a specific receptor on the surface of osteoblasts and fibroblasts resulting in internalization and degradation of the protease.

MMP-13 plays an important role in bone development and remodeling, as may be anticipated from its capability to cleave type II collagen (a major component of cartilage).

This rather specific function is reflected in a limited expression profile of MMP-13 during development and adulthood, which is restricted to developing skeletal tissue. MMP-13 has, contrary to the other collagenases, a relatively high specific activity toward gelatine, indicating that the proteolytic role of MMP-13 expands past the first step of cleavage of triple-helical collagens. Further identified substrates of MMP-13 include aggrecan and perlecan, transforming growth factor β , biglycan, the large protein species of tenascin-C, fibrillin-1 and -2, fibrinogen and two serpins (α 2-antichymotrypsin and plasminogen activator inhibitor-2). MMP-13 expression has been regularly referred to in the literature as indicative of various cancerous processes including chondrosarcoma, breast cancer, head and neck tumors and melanoma. In all cases, high expression of MMP-13 seems to be related to

aggressiveness of the tumor, and MMP-13 may even be required for metastasis of certain tumors as demonstrated for malignant melanoma. Regarding the important role of MMP-13 in bone turnover,

it is not surprising that this enzyme has been linked to various bone-related diseases. Since MMP-13 degrades both type II collagen and aggrecan, it has been linked to cartilage destruction in rheumatoid and osteoarthritis. The specialized role of MMP-13 in bone development and disease has made it an attractive target for selective MMP-13 inhibitors as therapeutic compounds.¹³

MMPs and cancer

MMPs have a relevant role in the pathophysiology of diseases such as arthritis, multiple sclerosis, periodontal disease, atherosclerosis, and cardiac injury and remodeling.¹⁵ A number of cancer studies have correlated MMP expression and disease outcome.

MMPs can contribute to tumor growth not only by degradation of the extracellular matrix (ECM) but by the release of sequestered growth factors or the generation of bioactive fragments. For instance, MMP-9 mobilizes VEGF from the ECM and cleaves type IV collagen to generate tumstatin, an angiogenesis inhibitor. MMPs are also important in tumor progression, promoting invasion, immune escape and many other events. However, particularly in carcinomas, MMPs are associated with the supporting ‘host’ cells rather than the tumor cells and this finding has emphasized the emerging theme of the importance of the microenvironment in tumorigenesis.

MMP-12, MMP-13 and cathepsin K showed an increase expression in human tumors compared with normal lung. Immunohistochemical analysis also confirmed MMP-12 expression in the stroma of human lung tumor samples.

It is notable that animal studies have shown that MMPs sometimes have ‘protective’ roles in cancer development. *Mmp8*-null male or ovariectomized female mice develop significantly larger numbers of skin papillomas after a chemical carcinogen treatment and higher grade and more aggressive skin tumors developed in *Mmp9*-null mice. In a human study of MMP-12 in squamous cell carcinoma it was found that high expression in tumor cells was associated with more aggressive tumors and high expression in tumor macrophages was correlated with lower grade tumors.

It is possible that obtaining a detailed understanding of the potential role of MMPs in the different cell types associated with tumors may be vital for the design of therapeutic anti-MMP strategies.¹⁶

Regulation of angiogenesis

MMPs also have complex roles in angiogenesis. It is known that MMPs can promote endothelial cell migration and trigger angiogenic switch. For example, MMP-9 participates in switching angiogenesis by releasing VEGF from ECM. Also, MMP-2 activity was suggested to be necessary for the switch to angiogenic phenotype in an animal model. Furthermore, MMPs increase the bioavailability of the pro-angiogenic growth factors, vascular endothelial growth factor (VEGF), fibroblast growth factor- 2 (FGF-2), and TGF- β , which stimulate proliferation and migration of endothelial cells. MT1-MMP regulates VEGF-A expression by promoting VEGFR-2 cell surface localization thereby activating VEGFR-2-Src-Akt-mTOR pathway. MMP-7 degrades soluble VEGF receptor-1 (sVEGFR-1/sFlt-1), an endogenous VEGF inhibitor that sequesters VEGF and blocks its access to VEGF receptors. The degradation of sVEGFR-1 then liberates VEGF from the endogenous trap and allows its access to membrane receptors on endothelial cells. However, MMPs may have adverse effects on angiogenesis. For example, MT1- MMP-mediated endoglin shedding inhibits tumor angiogenesis. The generation of angiostatin and endostatin, two potent angiogenesis inhibitors, also involves MMPs.

MMP-7 and MMP-9 hydrolyze plasminogen to generate angiostatin fragments. Endostatin is the C-terminal proteolytic product of the collagen XVIII α 1 chain and MMP-14 can cleave collagen XVIII to generate endostatin-spanning fragment. Hence, we speculate that the effects of MMPs on angiogenesis may be context-dependent. The outcome relies on the availability of specific MMPs and the balance between two opposing effects of individual MMPs on angiogenesis.⁴

MMP Inhibitors

As described above, matrix metalloproteinases are involved in the regulation of the cellular turnover and in the spreading of metastasis, and their regulation should be a very useful weapon for fight cancer.

Both small molecules (synthetic and natural products) and macromolecular endogenous inhibitors have been considered as potential therapies for diseases in which excess MMP activity has been implicated.

A tetracycline derivative, doxycycline (Periostat; CollaGenex Pharmaceuticals Inc., Newtown, PA, USA), is currently the only MMPI approved by the U.S. FDA and is used as an adjunct therapy in adult periodontitis. One of the main reasons for the limitations of hydroxamate-based inhibitors is due to its poor bioavailability and the toxicity arising from its metabolic stability limitations (the amide bond can be easily hydrolyzed with formation of hydroxylamine and the corresponding

carboxylic acids). On the other hand, most of the inhibitors tested were broad-spectrum MMP inhibitors that make no distinction between these enzymes.¹⁷

Many inhibitors have been developed either by pharmaceutical companies and academics.

Most MMP inhibitors (MMPi) are constituted from a functional groups which are capable to form H bonds with the structure enzyme and one or more residues that can interact through Van der Waals interactions with the enzyme subsite and a zinc-binding group (ZBG), which is deputate of the catalytic Zn²⁺ chelation. The most common moiety used for the synthesis of sudden inhibitors are hydroxamates, carboxylates, phosphinates and barbituric. The ZBG however is not always present, especially in the most recent and innovative inhibitors.

MMPsI can be classified in peptidomimetics and not peptidomimetics.

Either peptidomimetics and not peptidomimetics can be classified for their ZBG moiety.

Here under will be report the most important and innovative class of inhibitors.

Hydroxamates.

The hydroxamate is the most common and the most powerful moiety for the chelation of the catalytic zinc, it acts as a bidentate ligand and it's widely used for the developmental of MMPsI.

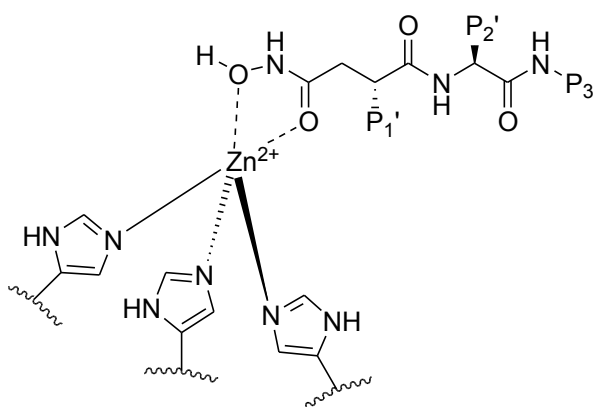


Figure 2.5. Hydroxamate chelation mechanism.¹⁸

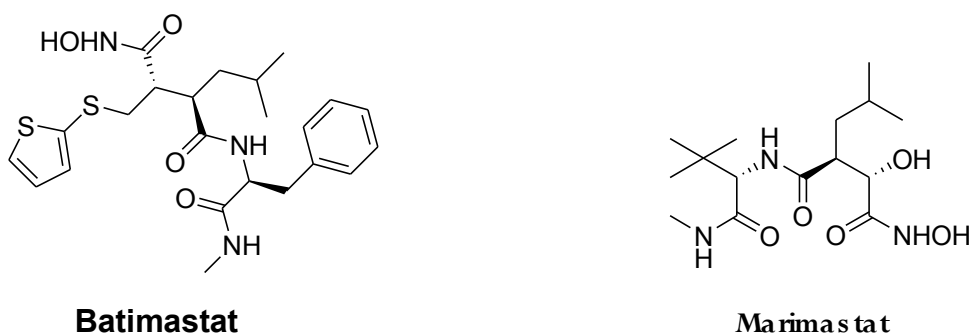
Efficiency of hydroxamates is supported by good *in vitro* activity data and a very huge amount of good selective nanomolar inhibitors have been synthesised, but unfortunately have result in a fail in clinical trials.

The failure of hydroxamic acid based MMPi at a clinical level may stem, in part, from the lack of selectivity of hydroxamic acids towards the Zn²⁺ ion, poor pharmacokinetics, and poor oral bioavailability.

Consequently, some efforts have been made to identify alternatives to the hydroxamic acid ZBG. In most of these studies there have been only a comparison between hydroxamic acids and the corresponding carboxylic acids (usually the synthetic precursor of most hydroxamic acids) and generally a loss in potency has been observed likely due to the change in binding mode and diminished donor ability of the carboxylate ligand.

Castelhamo and co-workers reported the selectivity and potency of MMPi with several different ZBGs such 'reverse' hydroxamates, carboxylates, thiols and phosphinates on a common indolactam/isobutyl backbone moiety.

As a result of these studies, the use of ZBGs other than a hydroxamate, resulted in a 10- to 250-fold loss in potency, but generally no changes in selectivity based on the nature of the ZBG. ¹⁵ Here under are report two of the most important MMP inhibitors that must be considered in this class as broad-spectrum MMPsI:



Scheme 2.6. Molecular structure of Batimastat and Marimastat.

Unfortunately these two MMPsI failed during clinical trials due to musculo-skeletal toxicity.

Pirones

A 2008 paper ¹⁵ report an interesting MMP inhibitory activity of some pyrone based molecules. Docking representation show the chelating effect of pyrone ring over zinc ion (figure 2.7).

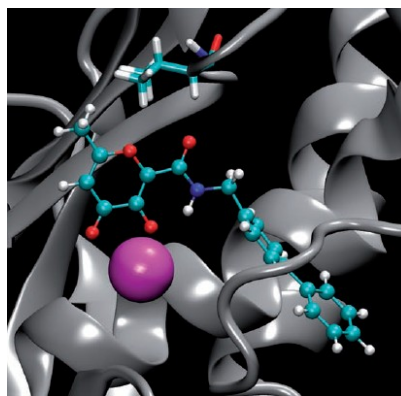
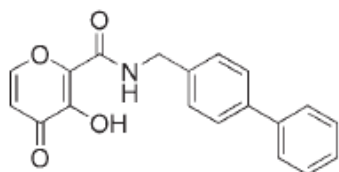


Figure 2.7. Pirone based scaffold in MMP-3 active site. ¹¹

X-ray structures of thiomaltol and maltol tris(pyrazolyl)borate zinc(II) complexes reveal that the hydroxythiopyrone and hydroxypyrene ligands coordinate to tris(pyrazolyl) borate zinc(II) in different geometries (Fig. 3),¹² suggesting that substituents at the same positions of thiopyrone and pyrone rings may interact with MMP active sites in different fashions. These findings promote us to investigate 5- and 6-substituted hydroxypyrones and hydroxythiopyrones. ¹¹

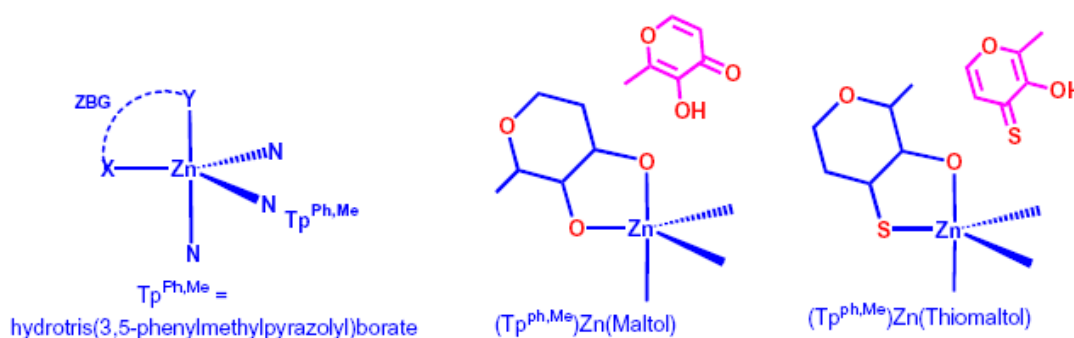


Figure 2.8. Geometries of maltol- and thiomaltol-tris(pyrazolyl)borate zinc(II) complexes. ¹¹

Barbiturates.

In 2001, following a random screen for anti-tumour agents, workers from the Hoffman La-Roche company reported a surprising discovery: certain 5,5-disubstituted pyrimidine-2,4,6,-triones

(barbiturates) are inhibitors of the MMPs with good gelatinase selectivity. This kind of MMP inhibitory with barbiturate-based scaffold are without the sedative effects of the classical agents, and impart a better in vivo stability respect to other zinc binding group (e.g., hydroxamates).

The ionised barbiturate ring chelates the zinc atom in a tridentate way directing the 5-substituents into the S1 and S2 substrate binding pockets. The class exhibit broadly similar SAR to non-barbiturate MMP inhibitor families. The 5-aromatic substituents (biphenyl or phenyloxyphenyl) bind in the deep hydrophobic S1 substrate pocket. The second 5-substituent is directed in this arrangement into the S2 pocket towards solvent. Several elegant studies have demonstrate that C5-piperazine or piperidine substitution is favourable for high potency and moreover that the heterocycle imparts flexibility in the design of a range of barbiturate- based pharmacological, clinical and biochemical tools.

The structural basis for barbiturate interactions with the MMPs was revealed in several X-ray studies.¹⁹

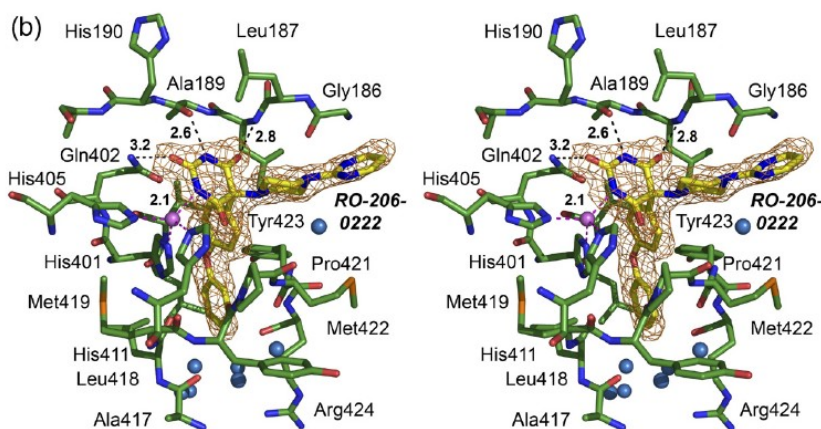
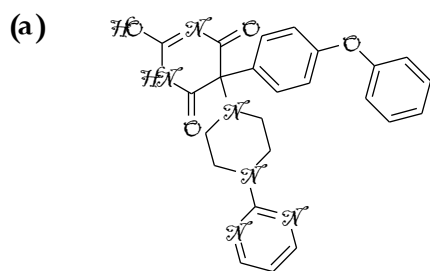


Figure 2.9. (a) Barbiturate inhibitor RO-206-0222 (b) Interaction between inhibitor and active site region of MMP-9. Ionic bonds to the catalytic zinc and intermolecular hydrogen bonds are shown as broken lines (distances in Å).²⁰

MMP inhibitors without a zinc-binding group

High-throughput screening of chemical libraries has led to the discovery of unusual MMP inhibitors, especially for MMP-13. Among these, MMP inhibitors with no zinc-binding group that do not engage in direct interactions with the zinc active site ion has emerged. These compounds without the zinc tether can be tailored to target the depth of the MMP S1' cavity keeping a reduced molecular weight, in contrast to inhibitors containing a zinc-binding group. The first highly potent and selective inhibitor of MMP-13 reported was compound 1 ($K_i = 8$ nM towards MMP-13 and no activity detected against MMP-1, -2, -3, -7, -8, -9, -10, -11, -12, -14 and -16 when tested at 100 μ M). The particular binding mode of 1 in MMP-13 active site is illustrated by comparing the X-ray structure of MMP-13 in interaction with compounds 1 and 2 (for chemical structures see Scheme 3 and 2 respectively). Compound 8 binds in the bottom part of the S1' cavity of MMP-13 and extends into an additional cavity termed the "S1' side pocket" as depicted in figure 2.10.

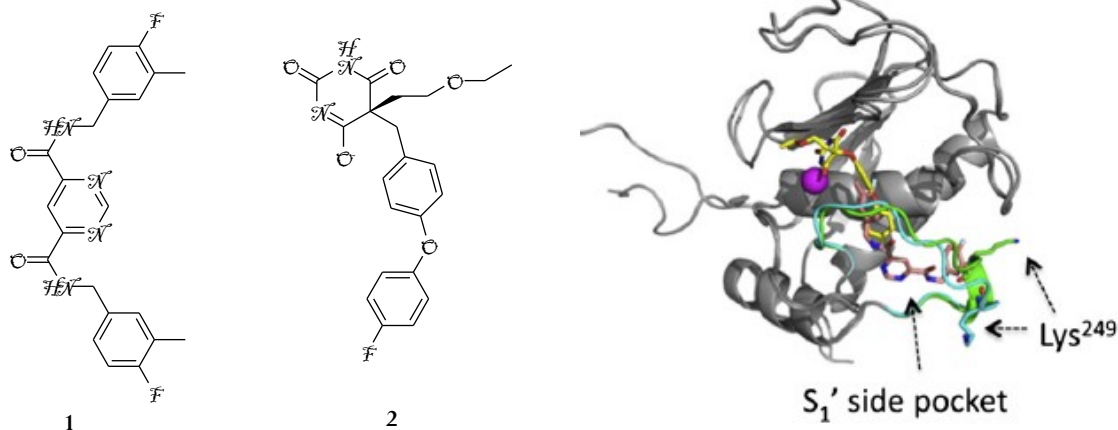


Figure 2.10. Superimposition and comparison of cartoon representations of two crystal structures of MMP-13 in complex with a non-chelating inhibitor 1 (pink stick, PDB code: 1XUD) and with a pyrimidinetrione inhibitor 2 (yellow stick, PDB code: 1YOU) illustrating the different S1' loop conformation and orientation of Lys249 in the two complexes.²¹

An excellent paper published from Gao et al. of Boehringer Ingelheim Pharmaceuticals²², report a library of compounds born from the same scaffold. Some of them show a very good activity joined to an exceptional selectivity for MMP-13. Here is report the main structure of sudden inhibitors.

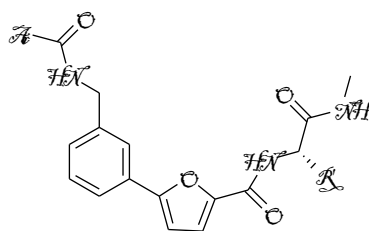


Figure 2.11. Main scaffold of selective MMP-13 inhibitors without zinc-binding group SAR studies of non-zinc-chelating MMP-13 inhibitors: Improving selectivity and metabolic stability.²²

Bibliography

1. Diaz, N; Sua, D.; Valdes, H.; From the X-ray Compact Structure to the Elongated Form of the Full-Length MMP-2 Enzyme in Solution: A Molecular Dynamics Study *J. Am. Chem. Soc.* **2008**, *130*, 14070–14071.
2. Page-McCaw, A.; Ewald, A. J.; Werb, Z. Matrix metalloproteinases and the regulation of tissue remodelling. *Nature review, Molecular cell biology* **2007**, *8*, 221-233.
3. Huxley-Jones, J.; Clarke, T.K.; Beck, C.; Toubaris, G.; Robertson, D.L.; Boot-Handford, R.P. The evolution of the vertebrate metzincins; insights from *Ciona intestinalis* and *Danio rerio*. *Bio Med Central Evol. Biol.*, **2007**, *7*, 1-20.

4. Hua, H.; Li, M.; Luo, T.; Yin, Y.; Jiang, Y.; Matrix metalloproteinases in tumorigenesis: an evolving paradigm. *Cell. Mol. Life Sci.* **2011** 68 3853–3868
5. Andrew, J.; Ewald, Werb, Z.; Page-McCaw, A.; Matrix metalloproteinases and the regulation of tissue remodelling. *Nature reviews, Molecular cell biology*, 2007, 8, 221-233.
6. Lovejoy B.; Cleasby A.; Hassell A.M.; Longley K.; Luther M.A.; Weigl D.; McGeehan G.; McElroy A.B.; Drewry D.; Lambert M.H.; Structure of the catalytic domain of fibroblast collagenase complexed with an inhibitor. *Science.* **1994**, 263, 375-7
7. Ra, H.J.; Parks, W.C.; Control of matrix metalloproteinase catalytic activity *Matrix Biology*, **2007**, 26, 587-596.
8. Maskos, K.; Crystal structures of MMPs in complex with physiological and pharmacological inhibitors *Biochimie* 87 (2005) 249–263
9. Whittaker, M.; Floyd, C.,D.; Brown, P.; Gearing, A., J. H.; Design and Therapeutic Application of Matrix Metalloproteinase Inhibitors. *Chem. Rev.* **1999**, 99, 2735-2776.
10. Overall, C. M. Molecular determinants of metalloproteinase substrate specificity: matrix metalloproteinase substrate binding domains, modules, and exosites. *Mol. Biotechnol.* **2002**, 22, 51–86.
11. Yan, Y.-L.; Miller, M.T.; Cao, Y.; Cohen, S.M.; Synthesis of hydroxypyrrone- and hydroxythiopyrrone-based matrix metalloproteinase inhibitors: Developing a structure–activity relationship. *Bioorganic & Medicinal Chemistry Letters* **2009** 19 1970–1976
12. Bourboulia, D.; Stetler-Stevenson W. G.; Matrix MetalloProteinases (MMPs) and Tissue Inhibitors of Metallo Proteinases (TIMPs): positive and negative regulators in tumor cell adhesion. *Semin Cancer Biol.* **2010**, 20, 161–168.
13. Klein, T.; Bischoff, R.; Physiology and pathophysiology of matrix metalloproteases *Amino Acids* **2011** 41 271–290.

14. Ramos-Fernandez, M.; Bellolio, M. F.; Stead, L. G.; Matrix Metalloproteinase-9 as a Marker for Acute Ischemic Stroke: A Systematic Review. *Journal of Stroke and Cerebrovascular Diseases* **2011** *20* 47-54.
15. Agrawal, A.; Romero-Perez, D.; Jacobsen, J., A.; Villarreal, F. J.; Cohen, S. M.; Zinc-binding groups modulate selective inhibition of MMPs. *ChemMedChem* **2008**, *3*, 812 – 820.
16. Murphy, G.; Nagase, H.; Progress in matrix metalloproteinase research. *Mol. Aspects Med*, **2008**, *29*, 290-308.
17. Marques, S. M.; Tuccinardi, T.; Nuti E.; Santamaria, S.; Andre, V.; Rossello, A.; Martinelli, A.; Santos, A.; Novel 1-Hydroxypiperazine-2,6-diones as New Leads in the Inhibition of Metalloproteinases. *J. Med. Chem.* **2011**, *54*, 8289–8298.
18. Jacobsen, F.,E., Lewis J., A.; Cohen S., M.; The design of inhibitors for medicinally relevant metalloproteins. *ChemMedChem* **2007**, *2*, 152 – 171.
19. Wang, J.; Medina, C.; Radomski, M., W.; Gilmer, J. F.; N-Substituted homopiperazine barbiturates as gelatinase inhibitors. *Bioorg. Med. Chem.* **2011** *19* 4985–4999.
20. Tochowicz A., Maskos K., Huber R., Oltenfreiter R., Dive V., Yiotakis A., Zanda M., Bode W, Goettig P. Crystal Structures of MMP-9 Complexes with Five Inhibitors: Contribution of the Flexible Arg424 Side-chain to Selectivity *J. Mol. Biol.* (**2007**) *371*, 989–1006.
21. Devel, L.; Czarny, B.; Beau, F.; Georgiadis, D.; Stura, E.; Dive, V. Third generation of matrix metalloprotease inhibitors: Gain in selectivity by targeting the depth of the S10 cavity. *Biochimie* **2010**, *921*, 501-1508.
22. Gao, D., A.; Xiong, Z.; Heim-Riether, A.; Amodeo, L.; August, E.,M.; Cao, X.; Ciccarelli, L.; Collins, B., K.; Harrington, K.; Haverty, K.; Hill-Drzewi, M.; Li, X.; Liang, S.; Margarit, S., M.; Moss, N.; *Bioorganic & Medicinal Chemistry Letters.* **2010**, *20*, 5039–5043.

CHAPTER 3

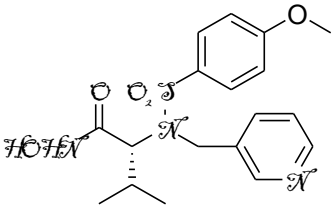
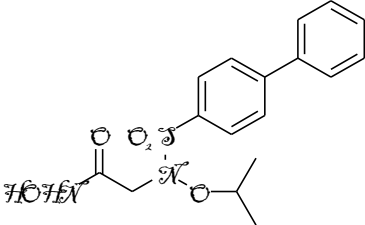
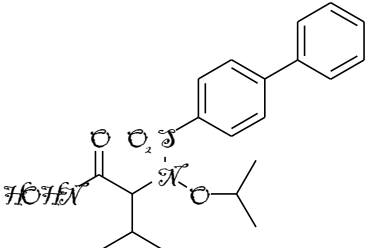
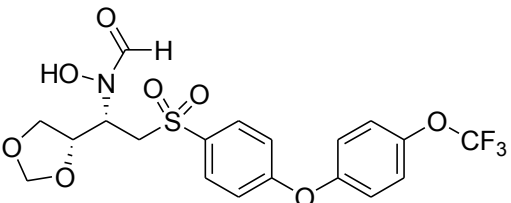
Developmental of Matrix Metalloproteinases Inhibitors

Benzo[*d*]isothiazol-3(2*H*)-one-1,1-dioxide Derivatives

I started my research program designing and synthesizing novel MMP-inhibitor (MMPI) candidates bearing a benzo[*d*]isothiazole heterocyclic core, developed as constrained analogues of the known sulphonamido-based non peptidic MMPIs of the literature.

Carrying out a throughout literature survey, I realized that the presence of a sulphonamide moiety in the non peptidic MMPIs scaffold often plays a pivotal role in allowing the compound to interact suitably with the protein binding site. As evidenced in the following Table (Table 1), a number of potent and effective MMPIs exploit this group as the key fragment of their templates.

Table 3.1. MMP-Inhibitors characterized by a sulphonamide moiety

	Inhibitor name	Inhibitory Activity (IC ₅₀ , nm)		
		MMP-2	MMP-9	MMP-13
	CGS 27023A ¹	20	9	--
	Compound 1 ³	12,46	12.4	
	Compound 2 ²	590	2.44	
	ABT-518 ³	0.61	0.32	--

It has been pointed out in many studies that a co-occurrent presence of a sulphonamide group and a zinc binding group, on the same heterocyclic scaffold, may promote a strong and effective coordination of the catalytic zinc ion within the MMP active site.

Literature examples clearly demonstrate that the sulphonamide group of the inhibitor may be involved in strong hydrogen bonds with amino acid residues from the active site cleft of the enzyme, thus stabilizing considerably the enzyme-inhibitor adduct.

The sulphonamide group does not participate in hydrogen bonds, but may enhance the participation of the two oxygen atoms, by donating them a major share of the lone pairs of electrons, to form coordinating bonds. This leads to the development of partial negative charges on the oxygen atoms, to the extent they attract lone pairs from the sulphur atom, turning out able to form hydrogen bonds. The strength of this latter clearly depends on the partial negative charges developed on the oxygen atoms.

Regarding the nitrogen atom, adjacent to the sulphur one, it has a free lone pair of electrons. Accordingly, it can be assumed to participate in some charge-transfer phenomena with the enzyme, acting either as a donor or as an acceptor of charges, depending upon the positive or negative charge.

A positive one implies that the nitrogen is acting as an acceptor, so that its ability to donate electrons decreases, decreasing the strength of charge transfer phenomenon.

A negative charge, on the other hand, means that the nitrogen would act as a donor so that it becomes more capable of donating electron, resulting in stronger charge-transfer phenomenon.

The sulphonamide moiety of the non peptidic MMPIs may not only be exploited to anchor the backbone of the protein through hydrogen bonds, but also used to direct properly the hydrophobic substituent of the MMPI to the S1' pocket of the enzyme, thus enabling it to plunge in deeply.

This is clearly emphasized by Ohtani and co-workers, who developed a number of sulphonamido and carboxamido derivatives as effective inhibitors of type IV collagenases, MMP-2 and MMP-9.⁷

As schematically represented in Figure 3.1, the C-N-S-C fragment, representing the sulphonamide portion of the 2-(biphenyl-4-ylsulfonamido)-N-hydroxy-3-phenylpropanamide, **3**, adopts exclusively a gauche conformation, thus allowing the biphenyl substituent of the compound to direct properly toward the S1' pocket.

On the contrary, when the same fragment is replaced by the C-N-(C=O)-C portion, as in the N-(1-(hydroxyamino)-1-oxo-3-phenylpropan-2-yl)biphenyl-4-carboxamide, **4**, the torsion adopts a trans conformation, thus directing the biphenyl substituent to the shallow S2' and S3' subsites. Such a change heavily affects the inhibitory efficacy of the resulting compound. Actually, while compound **3** proves to inhibit potently both MMP-2 and MMP-9, showing IC₅₀ values in the low micromolar range, derivative **4** turns out rather ineffective (Figure 1).

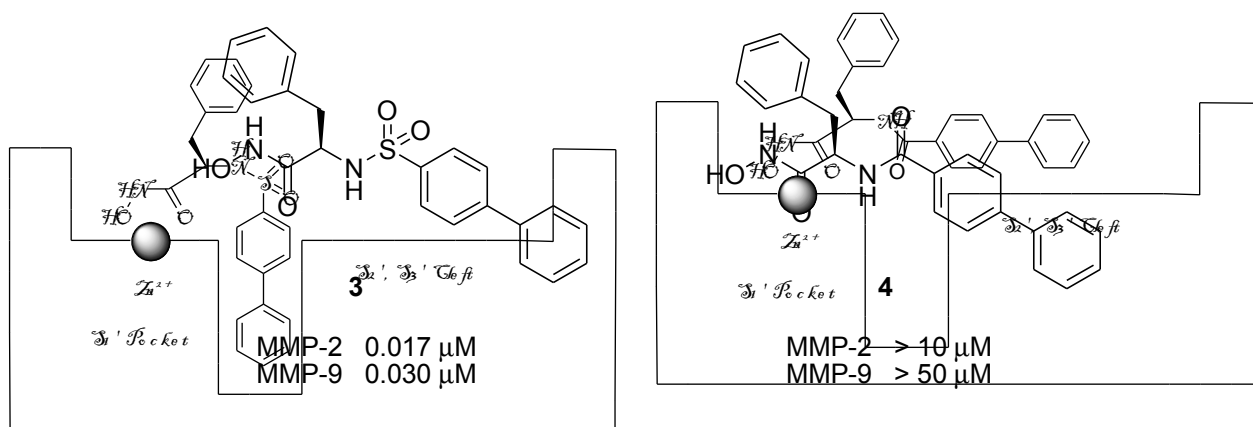


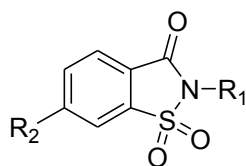
Figure 3.1. Schematic interaction of the sulphonamido and carboxamido inhibitors **3** and **4**.

Tetrahedral geometry at the sulphur atom, as opposed to planarity of the carboxamide linkage, provides ideal geometry to link $S1'$ directed hydrophobic substituent with ZBG.

Elongation of the sulphonamide substituent reduces the inhibitory activity against enzymes with shallower $S1'$ pocket, mainly MMP-1 and MMP-7, while retains efficacy against enzymes with open $S1'$ pockets, such as MMP-2, -8 and -13, and consequently enhances the selectivity.

Therefore, the sulphonamide substituent can be profitably manipulated somehow to alter the selectivity pattern of the resulting compounds.^{4,5}

Intrigued by the biological versatility of the sulphonamide portion, I focused my attention on the benzo[*d*]isothiazole heterocyclic core, in which this key fragment is constrained into a five membered skeleton. Aiming to disclose novel hits, to develop as MMPI leads, I explored the versatility of this scaffold designing and synthesizing a number of derivatives, summarized in Figure 3.2.



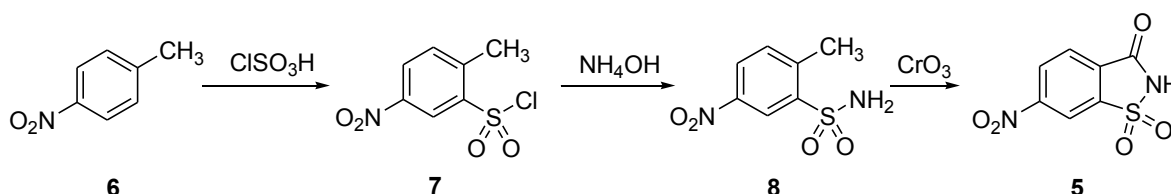
R_1 : H, $(CH_2)_nCOOH$
 R_2 : H, $NHCOCH_3$, $NHCOC_6H_5$, $NHCOC_6H_4-p-X$
 n : 1-3

Figure 3.2. General formula of benzo[*d*]isothiazole MMPIs

At first, to investigate a possible role of the sulphonimido moiety as distinctive ZBG, only alkyl- and aryl-amido substituents were inserted in the position 6 of the heterocyclic scaffold. Later, to verify any cooperation between the sulphonimido moiety and a well-known ZBG, carboxylic

residues of different length were inserted in the position 2 of the core. Finally, both the substitution patterns were explored.

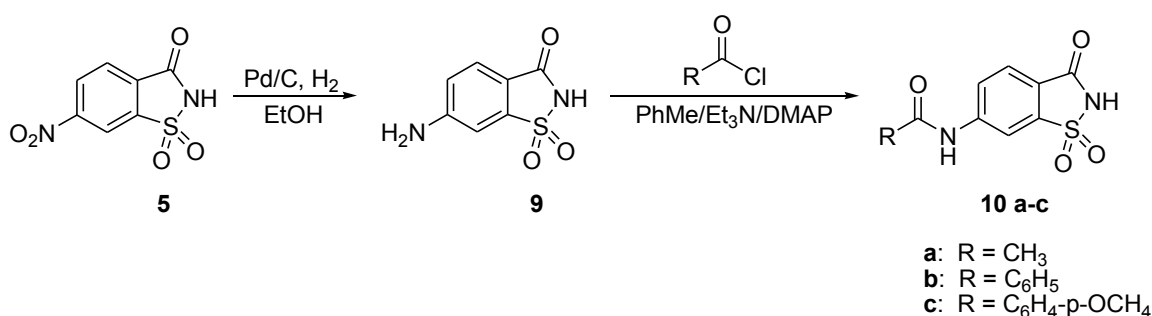
The novel benzisothiazole derivatives were prepared from the key intermediate **5**, 6-nitro-1,2-benzisothiazol-1,1-dioxide-3(2*H*)-one, which were synthesized following a previously reported procedure⁶ (Scheme 3.3).



Scheme 3.3. Synthetic Pathway of 6-nitro-1,2-benzisothiazol-1,1-dioxide-3(2*H*)-one.

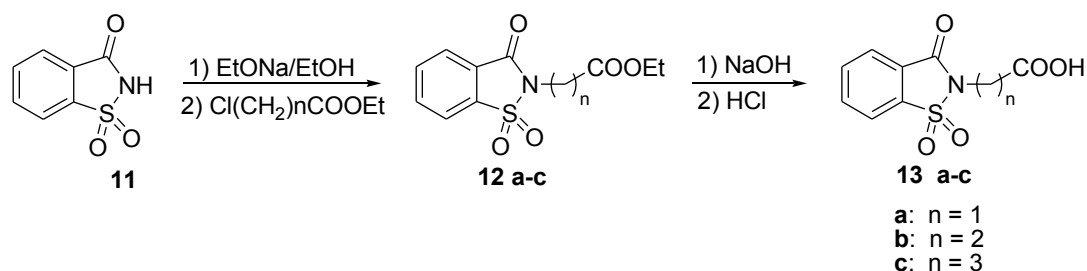
Reaction of the commercially available 4-nitrotoluene, **6**, with chlorosulfonic acid afforded the corresponding sulphonyl chloride, **7**. Treatment of **7** with concentrated ammonium hydroxide led to the sulphonamide **8**. Cyclization of **8**, by means of oxidation of benzylic carbon to carboxylic acid with chromium trioxide, afforded the target 6-nitro-1,2-benzisothiazol-1,1-dioxide-3(2*H*)-one, **5**.

To obtain MMPI hits **10 a-c**, bearing different substituents in the position 6 of the nucleus, the key intermediate **5** was reduced to the corresponding amino derivative, **9**, at room temperature and atmospheric pressure, *via* a catalytic hydrogenation performed in the presence of Palladium/Carbon as the catalyst. Compound **9** gave the target hits, **10 a-c**, by reaction with the suitable acyl chloride, in the presence of Et₃N and DMAP (Scheme 3.4).



Scheme 3.4. Synthetic Pathway to obtain MMPI hits **10 a-c**.

Scheme 3.5 describes the synthetic pattern employed to obtain inhibitors bearing a carboxylic group in the position 2 of the core.

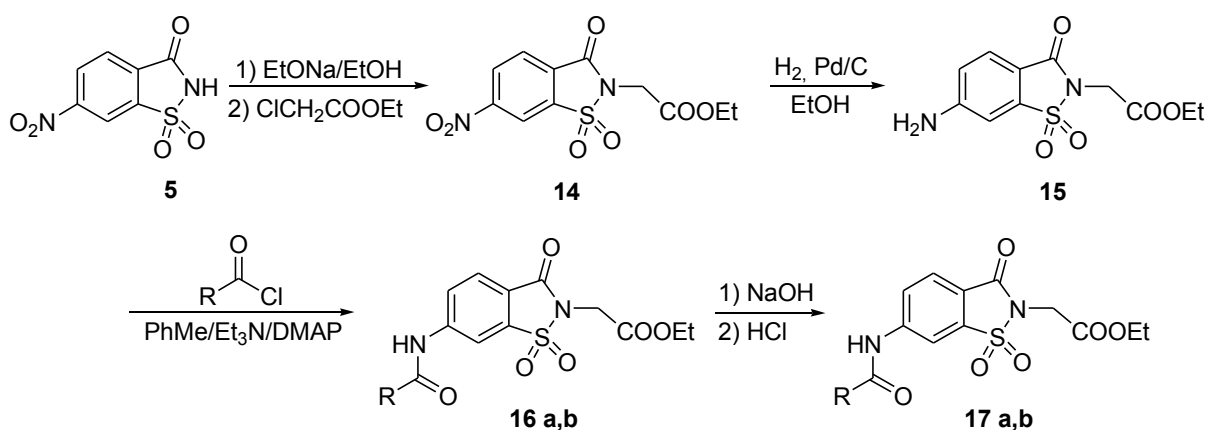


Scheme 3.5. Synthetic Pathway to obtain MMPI hits **13 a-c**.

Reaction started with the commercially available 1,2-benzisothiazol-1,1-dioxide-3(2*H*)-one, **11**, which was first converted to the corresponding sodium salt, through treatment with sodium ethoxide, than alkylated with the suitable α -esters, with a number of carbon atoms ranging from two to four, to give compounds **12 a-c**. Finally, the hydrolysis of the ester group, to achieve the target acids **13 a-c**, was performed with sodium hydroxide in methanol/water, followed by acidification with diluted hydrochloric acid.

Compounds substituted in both positions 2 and 6 of the benzisothiazole scaffold were synthesized as depicted in Scheme 3.6.

6-Nitro-1,2-benzisothiazol-1,1-dioxide-3(2*H*)-one, **5**, was converted to the corresponding sodium salt, then alkylated with ethyl bromoacetate to obtain the ester **14**. Catalytic hydrogenation of the nitro group afforded the amino derivative **15**, which gave the 6-substituted esters, **16 a,b**, by reaction with the suitable acyl chloride in the presence of triethyl amine and DMAP. Hydrolysis of the ester group, realized with sodium hydroxide in methanol/water, followed by acidification with diluted hydrochloric acid, gave the target MMPI hits **17 a,b**.



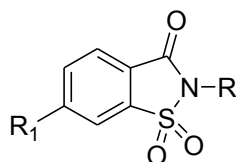
Scheme 3.6. Synthetic Pathway to obtain MMPI hits **17 a,b**.

All the novel hits were tested for their inhibitory activity and selectivity against specific MMPs, namely MMP-2, MMP-9 and MMP13. Assays were performed by the research group of Professor Armando Rossello, serving at our Faculty, exploiting a fluorescent method. Biological results are reported in Table 2 and expressed as IC₅₀.

All the synthesized compounds showed IC₅₀ values in the high micromolar range, thus turning out as novel and exploitable MMPIs hits.

Products **10 a-c**, characterized by the presence of the sulphonimido moiety as distinctive ZBG, showed the best inhibitory activity. On the contrary, the insertion of an additional carboxylic moiety, as in **13 a-c**, determined a reduction of efficacy, more marked for the propionic and the butyric residues.

Table 3.2. Inhibitory activity of MMPI hits **10 a-c**, **11**, **17 a,b** and **13 a-c**.



N	R	R1	IC ₅₀ (μM)		
			MMP-2	MMP-9	MMP-13
11	H	H	338	290	511
10a*	H	NHCOCH ₃	120	69	85
10b*	H	NHCOC ₆ H ₅	190	125	---
10c*	H	NHCOC ₆ H ₅ -4-OCH ₃	360	---	---

13a	CH ₂ COOH	H	190	250	230
13b	CH ₂ CH ₂ COOH	H	614	249	485
13c	CH ₂ CH ₂ CH ₂ COOH	H	545	274	443
17a*	CH ₂ COOH	NHCOPh	298	260	210
17b*	CH ₂ COOH	NHCOC ₆ H ₄ -4-Cl	280	195	422

* Previously synthesized by Sartini et al.

Values suggest that the only appreciable increase in activity is observable in compound *N*-acetylated with un-alkylated imidic position (**10a**).

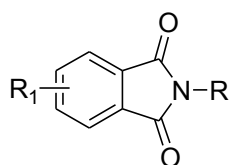
This has lead us to develop another series of compound with a very similar scaffold but without the solfonimidic function in order to evaluate the importance of the latter.

As a matter of fact phtalimide is closely related and the corresponding 5 and 6 nitro derivatives are commercially available.

The synthetic protocol used remained the same, no different conditions were used for the synthesis of the phtalimidic derivatives.

Isoindoline-1,3-dione Derivatives

Moving from the previously developed MMPiS, I planned to remove the sulphonimidic function, in order to evaluate its importance for a fruitful interaction with the enzymes' binding site. Accordingly, a number of isoindoline-1,3-dione derivatives were synthesized, summarized in Figure 3.7.

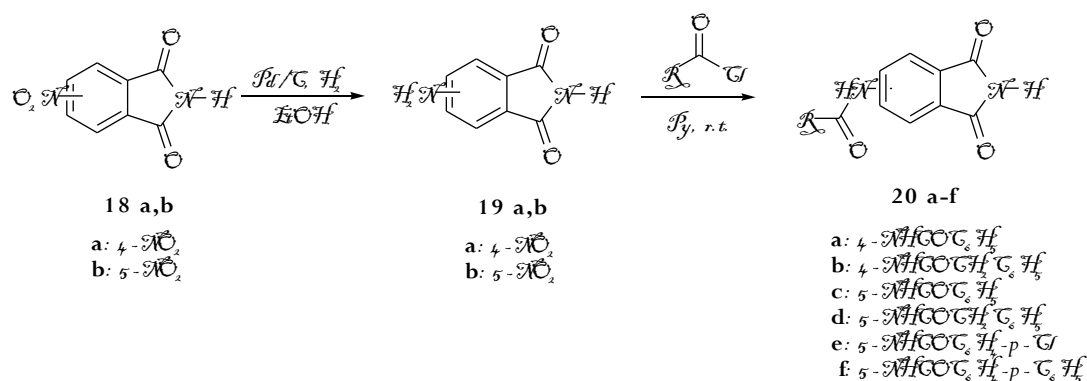


R: H, (CH₂)₃COOH
 R₁: NHCOC₆H₅, NHCOCH₂C₆H₅

Figure 3.7. General formula of isoindoline-1,3-dione MMPiS

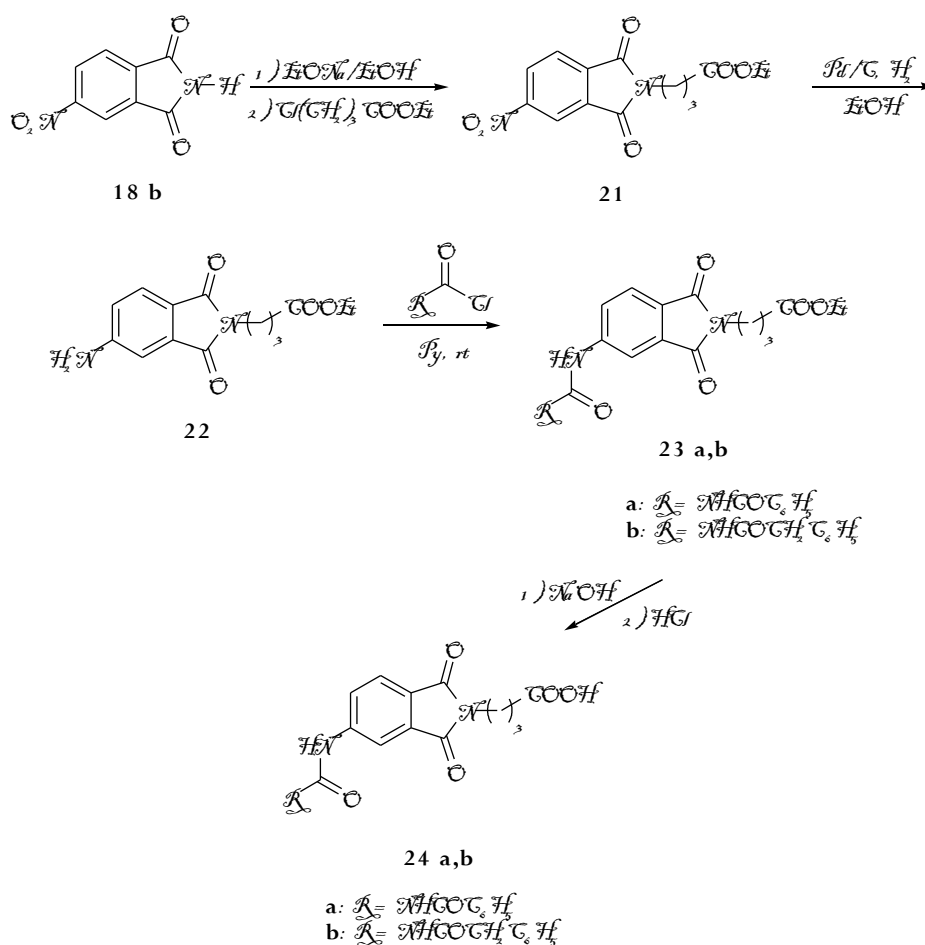
The novel compounds were easily synthesized from the commercially available 4- and 5-nitroisoindoline-1,3-diones, following the synthetic pathways reported in Schemes 1 and 2.

To obtain derivatives **20 a-d**, bearing an acyl amino substituent either in position 4 or in position 5 of the core, compounds **18 a,b** were first converted to the corresponding amino-isoindolines, **19 a,b**, by a catalytic hydrogenation performed in the presence of Palladium/Carbon as the catalyst, than treated with the suitable acyl chloride in pyridine (Scheme 3.8).⁷



Scheme 3.8. Synthetic Pathway to obtain MMPI hits **20 a-f**.

Inhibitors characterized by the presence of a carboxylic function, **24 a,b** were prepared as depicted in Scheme 3.9. The starting material, **18b**, was first alkylated to the corresponding ester, **21**, than reduced to the 5-amino derivative **22**. Reaction with the suitable acyl chloride, in pyridine⁷, gave the acylamino esters **23 a,b**, which were hydrolyzed to the desired inhibitors **24 a,b** through reaction with sodium hydroxide in methanol/water, followed by acidification with diluted hydrochloric acid.

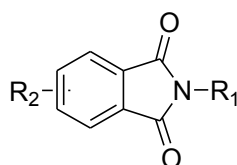


Scheme 3.9. Synthetic Pathway to obtain MMPI hits **24 a,b**.

All the novel compounds were tested for their ability to inhibit MMP-2, MMP-9 and MMP-13. Results obtained are reported in the following Table (Table 1), expressed as IC_{50} values. Similarly to what observed for the benzisothiazole derivatives, the insertion of a well-known ZBG on the heterocyclic core turned out detrimental for the biological efficacy, as compounds **24 a,b**, bearing a butyric chain, showed the lowest activity.

Otherwise, isoindolinone inhibitors showed an appreciable efficacy, more marked for compounds **20c** and **20f**, bearing respectively a benzoylamino and a 4-phenylbenzoylamino substituents in the position 5 of the heterocyclic core.

Table 3.3. Inhibitory activity of MMPI hits **20 a-f**, and **24 a,b**.



N	R ₁	R ₂	IC ₅₀ (□M)		
			MMP-2	MMP-9	MMP-13
20a	H	4-NHCOC ₆ H ₅	...	181	130
20b	H	4-NHCOCH ₂ C ₆ H ₅	232	120	181
20c	H	5-NHCOC ₆ H ₅	...	59	16
20d	H	5-NHCOCH ₂ C ₆ H ₅	>200
20e	H	5-NHCOC ₆ H ₄ -p-Cl	244	...	220
20f	H	5-NHCOC ₆ H ₄ -p-C ₆ H ₅	116	93	63
24a	CH ₂ CH ₂ CH ₂ COOH	5-NHCOC ₆ H ₅	450	590	620
24b	CH ₂ CH ₂ CH ₂ COOH	5-NHCOCH ₂ C ₆ H ₅	380	500	530

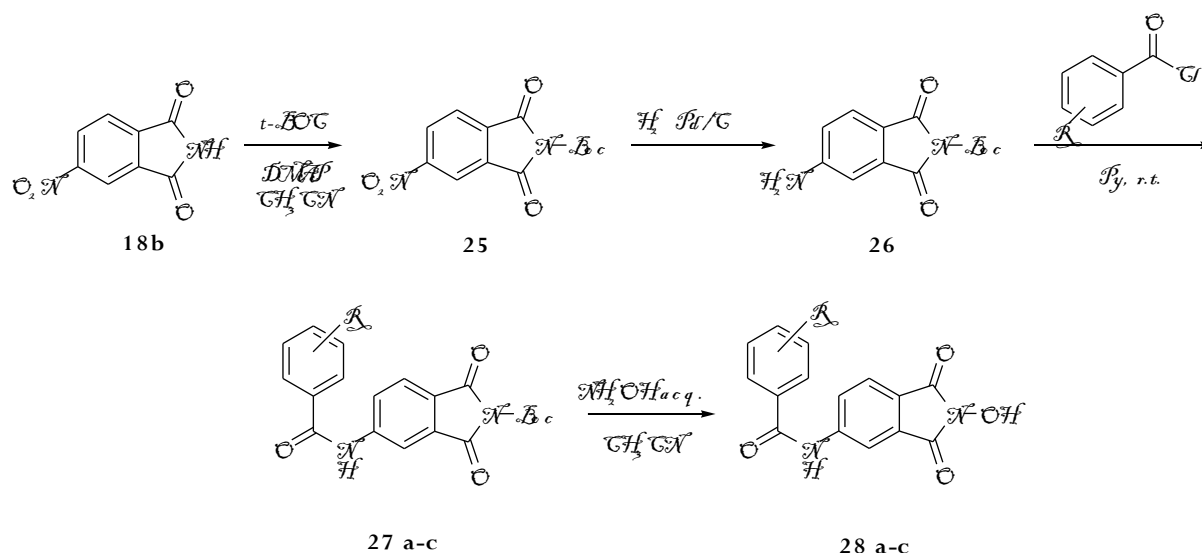
Going on with my studies on the isoindolinone derivatives, I considered the opportunity to substitute the imidic proton of the core with an hydroxy group.

The rational explanation consists in the well documented chelating capacity of a particular moiety extensively used for synthesis of MMPs inhibitor: hydroxamate. Numerous synthetic protocols are available in literature for the synthesis of these compounds, but a great disadvantage is the intrinsic toxicity due to the metabolic hydrolysis of hydroxamate as a matter small amount of hydroxylamine are liberated in-situ leading to unwanted dangerous side-effect.

An hydroxy moiety, bound to the imidic nitrogen, could be able to mime the chelating effects of an hydroxamate with the advantage of a major stability in a biological environment.

I developed a synthetic pathway which allowed to replace the imidic hydrogen with an hydroxy moiety, while the isoindolinone nucleus is conserved either for synthetic facilities or the better activities as the IC₅₀ values shown.

In the following Scheme (Scheme 3.10) the synthetic pathway for the manufacture of *N*-hydroxy phtalimides is depicted.



Scheme 3.10. Synthetic Pathway to obtain MMPI hits **28 a-c**.

Di *t*-butyldicarbonate was used for N protection of 5-nitroptalimide.⁸ Nitro group was catalytically reduced and consequently acylated with the corresponding acyl chloride.⁷ N-hydroxy group was introduced through treatment of **27 a-c** with a 50% hydroxylamine watery solution in acetonitrile.⁸ The biological efficacy of the novel synthesized compounds is reported in Table 3. Derivatives **28b** and **28c** showed appreciable inhibitory properties, above all against MMP-13.

Table 3.4. Inhibitory activity of MMPI hits **28 a-c**.

		IC ₅₀ (□M)		
N	R	MMP-2	MMP-9	MMP-13
28a	NHCOC ₆ H ₅	250
28b	NHCOC ₆ H ₄ -p-Cl	113	116	73
28c	NHCOC ₆ H ₄ -p-C ₆ H ₅	98	390	72

Thiazolidinedionic and thiohydantoinic core-based MMPs inhibitors:

Synthetic pathways, results and consideration.

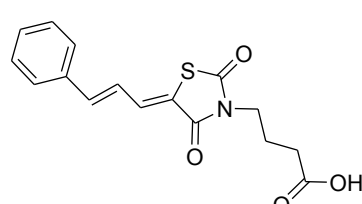
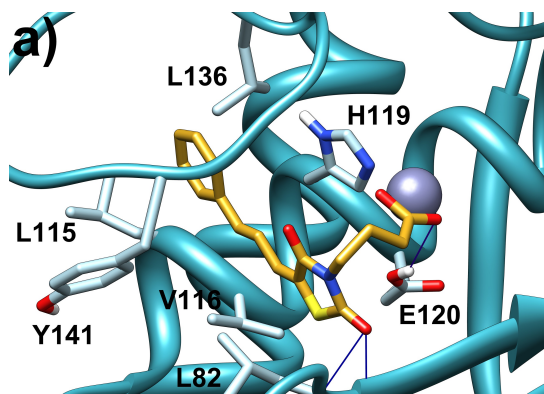
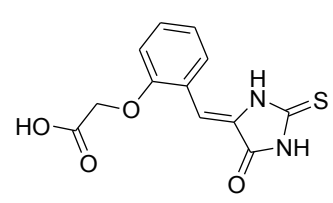
Compounds **29** and **30** respectively was promising lead compounds with a thiazolidinedionic and thiohydantoinic core advised from University of Napoli as zinc-chelating non-hydroxamate inhibitors of MMPs (Table 3.5).

The carboxylate moiety is directly linked to a thiazolidindione nucleus by a propyl-linker while in **2** an oxymethylene link the carboxylate group to a benzene. These compounds are characterized by a small number of rotatable bonds, indeed this rigidity allows the proper orientation of the ZBG for chelate the catalytic zinc ion and the adjustment of P1' group into the S1' pocket.

The thin olefinic chain ending with a phenyl ring gave to compound **1** a good selectivity on MMP-2.

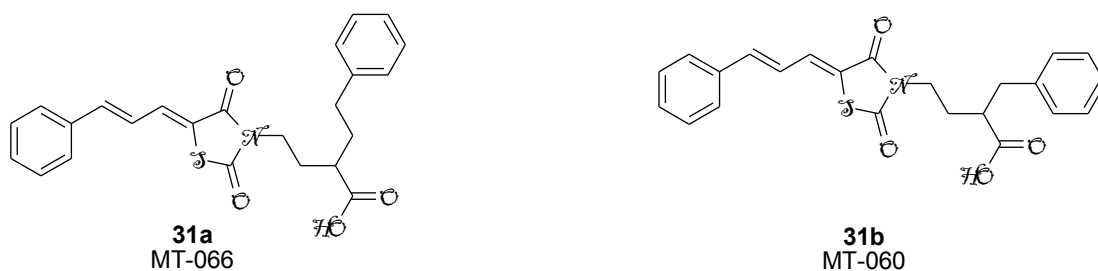
On computational chemists suggestions, some modification was necessary in order to increase efficacy of sudden compounds.

Table 3.5. Lead compounds from University of Napoli.

Chemical Structure	IC ₅₀ MMP-13 (μM)	
 a) 29	22	 a)
 b) 30	14	

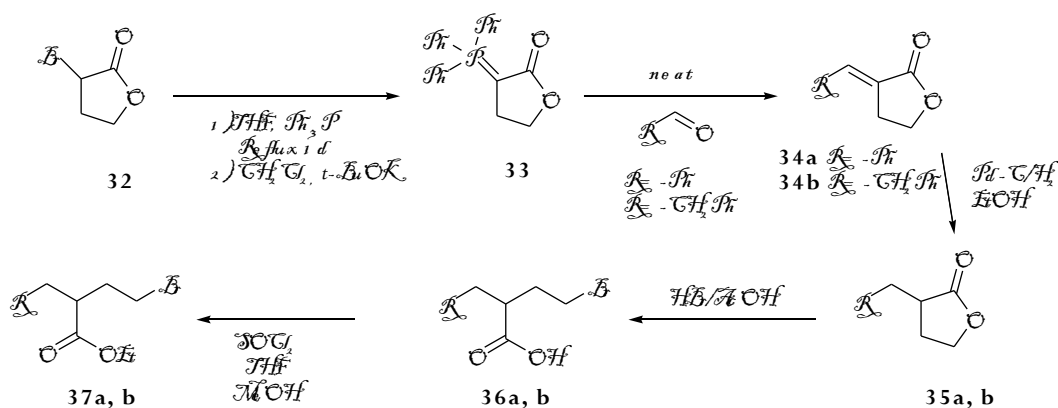
Modification on butyric acid chain of thiazolidinedionic compounds.

In the following scheme are depicted the variation on the α position of the butyric acid chain suggested from computational studies on lead compound 1 (Scheme 3.11).



Scheme 3.11. Compounds derived from lead molecule.

In scheme 3.12 the synthesis for the creation of the α substituted butyric acid is report:



Scheme 3.12. Synthesis of α - α -benzyl- α - α -bromo butyric acid.

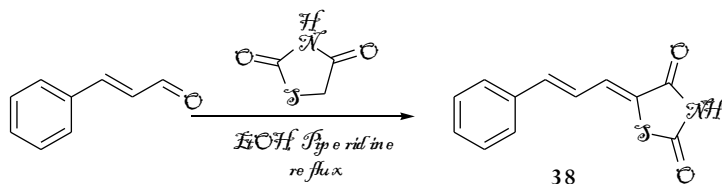
A Wittig reaction took place between phosphor ylide of butyrolactone **33**⁹ and benzaldehyde or phenyl acetaldehyde to obtain respectively **34a** or **34b** after flash chromatography purification.¹⁰

Catalytic reduction of insaturated compound is accomplished with Pd/C mediated hydrogenation, and the lactonic ring opening has been conducted with hydrobromic acid in glacial acetic acid.¹⁰

Esterification took place through the acyl chloride intermediate.

Then methyl α -benzyl- γ -bromo butyrate and Methyl α -phenylethyl- γ -bromo butyrate was obtained in a good overall yield.

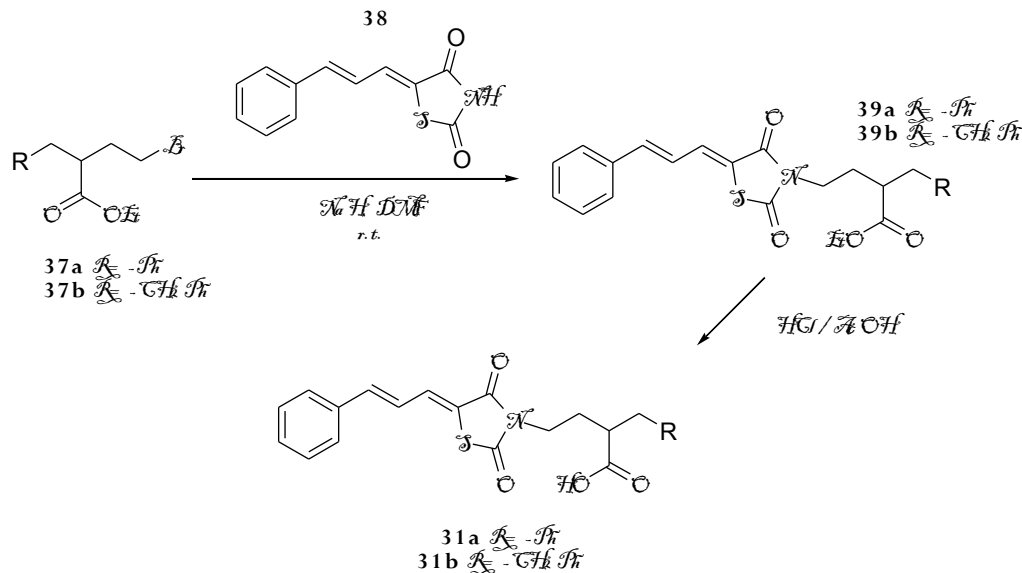
Then cinnamylidenthiazolidinedione core was synthesized through a Knoevenagel condensation refluxing thiazolidinedione and cinnamaldehyde in a mixture of acetic acid and sodium acetate to afford compound in **38** prevalently in *Z* form (Scheme 3.13).¹¹



Scheme 3.13. Cinnamylidenthiazolidinedione core.

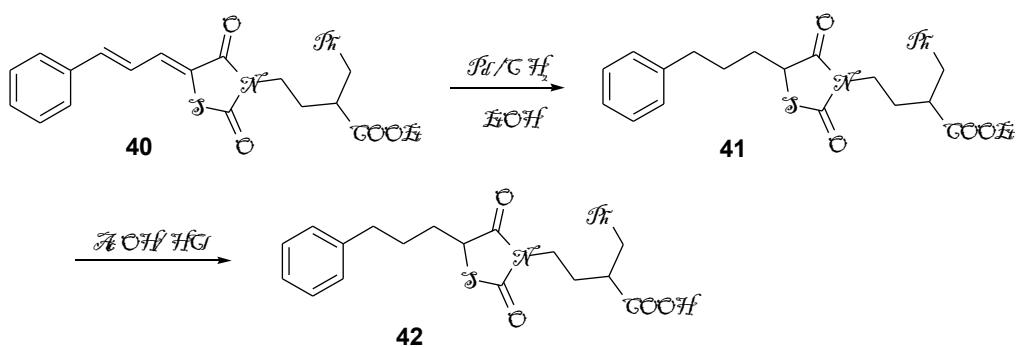
Sodium salt of sudden heterocyclic compound was obtained in DMF with the aim of sodium hydride, then after addition of ester **37a** or **37b** the mixture was left stirring at room temperature overnight. Compounds **39a** and **39b** were obtained in good yield and purified through flash chromatography.

Hydrolysis was achieved heating **39a** or **b** in a mixture of acetic and hydrochloric acid in a sealed tube.¹¹



Scheme 3.14. Synthesis of MT-060.

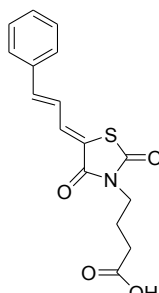
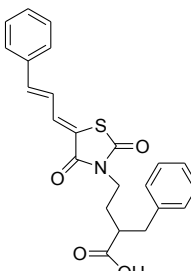
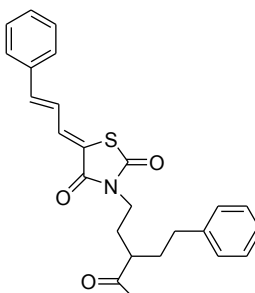
A saturated analogue was synthesized in order to compare inhibitory activity and evaluate the relevance of double bond in thiazolidinedionic compounds (scheme 3.15, compound **42**).

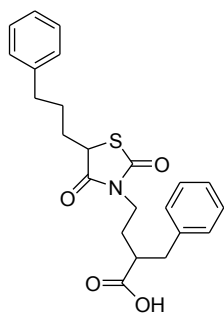


Scheme 3.15. Hydrogenated analogue **42**.

Inhibition activity are report in following the following table.

Table 3.6. IC₅₀ of the synthesized inhibitors.

Compd	IC ₅₀ (μM)					
	MMP-1	MMP-2	MMP-3	MMP-9	MMP-13	MMP-14
29						
	93±8	2.7±0.2	110±26	-	22±0.6	21±2
31a						
	50±6	3.6±0.4	35±3.6	8.3±0.9	15±1.2	17.8±1.9
31b						
	127±10	2.5±0.3	75±12	16±1.9	13±0.9	29±1.5
42	-	-	-	-	68±5.3	-



IC₅₀ values only slightly lower after this \square substitution and other designed analogues with chain elongation have been discharged, however, the difference in activity between hydrogenated compound **42** and other unsaturated inhibitors has led us to the consideration that a rigid carbon chain is necessary for increase in the activity.

However the IC₅₀ of **31a** and **31b** wasn't very good, so we have ask ourselves if activity of an enantiomer could be better than that of racemic mixture.

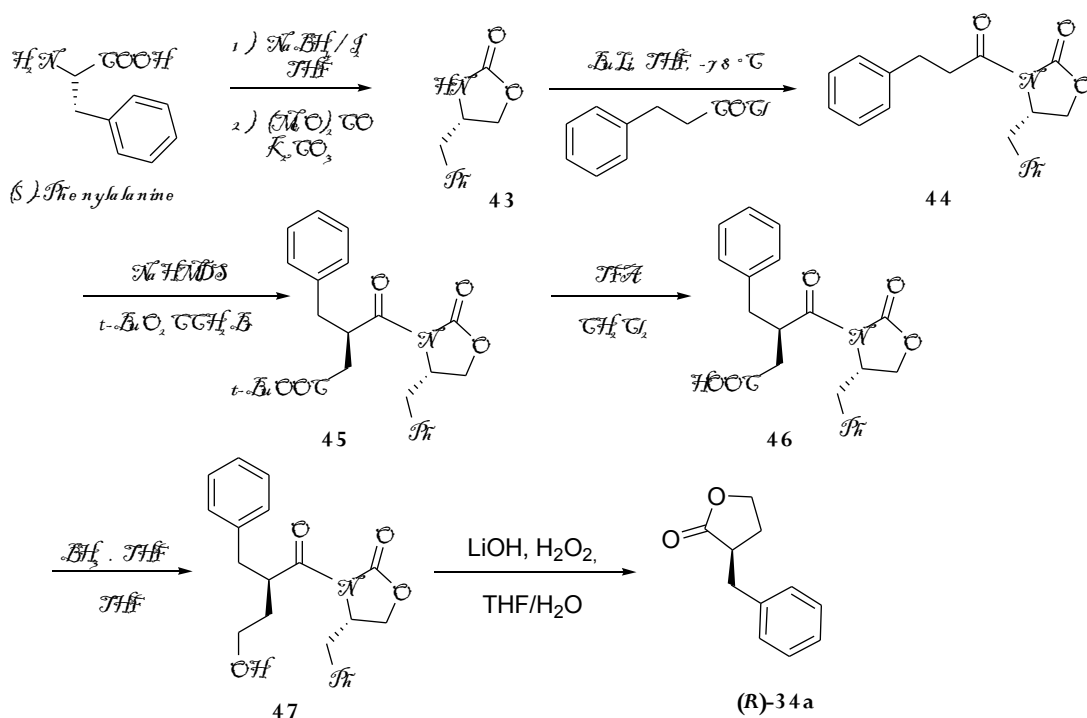
Literature report better IC₅₀ regard (*R*) enantiomer of some MMP inhibitors, so the presence of a chiral center on the butyric chain lead us to synthesize and to evaluate the IC₅₀ values of the two enantiomers.²

A stereoselective synthesis was developed for the obtainment of the optically active methyl \square -benzyl- \square -iodo butyrate.

We used the oxazolidinone derived from the corresponding (*S*) phenylalanine as optically active scaffold.¹² The alcohol obtained through a reduction with borane in THF was subsequently cyclised with dimethylcarbonate in basic conditions.¹³

The lithium salt of **43**, obtained by reaction of BuLi with oxazolidinone, was made reacted with hydrocinnamoyl chloride affording **44**. NaHMDS was used for the Claisen reaction between the optically active intermediate and *t*-Bu bromoacetate^{14, 15}, then **45** was hydrolyzed with TFA in CH₂Cl₂ and the carboxylic acid **46** was attempted to reduce with borane in THF.¹⁶

Unfortunately this last step afforded the alcohol **47** only in low yield, so the first approach resulted in a fail due to the low overall yield (Scheme 3.16).



Scheme 3.16. Theoretical synthetic plan for the obtention of **(R)-34a**

A different synthetic protocol was adopted.

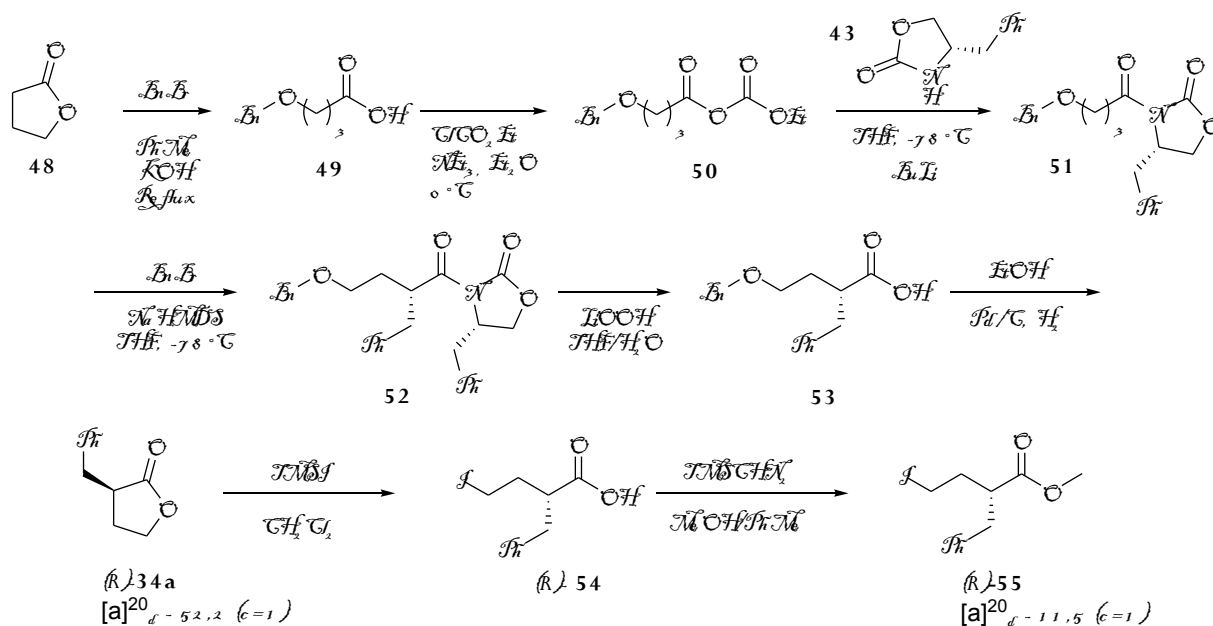
Acting through this pathway (scheme 3.17), was possible to achieve, in a reasonable overall yield, the optically active methyl γ -iodo- α -benzyl butyrate.

γ -benzyloxy butyric acid **49** was synthesized refluxing butyrolactone **48** in toluene with benzyl bromide and powdered potassium hydroxide. The carboxylic group of resulting acid was made reactive through the formation of a mixed anhydride with ethyl chloroformate (**50**).

Lithium salt of **43**, previously prepared from **43** and BuLi, was cannulated in the ethereal solution of **50** in order to obtain **51**.¹⁷

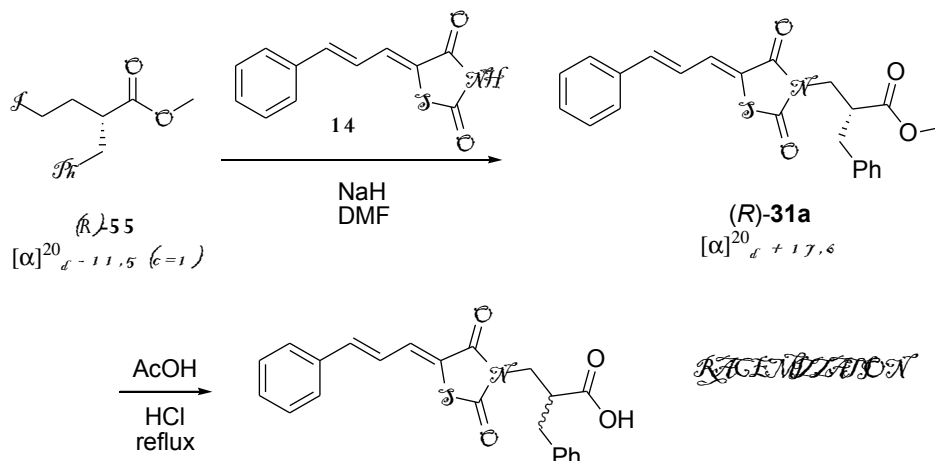
Claisen reaction between **51** and benzyl bromide in presence of NaHMDS afforded diastereoisomer **52**. Chiral oxazolidone was cleaved with lithium hydroxide and hydrogen peroxide¹⁷ and benzylic protection was removed through hydrogenolysis to afford the optically active lactone **(R)-34a**.

Lactone ring opening was made with trimethylsilyl iodide and the iodo carboxylic acid **(R)-54** was esterified almost immediately with trimethylsilyl diazomethane and purified through flash chromatography (scheme 3.17).¹⁸



Scheme 3.17. Synthetic pathway for (R)-55.

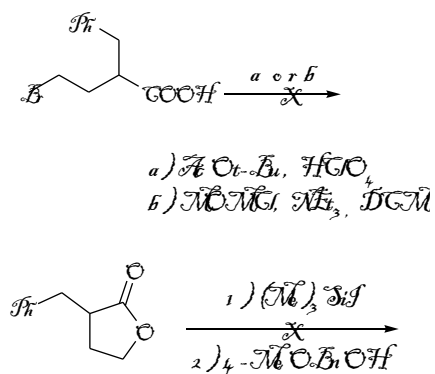
Manufacture of optically active ester (R)-31a followed the same synthetic pathway as for the racemic one, but the use of boiling acidic mixture led to a drop in optical activity of the resulting acid (Scheme 3.18).¹¹



Scheme 3.18. Acidic cleavage of ester led to racemisation.

A mild hydrolysis for the removal of the methyl ester was object of an intense research, so we've looking for a protecting group more easily removable.

In the following scheme, tried protecting groups are depicted.

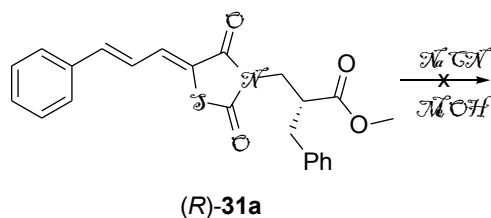


Scheme 3.19. Attempts for protection using **36a** and **35a**.

Methoxymethylene chloride was used for esterification of small amount of racemic acid in dry dichloromethane with poor results. A contemporary ring opening of lactone with trimethylsilyl iodide in DCM and esterification with 4-methoxybenzylic alcohol was attempted¹⁸, resulting in an unstable ester which underwent to lactonization. Same problem occurred with the introduction of a *t*-Bu using AcOt-*t*-Bu and perchloric acid.¹⁹

Despite the attempts, no one of the protections used afforded a stable ester.

Basic hydrolysis wasn't tolerated by thiazolidinedionic ring which undergo to decomposition, then a cleavage with NaCN in try methanol was tried with no results.

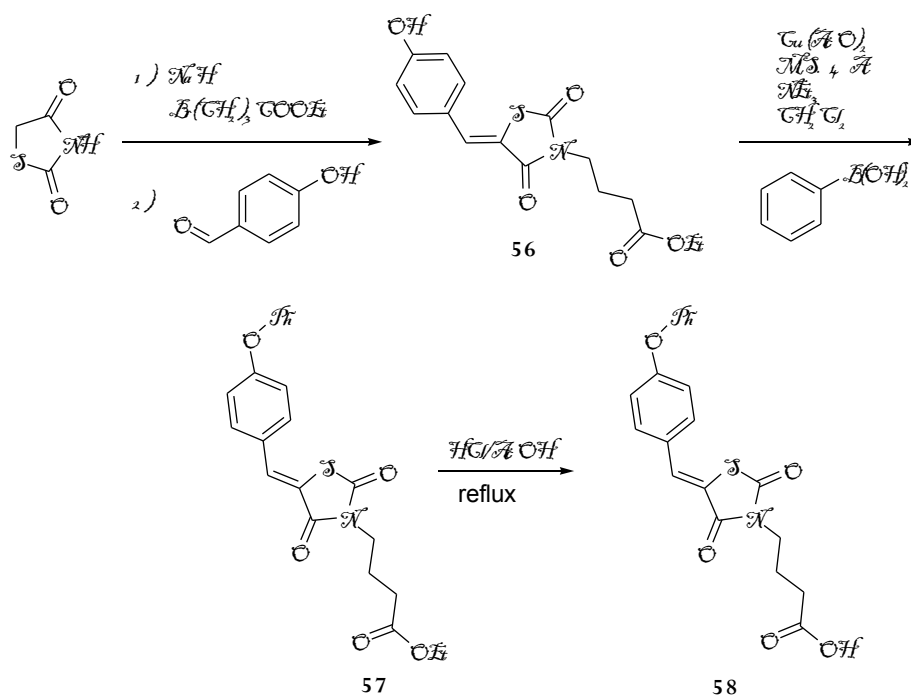


Scheme 3.20. No conversion with mild basic hydrolysis.

Modification on arylalkylidene portion.

Further modifications was made on the thiazolidinedionic lead **29** following computational chemists advice in order to increase the potency of inhibition and the selectivity over MMPs.

The cinnamylidene chain of the lead compound **29**, was substituted with a benzylidene one carrying, in para position, a substituted phenoxy moiety.



Scheme 3.21. Synthesis of compound **58**.

The designed synthesis was developed in order to obtain a library of compounds even if the activity of compound **58** led us to abandoned this scaffold.

After some attempts, we started from *N*-alkylated thiazolidinedione with butyric chain.

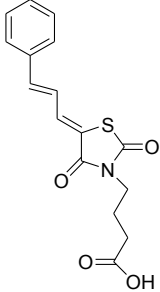
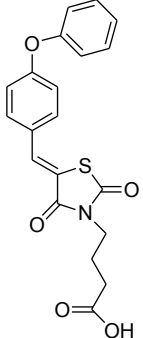
Then Knoevenagel condensation between 4-hydroxybenzaldehyde and alkylated thiazolidinedione led prevalently to the *E* form of compound **56**.²⁰

Compound **56** was the starting material for the developmental of a library due to the phenolic group easily etherifiable using the appropriate boronic acid through an Ullmann-like reaction.²¹

Basic hydrolysis was avoided due to side-reactions and consequent destruction of molecule. For this reason, acidic conditions are a “must” for thiazolidinedionic derivatives.

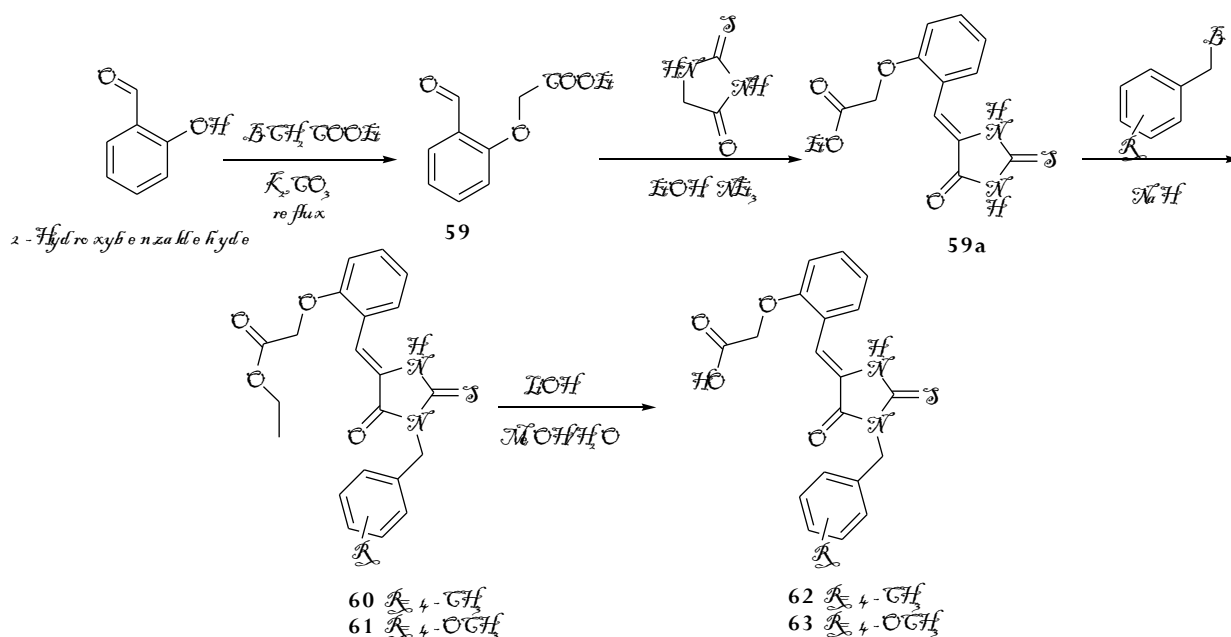
A comparison in the activity between lead and compound **58** is report in table 3.7.

Table 3.7 Comparison of the inhibitory activity of lead compound **29** versus **58**.

Compd	IC ₅₀ (μM)					
	MMP-1	MMP-2	MMP-3	MMP-9	MMP-13	MMP-14
29 	93±8	2.7±0.2	110±26	-	22±0.6	21±2
58 		18±1.7			20±2.6	

Synthesis of thiohydantoinic derivatives.

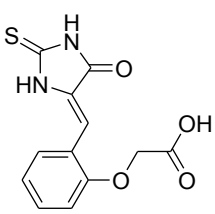
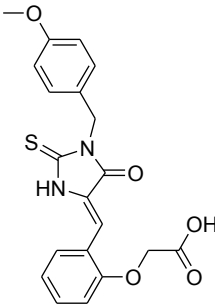
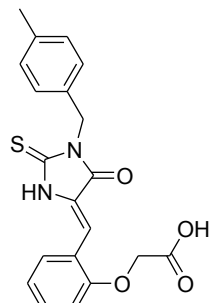
Regarding optimization of lead **30** (depicted in Table 3.5), an *N*-alkylation on the thiohydantoinic ring with a benzylic substituent was theorized as a good choice for raise inhibitory activity from computational chemists, then a synthetic plan was developed (scheme 3.21)



Scheme 3.22 Synthetic pathway for the manufacture of inhibitors **62** and **63**.

59 was obtained through condensation between salicylaldehyde and thiohydantoin in aqueous ethanol, in presence of triethylamine. Alkylation of the phenolic hydroxyl with ethyl bromoacetate gave compound **60**.^{22, 23} *N*-alkylation with substituted benzyl halide afforded compounds **61** or **62**. Hydrolysis has been carried out with lithium hydroxide using a mixture of methanol and water as solvent. Acidification with 1N hydrochloric acid, afforded the free carboxylic acid. However, the negative IC_{50} values, (table 3.8), led us to discard this kind of molecules.

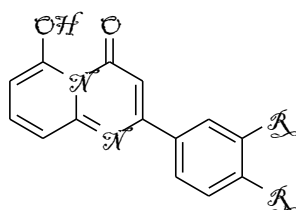
Table 3.8 IC₅₀ of compounds **62** and **63**.

Molecule	IC ₅₀ MMP-13 (μ M)
 30	67
 63	97 \pm 9.5
 62	27 \pm 3.5

Pyridopyrimidinone derivatives.

Synthesis and activity.

Sartini et al. in 2007 developed a pyridopyrimidinone scaffold based aldose reductase inhibitor with good activity.²⁴



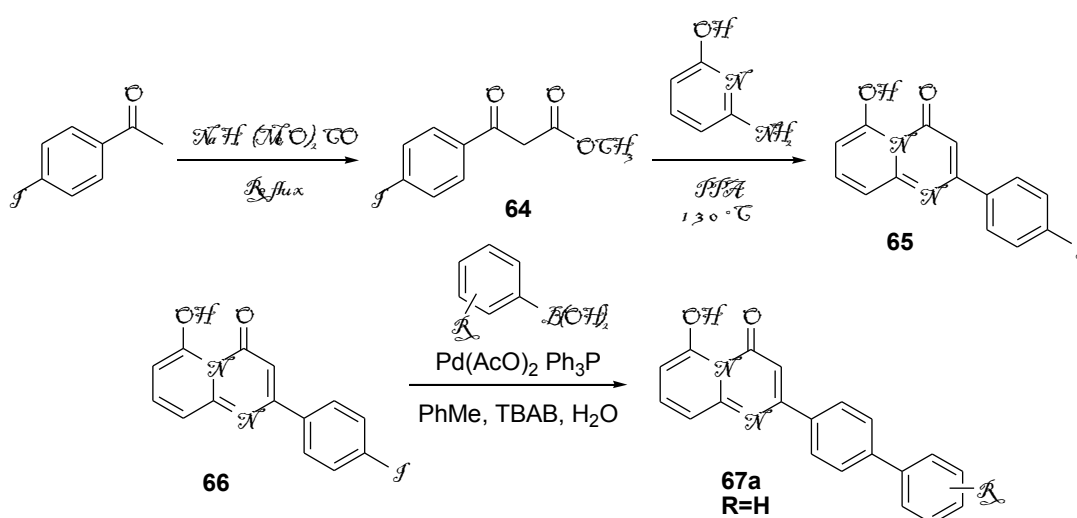
Scheme 3.23. General formula of Sartini's anti-oxidants.

The particular structure of pyridopyrimidinone similar to that of some pyrone-based inhibitors led us to explore the chelating properties of pyridopyrimidinone scaffold as zinc chelating agent.

A longer phenyl chain was advised for a better interaction with the lipophilic pocket S1' of target MMPs.²⁵

A synthesis for elongation of aromatic chain was elaborated (scheme 3.23). Claisen reaction between 4'-iodoacetophenone and dimethyl carbonate afforded the corresponding methyl oxopropanoate **64**. Heating **64** with 2-amino-6-hydroxy pyridine and polyphosphoric acid afforded pyridopyrimidinone **65** which was purified through flash chromatography.

A Suzuki reaction took place between **65** and substituted phenyl boronic acid. The product was recrystallized from a large amount of boiling AcOEt.



Scheme 3.24. Synthetic pathway for the manufacture of pyridopyrimidinone **67**.

Resulting products was very hard to purified. Only the biphenyl derivative was obtained (R=H). It was tested on MMP-13 and the resulting value of $42 \pm 3.6 \mu\text{M}$ led us to discontinue the synthesis of this kind of compounds.

Bibliography

1. MacPherson, L. J.; Bayburt, E. K.; Capparelli, M. P.; Carroll, B. J.; Goldstein, R.; Justice, M. R.; Zhu, L.; Hu, S.; Melton, R. A.; Fryer, L.; Goldberg, R. L.; Doughty, J. R.; Spirito, S.; Blancuzzi, V.; Wilson, D.; O'Byrne, E. M.; Ganu, V.; Parker, D. T. Discovery of CGS 27023A, a non-peptidic, potent, and orally active stromelysin inhibitor that blocks cartilage degradation in rabbits. *J. Med. Chem.*, **1997**, *40*, 2525-2532.
2. Tuccinardi, T.; Martinelli, A.; Nuti, E.; Carelli, P.; Balzano, F.; Uccello-Barretta, G.; Murphy, G.; Rossello, A. Amber force field implementation, molecular modelling study, synthesis and MMP-1/MMP-2 inhibition profile of (R)- and (S)-N-hydroxy-2-(N-isopropoxybiphenyl-4-ylsulfonamido)-3-methylbutanamides. *Bioorg. Med. Chem.*, **2006**, *14*, 4260-4276.
3. Wada, C. K.; Holms, J. H.; Curtin, M. L.; Dai, Y.; Florjancic, A. S.; Garland, R. B.; Guo, Y.; Heyman, H. R.; Stacey, J. R.; Steinman, D. H.; Albert, D. H.; Bouska, J. J.; Elmore, I. N.; Goodfellow, C. L.; Marcotte, P. A.; Tapang, P.; Morgan, D. W.; Michaelides, M. R.; Davidsen, S. K. Phenoxyphenyl sulfone N-formylhydroxylamines (retrohydroxamates) as potent, selective, orally bioavailable matrix metalloproteinase inhibitors. *J. Med. Chem.*, **2002**, *45*, 219-232.
4. Kiyama, R.; Tamura, Y.; Watanabe, F.; Homology Modeling of Gelatinase Catalytic Domains and Docking Simulations of Novel Sulfonamide Inhibitors *J. Med. Chem.* **1999**, *42*, 1723-1738.
5. Tamura, Y.; Watanabe, F.; Nakatani, T.; Yasui, K.; Fuji, M.; Komurasaki, T.; Tsuzuki, H.; Maekawa, R.; Yoshioka, T.; Kawada, K.; Sugita, K.; Ohtani, M. Highly selective and orally active inhibitors of type IV collagenase (MMP-9 and MMP-2): N-sulfonylamino acid derivatives. *J. Med. Chem.* **1998**, *41*, 640-649.
6. Rose, N. C. 6-Nitrosaccharin. *J. Heterocyclic Chem.* **1969**, *6*, 745-746.
7. Goetz, F. J., Hirsch, J. A., Augustine R. L.; Ring-Chain Tautomerism in Anions Derived from Substituted (Arylideneamino)toluenes and (Arylideneamino)oxindoles; *J. Org. Chem.*, **1983**, *48*, 2468-2472.

8. Einhorn, C.; Einhorn, J.; Marcadal-Abbadia C.; *Synthetic Communications* **2001**, *31*, 741-748.
9. S. Fliszár, R. F. Hudson and G. Salvadori *Helvetica chimica acta*, **1963**, *7*, 1580-1589.
10. Alonso A. et al. Preparation of carboxybenzylalkanoates as stimulators of soluble guanylate cyclase. **2001** DE 19943636 A1 20010315.
11. Bruno G.; Costantino L.; Curinga L.; Maccari R.; Monforte F.; Nicolò F. et al. Synthesis and aldose reductase inhibitory activity of 5-Arylidene-2,4-thiazolidinediones. *Bioorganic & Medicinal Chemistry*. **2002**, *10*, 1077-1084.
12. Hvidt, T.; Szarek, W. A.; Maclean, D. B.; Synthesis of enantiomerically pure β -amino- α -methylene- γ -butyrolactones by way of ozonolysis of aromatic α -amino acids, *Canadian Journal of Chemistry*, **1988**, *66* 779-782.
13. Gage, J. R.; Evans, D. A.; (S)-4-Phenylmethyl-2-oxazolidone *Organic Syntheses*, **1990**, *68*, 77.
14. Edmonds, M.K.; Abell, A.D.; Design and Synthesis of a Conformationally Restricted Trans Peptide Isostere Based on the Bioactive Conformations of Saquinavir and Nelfinavir *J. Org. Chemistry* **2001**, *66*, 3747-3752.
15. David A. Evans, Leester D. Wu, John J. M. Wiener, Jeffrey S. Johnson, David H. B. Ripin, and Jason S. Tedrow A General Method for the Synthesis of Enantiomerically Pure α -Substituted, β -Amino Acids through α -Substituted Succinic Acid Derivatives *J. Org. Chem.* **1999**, *64*, 6411-6417.
16. Pandya, B.A.; Dandapani, S.; Duvall, J. R.; Rowley, A.; Mulrooney, C., A.; Practical asymmetric synthesis of β -hydroxy γ -amino acids via complimentary aldol reactions *Tetrahedron* **2011** *67* 6131-6137
17. Lafontaine, J. A.; Provencal, D. P.; Gardelli, C.; Leahy, J. W.; The Enantioselective Total Synthesis of the Antitumor Macrolide Rhizoxin D (Supp. Info). *J. Org. Chem.* **2003**, *68*, 4215-4234.

18. Kolba, M.; Bartha, J.; A Convenient Preparation of Iodoalkyl Esters from Lactones *Synthetic Communications* **1981**, *11*, 763- 767.
19. Chen, H.; The total synthesis and reassignment of stereochemistry of dragonamide. *Tetrahedron* **2005** *61* 11132–11140.
20. Sepehr, S; Subrumanian, M.; Rhodanine derivatives as PPAR receptor modulators and their preparation, pharmaceutical compositions and use for treatment and prophylaxis of various diseases. WO **2006/041921** A2
21. Nuti, E.; Panelli, L.; Casalini, F.; Avramova, S., I.; Orlandini, E.; Santamaria, S.; Nencetti, S.; Tuccinardi, T.; Martinelli, A.; Design, Synthesis, Biological Evaluation, and NMR Studies of a New Series of Arylsulfones As Selective and Potent Matrix Metalloproteinase-12 Inhibitors *J.f Med. Chem.* **2009**, *52*, 6347-6361.
22. Mubammad A. et all. *J. Chem. Soc.: Perkin Trans.* (2) **2002**, pag 1662-1668
23. Garst, M., E.; Dolby, L, J.; Esdandiari, S.; Avey, A., A.; MacKenzie, V., R.; Muchmore, D., C.; Process for the synthesis of imidazole-2-thiones via thiohydantoin US **2007/0203344** A1.
24. La Motta, C; Sartini, S.; Mugnaini, L.; Simorini, F.; Taliani, S.; Salerno, S.; Marini, A., M.; Da Settimo, F.; Lavecchia, A.; Pyrido[1,2-a]pyrimidin-4-one Derivatives as a Novel Class of Selective Aldose Reductase Inhibitors Exhibiting Antioxidant Activity *J. Med. Chem.* **2007**, *50*, 4917-4927.
25. Agrawal, A.; Romero-Perez, D.; Zinc-Binding Groups Modulate Selective Inhibition of MMPs. *ChemMedChem* **2008**, *3*, 812 – 820.

CHAPTER 4

Experimental Section

General

Commercially available chemicals were purchased from SigmaAldrich or Alfa Aesar and used without further purification, NMR spectra were obtained with a Varian Gemini 200 MHz spectrometer. Chemical shifts (δ) are reported in parts per million downfield from tetramethylsilane and referenced from solvent references. Melting points were measured with a Kofler apparatus. Chromatographic separations were performed on silica gel columns by flash (Kieselgel 40, 0.040e0.063 mm; Merck) or gravity column (Kieselgel 60, 0.063e0.200 mm; Merck) chromatography. Reactions were followed by thin-layer chromatography (TLC) on Merck aluminium silica gel (60 F254) sheets that were visualized under a UV lamp.

Evaporation was performed in vacuo (rotating evaporator).

Scheme 3.8, 3.9

General procedure for the N alkylation of either saccharines and phtalimides.

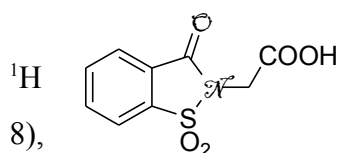
50 mmol of either saccharines or phtalimides were dissolved in 150 ml of absolute ethanol. An equimolar amount of fresh sodium metallic was allowed to react in 150 ml of absolute ethanol and once dissolved, resulting sodium ethoxide solution was added to the saccharine or phtalimide solution.

A precipitate formed, and after stirred for one hour, the solvent was removed under reduced pressure. The remaining solid consist in the sodium salt of the corresponding heterocycle was pure enough for successive steps.

Phthalimidic or saccarinic sodium salt (10 mmol) was dissolved in 5 ml of dry DMF, and an equimolar amount of bromoalkanoic ester was added. The reaction mixture was stirred and heat to reflux and allowed to react.

After completion (generally at least 3 hours), the mixture was cooled to room temperature and all the volatile materials were removed under vacuum. The residue was dissolved in CH_2Cl_2 and washed with water. The CH_2Cl_2 was evaporated under vacuum, and the residue was purified by recrystallization.

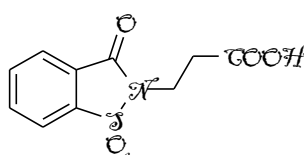
The pure ester was hydrolyzed with the aim of NaOH (1.5 eq, 1.5 mmol, 59 mg) in 20 ml of a 2:1 MeOH/ Water mixture. The solvent was removed under vacuo and the residue was dissolved in water. Acidification of the solution with HCl 1N afforded a precipitate which was filtered and crystallized from methanol.



Melting Point 212-215°C

13a. N-acetylsaccharin.

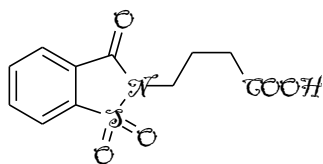
NMR 12.48 (DMSO-*d*₆) (s, 1H, -COOH), 8.32 – 8.28 (d, 1H, ArH, J = 8.14- 8.00 (m, 3H, ArH), 4.01 (s, 1H, -CH₂COOH).



Melting Point 164-165°C

13b. N-propionylsaccharin.

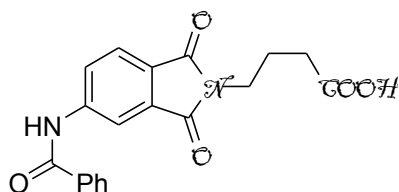
¹HNMR (DMSO-*d*₆) 12.41 (s, 1H, -COOH), 8.33 – 8.29 (d, 1H, ArH, J = 8), 8.14- 8.00 (m, 3H, ArH), 3.99 – 3.92 (t, 2H, J_{min} = 6 J_{max} = 14, -CH₂CH₂COOH), 2.77 – 2.70 (t, 2H, -CH₂COOH).



Melting Point 117-118°C

13c. N-butyrylsaccharin.

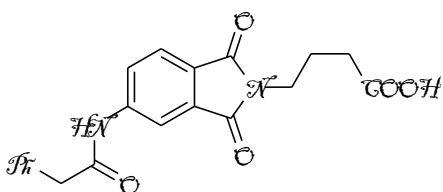
¹HNMR (DMSO-*d*₆) 12.41 (s, 1H, -COOH), 8.33 – 8.29 (d, 1H, ArH, J = 8), 8.14- 8.00 (m, 3H, ArH), 3.99 – 3.92 (t, 2H, J_{min} = 6 J_{max} = 14, -CH₂CH₂COOH), 2.77 – 2.70 (t, 2H, -CH₂COOH), 1.92 – 1.99 (q, -CH₂CH₂CH₂COOH).



^{max} =14, -CH₂COOH), 1.83–1.77 (q, 2H, -CH₂CH₂CH₂COOH).

23a. N-butyrylphtalimide-5-benzamide.

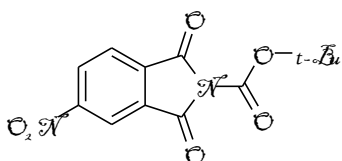
¹HNMR (DMSO-*d*₆) 12.48 (s, 1H, -COOH), 10.44 (s, 1H, -NH-), 8.20 (s, 1H, ArH), 8.00 – 7.53 (m, 7H, ArH), 3.55 -3.48 (t, 2H, J_{min} = 6, J_{max} = 14, -CH₂CH₂COOH), 2.34 – 2.27 (t, 2H, J_{min} =8, J



23b. N-butyrylphtalimide-5-phenylacetamide.

¹HNMR (DMSO-*d*₆) 12.48 (s, 1H, -COOH), 10.44 (s, 1H, -NH-), 8.20 (s, 1H, ArH), 8.01 – 7.53 (m, 7H, ArH), 3.67 (s, 1H, -COCH₂Ph), 3.56 -3.49 (t, 2H, J_{min} = 6, J_{max} = 14,

$-\text{CH}_2\text{CH}_2\text{COOH}$), 2.36 – 2.29 (t, 2H, $J_{\text{min}} = 8$, $J_{\text{max}} = 14$, $-\text{CH}_2\text{COOH}$), 1.83–1.77 (q, 2H, $-\text{CH}_2\text{CH}_2\text{CH}_2\text{COOH}$).



18b. N-Boc-5-nitroftalimide. To a magnetical stirred suspension of 4-nitroftalimide (1,92 g, 10,0 mmol) in 5 ml of anhydrous acetonitrile in a three necked round bottomed flask, flame-dried and purged with nitrogen, is added di-*t*-butylbcarbonate (2.29 g, 10.5 mmol) and a catalytical amount of DMAP (2 mol%, 24 mg).

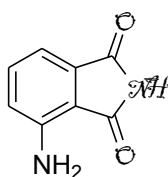
A carbon dioxide evolution occur.

After 4 h, the reaction is end. The solvent is evaporated under r.p. and the residue is crystallized dissolving it in the minimum amount of AcOEt and crashing the solubility with P.E. 60-80°C.

The obtained crystals are filtered on a Buchner funnel, washed with fresh P.E. and dried.¹

Yield 96%

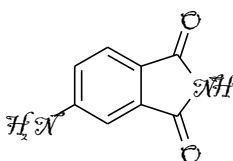
¹HNMR (CDCl₃) 8.77 (s, 1H, ArH), 8.71 – 8.67 (d, 1H, $J = 8$ Hz, ArH), 8.19 – 8.15 (d, 1H, $J = 8$ Hz, ArH), 1.66 (s, 9H, $-\text{C}(\text{CH}_3)_3$).



19a. 4-aminoisindoline-1,3-dione.

Same procedure used for **26**.

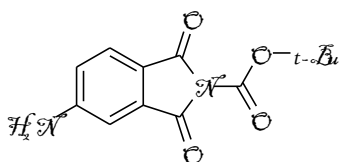
¹HNMR (DMSO-*d*₆) 10.68 (s, 1H, NH), 8.49 – 8.45 (d, 1H, ArH), 7.77 – 7.69 (t, 1H, ArH), 7.48 – 7.45 (d, 1H, ArH), 6,34 (s, 2H, $-\text{NH}_2$).



19b. 5-aminoisindoline-1,3-dione.

Same procedure used for **26**.

¹HNMR (DMSO-*d*₆) 10.71 (s, 1H, NH), 7.44- 7.40 (d, 1H, $J = 8$) 6.84 – 6.75 (t, 2H), 6,39 (s, 2H, $-\text{NH}_2$).



26. N-Boc-5-aminophthalimide. A flame-dried 500 ml round bottomed flask is charged with 4-nitroftalimide (x g), 150 ml absolute ethanol and Pd/C (5mol%).

After consumption of starting material (TLC, overnight), the mixture is filtered on celite and the filtrate concentrated at r.p.

The yellow flakes product were pure enough for successive steps.

Yield Quantitative

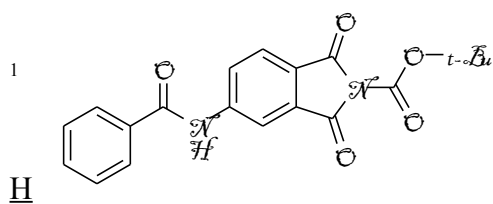
¹HNMR (CDCl₃) 7,57-6,86 (m, 3H, ArH), 6,68 (s, 2H, $-\text{NH}_2$), 1,51 (s, 9H, $-\text{C}(\text{CH}_3)_3$)

Melting Point 290-295°C

General procedure for the amide formation.

A solution of 100 mg (0.010 mol) of **19a**, **19b** or **26** in 1.9 mL of anhydrous pyridine (5 ml/ mmol) was cooled to 0 °C under nitrogen, and 1.1 eq. of the corresponding acyl chloride was added with stirring.

After 24 h at room temperature under nitrogen, the mixture was concentrated, and 1 mL of absolute methanol was added. The resulting mixture was poured into 10 ml of a stirred solution of 5:5 ml of water/glacial acetic acid. Separated solid was recrystallized from 95% ethanol and then recrystallized from absolute methanol to give the title compounds.²

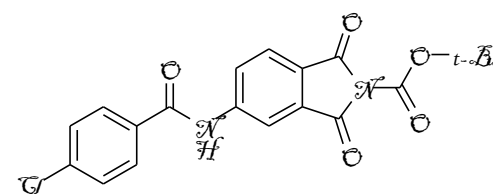


27a. *N*-Boc-5-(phenylbenzamido)phtalimide.

HNMR (CDCl₃) 10.78 (s, 1H, -NH), 8.31 (s, 1H, C-H), 8.13 – 8.09 (d, 1H, J= 8, C-H), 7.97 – 7.93 (d, 2H, J= 8, C-H), 7.84 – 7.78 (dd, 1H, J_{min} = 2.9, J_{max} = 8.2), 7.58 (m, 3H, ArH). ¹³CNMR (CDCl₃)170.03, 168.12, 164.11, 135.72, 135.02, 132.61, 132.21, 128.44, 126.49, 124.24, 117.91, 117.39, 80.92, 27.83.

Yield 89%

Melting Point >300°C

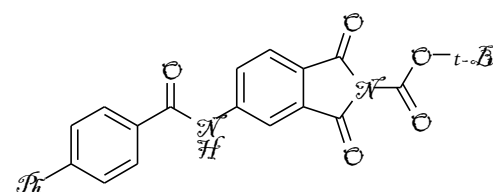


27b. *N*-Boc-5-(4-chlorobenzamido)phtalimide.

Yield 76%

¹H NMR (CDCl₃) 8.27-7.50 (m, 8H) 1.60 (s, 9H, -C(CH₃)₃) ¹³CNMR (CDCl₃) 164.42, 163.25, 155.22, 144.06, 136.29, 132.04, 129.39, 129.26, 127.84, 123.76, 123.33, 122.18, 113.47, 81.54, 27.98.

Melting Point > 300°C



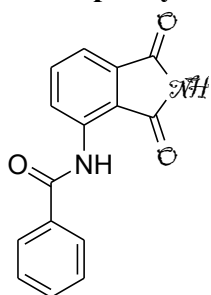
27c. *N*-Boc-5-(4-phenylbenzamido)phtalimide.

Yield 63%

^1H NMR (CDCl_3) 8.28-7.43 (m, 13H C-H), 1.64 (s, 9H $-\text{CCH}_3$) ^{13}C NMR (CDCl_3) 170.05, 168.15, 164.12, 135.75, 135.00, 132.61, 132.21, 129.51 128.44, 128.01, 126.49, 124.20, 117.81, 117.34, 80.88, 27.83.

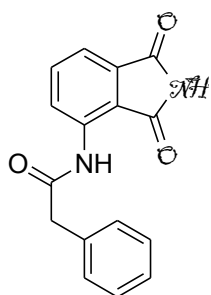
Melting Point $>300^\circ\text{C}$

20a. 3-phenylbenzamidophthalimide.



^1H NMR ($\text{DMSO}-d_6$) 11.50 (s, 1H, NH), 10.37 (s, 1H, ammidic NH), 8.72 – 8.68 (d, 1H, ArH), 7.77 – 7.69 (t, 1H,), 7.51 – 7.48 (d, 1H, $J = 6$), 7.42 – 7.34 (m, 5H, ArH). ^{13}C NMR ($\text{DMSO}-d_6$) 170.14, 168.03, 164.17, 135.82, 135.22, 132.68, 131.99, 128.44, 126.49, 124.24, 117.99, 117.39.

Melting Point 285 – 289 $^\circ\text{C}$



20b. 4-phenylacetamidophthalimide.

^1H NMR ($\text{DMSO}-d_6$) 11.37 (s, 1H, NH), 9.73 (s, 1H, ammidic NH), 8.49 – 8.45 (d, 1H, ArH), 7.77 – 7.69 (t, 1H,), 7.48 – 7.45 (d, 1H,), 7.38 – 7.30 (m, 5H, ArH), 3.83 (s, 2H, PhCH_2CO -). ^{13}C NMR ($\text{DMSO}-d_6$) 169.52, 169.32, 167.95, 135.60, 135.01, 133.94, 132.08, 128.86, 127.97, 126.37, 124.05, 117.08, 43.03.

Melting Point $>290^\circ$

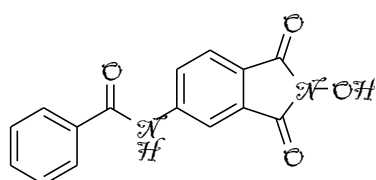
Scheme 3.10

General procedure for the formation of *N*-hydroxyphthalimide derivatives.

0,50 mmol of a *N*-Boc derivative (**27a-c**) was dissolved in 1 ml of CH_3CN in a 10 ml round bottomed flask, then 0,1 ml of an aqueous solution (50% w/w) of Hydroxylamine is added.

After 4.5 h, the reaction is quenched with 5 ml of diethyl ether, and the precipitate (white to pink) is filtered on a Buchner funnel and washed twice with small portion of fresh Et_2O (10 ml x 2).

Mild and convenient one pot synthesis of *N*-Hydroxyimides from *N*-unsubstituted imides.¹

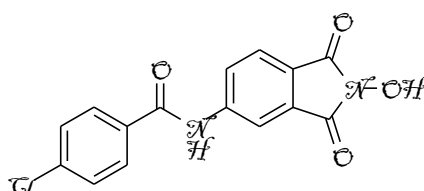


28a. *N*-Hydroxy-4-benzamidophthalimide.

Yield 76%

^1H NMR (DMSO- d_6) 10.78 (s, 1H, -OH), 8.31 (s, 1H, C-H), 8.13 – 8.09 (d, 1H, $J=8$, C-H), 7.97 – 7.93 (d, 2H, $J=8$, C-H), 7.84 – 7.78 (dd, 1H, $J_{\min}=2.9$, $J_{\max}=8.2$), 7.58 (m, 3H). ^{13}C NMR (DMSO- d_6) 170.14, 168.03, 164.17, 135.82, 135.22, 132.68, 131.99, 128.44, 126.49, 124.24, 117.91, 117.39.

Melting Point 212 – 213°C

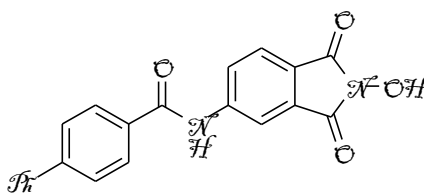


28b. N-Hydroxy-4-(4-chlorobenzamido)phtalimide.

Yield 18%

^1H NMR (DMSO- d_6) 11.13 (s, 1H, -OH), 10.85 (s, 1H, -NH-), 8.36 (s, 1H, C-H), 8.21-8.18 (d, 2H, $J=6$), 8.08 – 8.05 (d, 1H, $J=6$), 7.80-7.76 (d, 1H, $J=8$), 7.60 – 7.56 (d, 2H, $J=8$) ^{13}C NMR (DMSO- d_6) 164.42, 163.25, 144.06, 136.29, 132.04, 129.39, 129.26, 127.84, 123.76, 123.33, 122.18, 113.47.

Melting Point > 290°C dec.



28c. N-Hydroxy-4-(4-phenylbenzamido)phtalimide.

Yield 33%

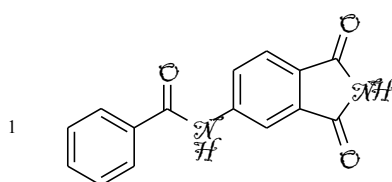
^1H NMR (DMSO- d_6) 10.84 (s, 1H, -OH), 10.63 (s, 1H, -NH-), 8.28-7.46 (m, 12H, ArH). ^{13}C NMR (DMSO- d_6) 170.11, 168.22, 164.35, 135.75, 135.01, 132.67, 132.19, 129.49, 128.38, 128.00, 126.33, 124.19, 117.81, 117.37.

Melting Point > 300°C dec.

General Method for N-Boc deprotection.

N-Boc aryl phtalimide was placed in a flame dried round bottomed flask, protected from moisture with a drying tube and dissolved in dry dichloromethane, then trifluoroacetic acid was added and the reaction was allowed to stir at room temperature.

After 1 hour TLC shown completion of reaction. All volatile substances were removed and residue was crystallized with methanol.



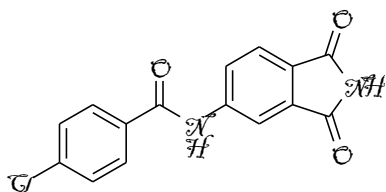
20c. 4-benzamidophthalimide.

Yield 90%

^1H NMR (DMSO- d_6) 11.50 (s, 1H, NH) 10.78 (s, 1H, amidic -NH), 8.31 (s, 1H, C-H), 8.13 – 8.09 (d, 1H, $J=8$, C-H), 7.97 – 7.93 (d,

2H, $J = 8$, C-H), 7.84 – 7.78 (dd, 1H, $J_{\min} = 2.9$, $J_{\max} = 8.2$), 7.58 (m, 3H). ^{13}C NMR (DMSO- d_6) 170.14, 168.03, 164.17, 135.82, 135.22, 132.68, 131.99, 128.44, 126.49, 124.24, 117.91, 117.39.

Melting Point $>290^\circ\text{C}$



20e. 4-(4-chlorobenzamido)phtalimide.

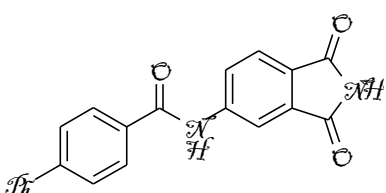
Yield 93%

^1H NMR (DMSO- d_6) 11.13 (s, 1H, -NH), 10.85 (s, 1H, amidic -NH-), 8.36 (s, 1H, C-H), 8.21-8.18 (d, 2H, $J = 6$), 8.08 – 8.05 (d,

1H, $J = 6$), 7.80-7.76 (d, 1H, $J = 8$), 7.60 – 7.56 (d, 2H, $J = 8$)

^{13}C NMR (DMSO- d_6) 164.42, 163.25, 144.06, 136.29, 132.04, 129.39, 129.26, 127.84, 123.76, 123.33, 122.18, 113.47.

Melting Point $> 290^\circ\text{C}$



20f. (4-phenylbenzamido)phtalimide.

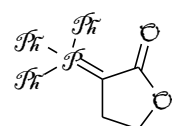
Yield 89%

^1H NMR (DMSO- d_6) 10.84 (s, 1H, -NH), 10.63 (s, 1H, amidic -NH-), 8.28-7.46 (m, 12H, ArH). ^{13}C NMR (DMSO- d_6) 169.87,

168.01, 164.35, 135.75, 135.01, 132.67, 132.19, 129.49, 128.38, 128.00, 126.33, 124.19, 117.81, 117.37.

Melting Point $> 290^\circ\text{C}$

Scheme 3.12, 3.13, 3.14, 3.15



33. γ -butyrolactone triphenylphosphonium bromide

A mixture of 2 g of α -bromo butyrolactone and 6 grams of triphenylphosphine was mechanically stirred and refluxed in 20 ml of THF for six hours. A white to grey powder formed copiously.

Heating was removed and the mixture was allowed to reach room temperature.

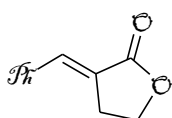
About 100 ml of diethyl ether was added, the precipitate was filtered on a Buchner funnel and washed several times with fresh ether.

Quantitative Yield.

Spectroscopic data correspond to that reviewed in literature. ³

The triphenylphosphine bromide salt obtained was dissolved in DCM and a stoichiometrical amount of t-BuOK was added. After 30 minutes, the inorganic solid constituted of potassium bromide was filtered and the solvent was removed at reduced pressure from the filtrate.

The white-to-grey solid can was used in the successive step without further purification. ⁴



34a □ **α-benzylidenebutyrolactone.**

In a 50 ml round bottomed flask with magnetic agitation, the phosphor ylide and the benzaldehyde are mixed together without solvent.

In few second a very strong exothermic reaction take place, with the complete melting of the solid compound and the formation of a very viscous amber liquid. The reaction mustn't be cooled.

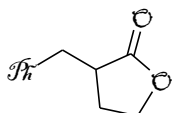
The liquid which was mainly constituted of triphenylphosphine oxide and the olefinic compound will turn in solid on cooling.

Flash chromatography (P.E./AcOEt 5:5) afforded the title compound as a crystalline solid.

If a purer stuff was desired, diethyl ether can be use as washing solvent in order to remove all of coloured impurities. ⁵

Yield 91%

Spectroscopic data correspond to that reviewed in literature. ⁶



35a. **α-benzylbutyrolactone.**

In a flame-dried 250 ml round bottomed flask, compound X was added in 100 ml of absolute ethanol.

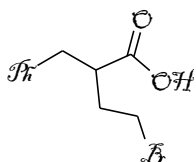
Palladium on carbon was added (5mol%).

The reaction was stirred under an hydrogen atmosphere for two hours, until all the starting material reacts (TLC).

The green solution was then filtered on a pad of celite and the alcohol in the filtrate was removed at reduced pressure. A slightly yellow oil was obtain.

Yield almost quantitative. ^{5,6}

¹HNMR (CDCl₃) 7.38 – 7.20 (m, 5H, ArH), 4.26 – 4.13 (m, 2H, -CH₂CH₂OOC-), 3.31 – 3.23 (m, 1H,), 2.90 – 2.70 (m, 2H,), 2.35 – 2.21 (m, 1H), 2.11 – 1.95 (m, 1H). ¹³CNMR (CDCl₃) 177.84, 138.24, 128.19, 127.73, 125.69, 65.68, 39.64, 34.72, 27.02.



36a. **α-benzyl-β-bromobutyric acid.**

In a 100 ml round bottomed flask, 1g Of **35a** and 20 ml of AcOH/HBr 33% are stirred and heated at 80°C for one hour.

(The formation of the acid was easily detected using PhMe/AcOEt/AcOH 6,5:3:0.5 as eluant for TLC).

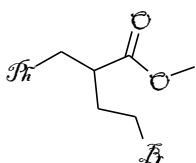
Reaction was left to cool and 20 ml of water are added.

Petroleum ether was used as solvent for the extraction (50 ml x 3) to avoid formation of emulsions.

The organic layer was washed with brine (20 ml x 2), 20% sodium thiosulphate solution (20 ml x 2) and again with brine (10 ml x 2), dried over magnesium sulphate, filtered and concentrated under reduced pressure. ⁵

Yield 79% as a brown oil

NMR (CDCl₃) 7.35 – 7.28 (m, 5H, Ph), 3.46 – 3.35 (q, 2H, J_{min} = 8, J_{max} = 22, -CH₂CH₂Br), 2.67 – 2.59 (t, 2H, J_{min} = 8, J_{max} = 16, PhCH₂CH₂-), 2.39 – 2.11 (m, 1H, =CH-), 2.05 – 1.77 (m, 2H, -COOCH₂CH₂-).



37a. Methyl α -benzyl- γ -bromobutyrate.

In a 50 ml round bottomed flask the compound from the previous reaction was dissolved in 10 ml of anhydrous THF.

A large excess of thionyl chloride was added together to few drops of DMF.

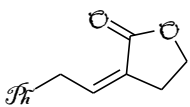
The reaction was stirred for 15 minutes, then THF and unreacted thionyl chloride were removed with the aid of reduced pressure.

A large excess of absolute ethanol was added to the acyl chloride (25 ml) and the mixture was left on stirring for ten minutes.

After stripping of ethanol a brown oil pure enough for successive step was obtained. If a purer ester was desired a flash chromatography (P.E./AcOEt 7:3) can be carried out. ⁵

Yield = 75% as a white oil.

¹HNMR (CDCl₃) 7.35 – 7.28 (m, 5H, Ph), 3.65 (s, 3H, -COOCH₃), 3.46 – 3.35 (q, 2H, J_{min} = 8, J_{max} = 22, -CH₂CH₂Br), 2.67 – 2.59 (t, 2H, J_{min} = 8, J_{max} = 16, PhCH₂CH₂-), 2.39 – 2.11 (m, 1H, =CH-), 2.05 – 1.77 (m, 2H, -COOCH₂CH₂-).

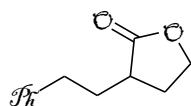


34b. α -phenethylidenbutyrolactone.

Same procedure used for the manufacture of α -benzylidenbutyrolactone.

$^1\text{H NMR}$ (CDCl_3) 7.47 – 7.43 (d, 1H, $J = 8$ PhCH $\underline{2}$ CH-), 7.36-7.22 (m, 5H, Ph), 4.39-4.32 (t, 2H, $J_{\text{min}} = 8$, $J_{\text{max}} = 16$ Hz -COOCH $\underline{2}$ CH $\underline{2}$ -), 3.56 – 3.52 (d, 2H, $J = 8$, PhCH $\underline{2}$ CH=), 2.52 – 2.44 (m, 1H, -COOCH $\underline{2}$ CH $\underline{2}$ -), 2.29 – 2.10 (m, 1H, -COOCH $\underline{2}$ CH $\underline{2}$ -).

Yield 68% as a white oil.⁵

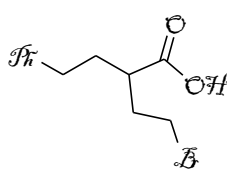


35b. α -phenethylbutyrolactone.

Same procedure used for the manufacture of β -benzylbutyrolactone

$^1\text{H NMR}$ (CDCl_3) 7.36 – 7.22 (m, 5H, Ph), 4.42 – 4.33 (t, 1H, $J_{\text{min}} = 9$, $J_{\text{max}} = 18$, -COOCH $\underline{2}$ CH $\underline{2}$ -), 4.26 – 4.18 (t, 1H, $J_{\text{min}} = 8$, $J_{\text{max}} = 14$, -COOCH $\underline{2}$ CH $\underline{2}$ -), 2.80 – 2.73 (t, 2H, $J_{\text{min}} = 6$, $J_{\text{max}} = 14$, PhCH $\underline{2}$ CH=), 2.56 – 2.26 (m, 3H), 2.03 – 1.74 (m, 2H).

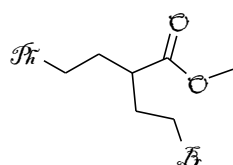
Yield = 98% as a white oil.⁵



36b. 4-bromo-2-phenethylbutanoic acid.

$^1\text{H NMR}$ (CDCl_3) 7.35 – 7.17 (m, 5H, Ph), 3.73 (s, 3H), 3.46 – 3.35 (q, 2H, $J_{\text{min}} = 8$, $J_{\text{max}} = 22$), 2.67 – 2.59 (t, 2H, $J_{\text{min}} = 8$, $J_{\text{max}} = 16$, PhCH $\underline{2}$ CH $\underline{2}$ -), 2.39 – 2.11 (m, 1H, =CH-), 2.05 – 1.77 (m, 4H, -COOCH $\underline{2}$ CH $\underline{2}$ -).

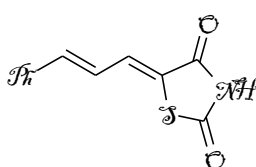
Yield = 90% as a brownish oil.⁵



37b. Methyl 4-bromo-2-phenethylbutanoate.

$^1\text{H NMR}$ (CDCl_3) 7.35 – 7.17 (m, 5H, Ph), 3.73 (s, 3H), 3.74 (s, 3H, -COOCH $\underline{3}$), 3.46 – 3.35 (q, 2H, $J_{\text{min}} = 8$, $J_{\text{max}} = 22$), 2.67 – 2.59 (t, 2H, $J_{\text{min}} = 8$, $J_{\text{max}} = 16$, PhCH $\underline{2}$ CH $\underline{2}$ -), 2.39 – 2.11 (m, 1H, =CH-), 2.05 – 1.77 (m, 4H, -COOCH $\underline{2}$ CH $\underline{2}$ -).

Yield = 77% as a white oil.⁵



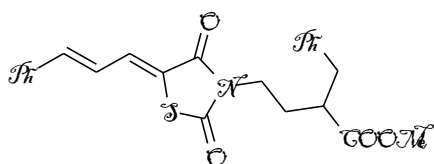
38. (5Z)-5-((E)-3-phenylallylidene)thiazolidine-2,4-dione. In a 250 ml round bottomed flask x g of thiazolidinedione and x g of trans cinnamaldehyde are stirred in x ml of ethanol. Piperidine was added as catalyst and the blend was stirred under reflux for 24 hours.

Ethanol was stripped and the concentrated solution was dropped in cold water, acidified with glacial acetic acid and the resulting yellow solid filtrate on a Buchner funnel.

A small sample for analytical purpose can be made using toluene as crystallizing solvent.⁸

Yield 64%

¹HNMR (DMSO-*d*₆) 12.42 (s, 1H, NH), 7.70-7.66 (d, 1H, PhCHCHCH-), 7.53-7.39 (m, 5H, Ph) 7.34-7.27 (d, 1H, PhCHCHCH), 7.26 (s, 1H, PhCHCHCH-), 7.00-6.87 (dd, 1H, PhCHCHCH-).



39a. methyl 2-benzyl-4-((5Z)-2,4-dioxo-5-((E)-3-phenylallylidene)thiazolidin-3-yl)butanoate.

In a flame-dried 50 ml three necked round bottomed flask equipped for magnetic stirring and purged with nitrogen, was charged with 475.6 mg (2.05 mmol) of **38** in 5 ml of anhydrous DMF. When the solid was dissolved, NaH (60% mineral oil dispersion, 82 mg, 2.05 mmol) was added.

A visible evolution of hydrogen take place, and a clear yellow solution was obtained.

Then 372 mg of **36a** (1.37 mmol) was added dropwise, and the mixture stirred overnight at r.t.

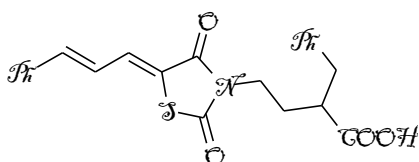
After consumption of ester (tlc), DMF was removed, and a yellow solid was obtained.

Flash chromatography (P.E./AcOEt 7:3) afforded title compound as a yellowish solid.

Yield 64%

¹HNMR (CDCl₃) 7.61-7.55 (d, 1H, J = 12, PhCHCHCH-), 7.51-7.14 (m, 10H 2xPh), 7.10-7.03 (d, 1H, J= 14 Hz, PhCHCHCH-), 6.79-6.66 (dd, 1H, J_{min} = 12, J_{max} = 15 PhCHCHCH-), 3.81 – 3.74 (t, 2H, J_{min} = 8, J_{max} = 14 Hz), 3.64 (s, 3H) 3.04-2.71 (m, 3H), 2.16 – 1.98 (m, 1H) 1.94 – 1.80 (m, 1H). ¹³CNMR (CDCl₃) 175.40, 175.16, 165.68, 143.90, 141.31, 138.00, 135.61, 133.50, 130.15, 129.17, 128.92, 128.59, 127.82, 127.15, 126.20, 123.01, 120.69, 52.04, 42.52, 42.28, 40.13, 29.95.

Melting Point 50-52°C



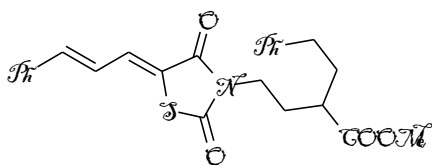
31a. 2-benzyl-4-((5Z)-2,4-dioxo-5-((E)-3-phenylallylidene)thiazolidin-3-yl)butanoic acid.

In a 25 ml round bottomed flask 270 mg (0.65 mmol) of **39a** was dissolved in 6 ml of AcOH, then 1.5 ml of concentrated HCl 36% was added to the clear solution. Reaction was heat to 120°C for four hours and the acid mixture was removed at reduced pressure. The yellow residue was purified throught flash chromatography (gradient elution CH₂Cl₂ 10 CH₂Cl₂/MeOH 9.5:0.5)

Yield 71%

¹HNMR (CDCl₃) 7.61-7.55 (d, 1H, J = 12, PhCHCHCH-), 7.51-7.14 (m, 10H 2xPh), 7.11-7.04 (d, 1H, J= 14 Hz, PhCHCHCH-), 6.93 - 6.80 (dd, 1H, J_{min} = 12, J_{max} = 15 PhCHCHCH-), 3.84 – 3.77 (t, 2H, J_{min} = 8, J_{max} = 14 Hz), 3.04-2.71 (m, 3H), 2.12 – 1.99 (m, 1H) 1.93 – 1.80 (m, 1H). ¹³CNMR (CDCl₃) 174.47, 174.34, 164.53, 138.60, 137.85, 136.69, 129.22, 129.17, 129.11, 128.90, 128.60, 127.84, 127.53, 126.73, 45.14, 40.24, 38.53, 29.99.

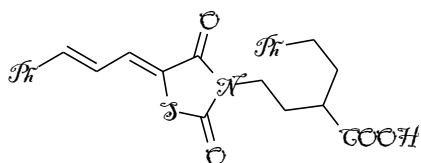
Melting Point 109-112°C



39b. Methyl 4-((5Z)-2,4-dioxo-5-((E)-3-phenylallylidene)thiazolidin-3-yl)-2-phenethylbutanoate.

Same procedure used for **39a**.

¹HNMR (CDCl₃) 7.61-7.55 (d, 1H, J = 12, PhCHCHCH-), 7.51-7.14 (m, 10H 2xPh), 7.10-7.03 (d, 1H, J= 14 Hz, PhCHCHCH-), 6.79-6.66 (dd, 1H, J_{min} = 12, J_{max} = 15 PhCHCHCH-), 3.81 – 3.74 (t, 2H, J_{min} = 8, J_{max} = 14 Hz), 3.64 (s, 3H) 3.04-2.71 (m, 3H), 2.22 – 1.75 (m, 3H). ¹³CNMR (CDCl₃) 175.40, 175.16, 165.68, 143.90, 141.31, 138.00, 135.61, 133.50, 130.15, 129.17, 128.92, 128.59, 127.82, 127.15, 126.20, 123.01, 120.69, 52.04, 42.52, 42.28, 40.13, 34.01, 29.95.

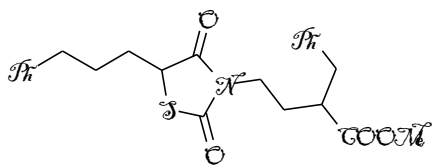


31b. 4-((5Z)-2,4-dioxo-5-((E)-3-phenylallylidene)thiazolidin-3-yl)-2-phenethylbutanoic acid.

Same procedure used for **31a**.

¹HNMR (CDCl₃) 7.61-7.55 (d, 1H, J = 12, PhCHCHCH-), 7.51-7.14 (m, 10H 2xPh), 7.10-7.03 (d, 1H, J= 14 Hz, PhCHCHCH-), 6.79-6.66 (dd, 1H, J_{min} = 12, J_{max} = 15 PhCHCHCH-), 3.81 – 3.74 (t, 2H, J_{min} = 8, J_{max} = 14 Hz), 3.04-2.71 (m, 3H), 2.22 – 1.75 (m, 3H). ¹³CNMR (CDCl₃) 175.47, 175.14, 165.60, 143.50, 141.29, 138.10, 135.61, 133.50, 130.15, 129.17, 128.92, 128.86, 127.82, 127.15, 126.20, 123.01, 120.69, 42.52, 42.28, 40.73, 34.01, 29.95.

Melting Point 203-204° C

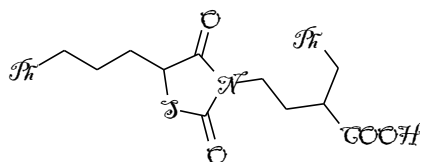


41. methyl 2-benzyl-4-(2,4-dioxo-5-(3-phenylpropyl)thiazolidin-3-yl)butanoate.

39a (100mg, 0.24 mmol) was dissolved in absolute ethanol. Pd/C was added (5 mol%) and the mixture was left stirring at rt

overnight. Reaction mixture was filtered through celite and concentrated. **41** was pure enough for next step. ¹HNMR (CDCl₃) 7.51-7.14 (m, 10H 2xPh), 3.77 (t, 1H), 3.64 (s, 3H), 3.04-2.71 (m, 3H), 2.55 (t, 2H), 2.12 – 1.99 (m, 3H) 1.93 – 1.80 (m, 2H), 1.55 (m, 2H).

Yield = 70% as a sticky liquid.



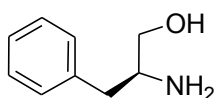
42. 2-benzyl-4-(2,4-dioxo-5-(3-phenylpropyl)thiazolidin-3-yl)butanoic acid

Hydrolysis procedure is the same for **39a** o **39b**.

^1H NMR (CDCl_3) 7.51-7.14 (m, 10H 2xPh), 3.77 (t, 1H), 3.04-2.71 (m, 3H), 2.55 (t, 2H), 2.12 – 1.99 (m, 3H) 1.93 – 1.80 (m, 2H), 1.55 (m, 2H).

Yield = 42% as a sticky liquid.

Scheme 3.16.



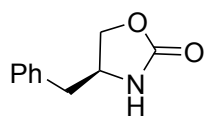
43. (S)-2-amino-3-phenylpropan-1-ol.

A 500 ml three-neck round-bottom flask was fitted with a magnetic stirbar, was fitted with a reflux condenser, and an addition funnel. The flask was charged with 6.92 g (183 mmol) sodium borohydride and 200 mL of THF (predried over sodium). L-phenylalanine (12,54 g, 76 mmol) was added in one portion. The remaining neck was sealed with a septum and an argon line attached, and the flask was cooled to 0 °C in an ice bath. A solution of 19.30 g (76 mmol of iodine dissolved in 50 mL of THF was poured into the addition funnel and added slowly and dropwise over 30 min resulting in vigorous evolution of hydrogen. After addition of the iodine was complete and gas evolution had ceased, the flask was heated to reflux for 18 h and then cooled to room temperature, and methanol was added cautiously until the mixture became clear. After stirring 30 min, the solvent was removed by rotary evaporation leaving a white paste which was dissolved by addition of 150 mL of 20% aqueous KOH. The solution was stirred for 4 h and extracted with 3 X 150 mL of methylene chloride. The organic extracts were dried over sodium sulfate and concentrated in vacuo, affording a crude product.

Cristallization from toluene yield 6.8 g of amino alcohol.

Yield 59%

Spectroscopic datas correspond to that reviewed in literature. ⁹

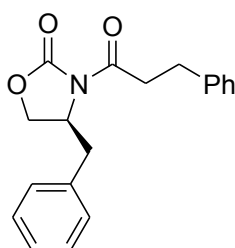


43a. (S)-4-benzyloxazolidinone

A dry, 50 ml, three-necked flask was equipped with a magnetic stirrer and a distillation head. The flask was charged with 3.1 g (20.7 mmol) of (S)-phenylalanol, 0.3 g (2.02 mmol) of anhydrous potassium carbonate, and 3.4 mL (40.33 mmol) of dimethyl carbonate. The mixture was lowered into an oil bath, preheated to 100°C, and was stirred until dissolution was achieved (ca. 5 min). The theoretical amount of methanol was collected from the reaction over a 2.5-hr period. The oil bath was removed on cessation of the methanol distillation. After the light-yellow solution was cooled to ambient temperature, it was diluted with 30 mL of dichloromethane, transferred to a separatory funnel, and washed with 10 mL of water. The organic phase was dried over anhydrous magnesium sulfate, filtered, and concentrated on the rotary evaporator affording 200 g a white crystalline solid. This material was taken up into 30 mL of a hot 2:1 ethyl acetate–hexane solution, filtered while hot, then allowed to crystallize to afford large white plates.¹⁰

Obtained: 2.2 g

Yield 60%



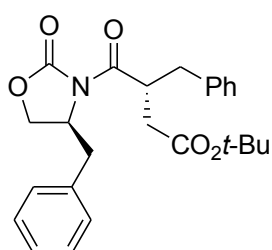
44. (S)-3-(3-phenylpropanoyl)-4-benzyloxazolidin-2-one.

To **43a** (704 mg, 4.0 mmol) in THF (8 mL), was added n-BuLi (2.5 M in hexane, 2.5 mL, 4.0 mmol) dropwise at -78°C. After complete addition, the solution was stirred for 5 min at -78 °C. A solution of Hydroxycinnamoyl chloride in 5 mL of THF was then added dropwise at -78 °C over 10 minutes and the mixture was stirred at -78 °C for 1 h. The reaction was quenched with 1 mL of saturated NH₄Cl solution and extracted with ethyl acetate (3 x 20 mL). The extracts were combined, washed with brine (2 x 5 mL), dried over MgSO₄, and concentrated to afford a yellow oil. Crystallization (from ethyl acetate/P.E.) provided a colorless solid.

Obtained 915 mg as a solid.

Yield 74%.

Spectroscopic data and melting point are referred.¹¹



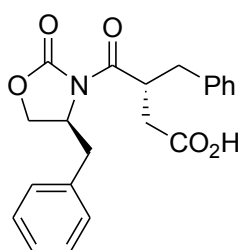
45. (R)-tert-butyl 3-benzyl-4-((S)-4-benzyloxazolidin-3-yl)-4-oxobutanoate.

To a solution of 1,20 g of **44** (3.9 mmol) in dry THF (10 ml/ mmol) at -78 °C was added 7.15 ml of sodium hexamethyldisilazide (4.29 mmol, 1.1 equiv, 1.0

M in THF) via syringe. The solution was then stirred at $-78\text{ }^{\circ}\text{C}$ for 1.5-2 h. To the reaction was added 0.86 ml of tert-butyl bromoacetate (5.85 mmol, 1.5 eq.) via syringe. Alkylation was allowed to proceed at $-78\text{ }^{\circ}\text{C}$ until TLC analysis indicated complete consumption of the starting material (3-6 h). The reaction flask was allowed to warm to $0\text{ }^{\circ}\text{C}$ before the contents were partitioned between saturated aqueous NH_4Cl (10 ml) and 50 mL of EtOAc. The layers were separated, and the aqueous layer was extracted with three 20 mL portions of EtOAc. The combined organic extracts were dried (MgSO_4), filtered through cotton, and concentrated in vacuo to yield a solid which was recrystallized from a minimal volume of hexane/ether to afford white crystals or purified through flash chromatography (P.E. / AcOEt 9:1).

Spectroscopic data match to that reviewed in literature.¹²

Yield = 74%

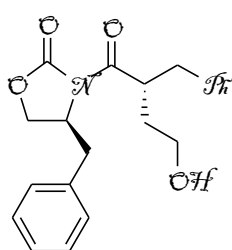


46. (R)-3-benzyl-4-((S)-4-benzyl-2-oxooxazolidin-3-yl)-4-oxobutanoic acid.

To a $0\text{ }^{\circ}\text{C}$ solution of the ester (0.312 mmol) X ml of a 70:30 (v/v) CH_2Cl_2 /trifluoroacetic acid solution was added. The solution was stirred at room temperature for 3.5 h, and the contents were concentrated in vacuo and under high vacuum to yield a residue. The residue was dissolved in the minimum amount of ethyl ether and precipitate with Petroleum ether 60-80. A white solid was obtained.¹²

Yield 89%

$^1\text{H NMR}$ (CDCl_3) $\square\square$ 7.39-7.18 (m, 10 H), 4.59-4.44 (m, 2H), 4.13-4.08 (dd, $J = 8.9$, 1H), 3.99-3.91 (m, 1H), 3.37-3.29 (dd, $J = 13.3$, 1H), 3.01 (dd, $J = 13.1$), 2.85 (dd, $J = 16.9$, 1H), 2.76 (dd, $J = 13.5$, 1H), 2.45 – 2.34 (dd, $J = 13.1$, 1H).



47. (R)-3-benzyl-4-((S)-4-benzyl-2-oxooxazolidin-3-yl)-4-oxobutanol.

430 mg of **46** (1.16 mmol) was dissolved in 9 ml of dry THF. $\text{BH}_3\cdot\text{THF}$ was added dropwise (1.16 ml, 1.16 mmol) at $0\text{ }^{\circ}\text{C}$. The mixture was stirred for six hours, then quenched with MeOH. The solvents was removed in vacuo and the residue was purified through flash chromatography. (P.E./AcOEt 7:3)

$^1\text{H NMR}$ (CDCl_3) $\square\square$ 7.37-7.20 (m, 10 H), 4.99 (s, 1H, $-\text{OH}$), 4.59-4.44 (m, 2H), 4.05- 3.99 (dd, $J = 8.9$, 1H), 3.76 -3.70 (t, 2H, $J_{\text{min}} = 6$, $J_{\text{max}} = 12$ Hz), 3.37-3.29 (dd, $J = 13.3$, 1H), 3.01 (dd, $J = 13.1$), 2.85 (dd, $J = 16.9$, 1H), 2.76 (dd, $J = 13.5$, 1H), 2.45 – 2.34 (dd, $J = 13.1$, 1H).

Yield = 9% as a viscous oil.¹³

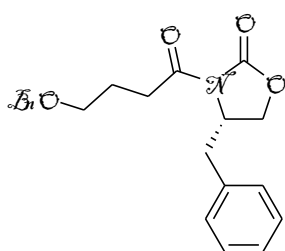
Scheme 3.17

49. α -(benzyloxy)butanoic acid.

To a solution of 83 mL (0.70 mol) of benzyl bromide and 15.0 g (0.174 mol) of γ -butyrolactone in 300 mL of toluene was added 49.2 g (0.745 mol) of freshly crushed 85% KOH. The mixture was stirred at reflux, under N₂, for three days, then partitioned between 300 mL of H₂O and 150 mL of diethyl ether. The layers were separated, and the aqueous layer was extracted with additional ether (2 x 150 mL). The ether/toluene layers were set aside, and the aqueous layer was cooled with an ice bath, then acidified with 150 mL of 3 M H₂SO₄ solution. The acidic suspension was then extracted with CH₂Cl₂, (3 x 150 mL). The combined CH₂Cl₂ layers were dried and concentrated to 8.85 g (26.2%) of a colorless oil.

The ether/toluene layer was concentrated to remove most of the diethyl ether, and the residue was heated at reflux with 80 mL of H₂O and 16 g of NaOH for 20 h. The layers were separated, then the aqueous layer was diluted to 200 mL. This was extracted with ether (3 x 50 mL). The aqueous layer was treated with a slurry of 20 mL H₂SO₄, in 100 mL of ice. The acidic suspension was then extracted with CH₂Cl₂, (3 x 100 mL). The combined CH₂Cl₂ layers were dried and concentrated to 22.44 g (66%) of additional product for a total yield of 31.29 g (92%). This acid was used without purification in the next step.

14, 15



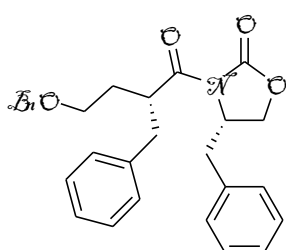
51. (S)-3-(4-(benzyloxy)butanoyl)-4-benzyloxazolidin-2-one.

In a three-necked flask equipped with a mechanical stirrer, **49** (1.1 g, 5.65 mmol) was dissolved in dry Et₂O (9.5 mL/ mmol). Triethylamine (0.8 mL, 5.65 mmol) was added, and the mixture was stirred at rt for 15 min. This solution was cooled to 0 °C, and ethyl chloroformate (0.54 mL, 5.65 mmol) was added. A thick white precipitate immediately formed. This solution was warmed to rt and stirred for an additional 1 h. In a separate flask, (4*S*)-benzyl oxazolidinone **43a** (1 g, 5.65 mmol) was dissolved in THF (1.5 ml/ mmol) and cooled to -78 °C.

n-butyllithium (1.6 M in hexanes, 3.53 mL, 5.65 mmol) was added dropwise to this solution. The **43a** solution was transferred via cannula into the solution containing the anhydride, the mixture was stirred for 30 min at -78 °C, and then was warmed to 0 °C for an additional 30 min. The solution was quenched with satd. aq. NH₄Cl and extracted with Et₂O. The combined organic extracts were

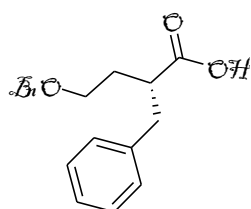
washed with brine, dried over Na₂SO₄, filtered, and concentrated in vacuo. Purification by column chromatography (9:1 hexanes/EtOAc) afforded 15.2 g (46.3 mmol, 88 %) of the product as a pale yellow oil.¹⁶

Report: [α]₂₃^D + 44.8 (c 1.0, CHCl₃),¹⁶ found: [α]₂₃^D + 40.2 (c 1.0, CHCl₃).



52. (S)-3-((R)-2-benzyl-4-(benzyloxy)butanoyl)-4-benzyloxazolidin-2-one.

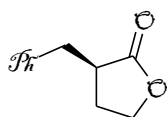
In a three-necked flask equipped with an internal thermometer, NaHMDS (1 M in THF, 3.1 mL, 3.05 mmol) was cooled to -78°C, and a solution of **51** (900 mg, 2.54 mmol) in 2.5 mL of THF (1 ml/ mmol) was added dropwise via syringe at a rate such that the internal temperature was maintained below -70 °C. This mixture was stirred for 30 min, after which benzyl bromide (638 mg, 1.5 eq., 3.80 mmol) in THF (1 ml/ mmol) was added dropwise. The reaction mixture was allowed warm to -50 °C and stirred for an additional 24 h at this temperature. The solution was then quenched with satd. aq. NH₄Cl and was extracted with Et₂O. The combined organic extracts were washed with brine, dried over MgSO₄, filtered, and concentrated in vacuo. The crude product was purified by column chromatography (8:2 P.E./EtOAc) to afford 640 mg of the alkylated product as a clear oil.¹⁶ Yield: 57%



53. (R)-2-benzyl-4-(benzyloxy)butanoic acid.

To a solution of 620 mg of **52** (1.4 mmol) dissolved in 4.5 ml of a mixture 3:1 THF/water poured to 0°C, was added hydrogen peroxide (6 eq., 8.4 mmol 0.85 ml 30% aqueous solution) and 118 mg of LiOH idrate (2 eq. 2.8 mmol). Hydrolysis proceeded for 1 h. Acidification of the aqueous layer, extraction, and concentration yielded the carboxylic acid as a clear oil, pure enough for next step.

¹HNMR (CDCl₃) 11.27 (s, 1H, -COOH), 7.36- 7.18 (m, 10H, ArH), 4.47 (s, 2H, PhCH₂O-), 3.55 – 3.49 (t, 2H, J_{min} = 6, J_{max} = 12 Hz, -OCH₂CH₂-), 3.09 – 2.74 (m, 3H, -CH-, CH₂Ph), 2.07 – 1.57 (m, 2H, -OCH₂CH₂-).



(R) – 34a. (R)-2-benzylbutyrolactone.

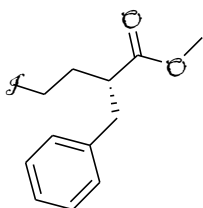
In a dried 50 ml round bottomed flask, was dissolved **53** (350 mg, 1.23 mmol) in 25 ml of absolute ethanol, Pd/C was added to the mixture (5 mol%). The flask was purged with hydrogen and the mixture was left stirred for one hour.

The mixture was filtered through a short pad of celite and on concentration yielded **(R) – 34a** as a white oil.

$[\alpha]_D^{20}$ (c 1.0, MeOH) + 52.2

Yield = 97%

$^1\text{H NMR}$ (CDCl_3) 7.38 – 7.20 (m, 5H, ArH), 4.26 – 4.13 (m, 2H, $-\text{CH}_2\text{CH}_2\text{OOC}-$), 3.31 – 3.23 (m, 1H, CH), 2.90 – 2.70 (m, 2H, PhCH_2-), 2.35 – 2.21 (m, 1H, $-\text{CH}_2\text{CH}_2\text{OOC}-$), 2.11 – 1.95 (m, 1H, $-\text{CH}_2\text{CH}_2\text{OOC}-$). $^{13}\text{C NMR}$ (CDCl_3) 177.84, 138.24, 128.19, 127.73, 125.69, 65.68, 39.64, 34.72, 27.02.



(R) – 55. (R)-methyl 2-benzyl-4-iodobutanoate.

(R) – 34a (88 mg, 0.5 mmol) was dissolved in dry CH_2Cl_2 (1ml/mmol). Trimethylsilyl iodide (1 eq., 0.5 mmol, 0.07 ml) was added, and mixture was allowed to react avoiding light.

After 2 hours lactone was hydrolyzed. Reaction was quenched with 20 ml of moist CH_2Cl_2 .

Sudden organic phase was then washed with sodium thiosulphate 5% strength (5 ml x 2), dried over MgSO_4 , and concentrated afford 137 mg (90% of yield).

This residue was dissolved in 3 ml of a mixture of PhMe / MeOH 2:1, treated with 0.3 ml of trimethylsilyl diazomethane (2.0 M in Hexanes) and left stirred at r.t. for half hour.

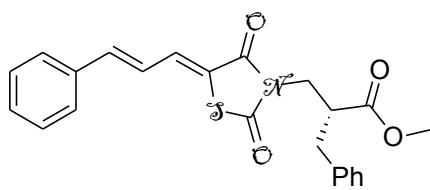
Concentration afforded an oily residue which was purified through flash chromatography (P.E./ AcOEt 8:2). Obtained 138 mg.¹⁷

Yield = 98% as a white oil.

$[\alpha]_D^{20}$ (c 1.0, MeOH) + 11.5

$^1\text{H NMR}$ (CDCl_3) 7.32 – 7.15 (m, 5H, ArH), 3.66 (s, 3H, $-\text{COOCH}_3$), 3.24 – 3.18 (m, 2H, ICH_2CH_2-), 2.97 – 2.78 (m, 3H,), 2.37 – 1.95 (m, 2H).

Scheme 3.18

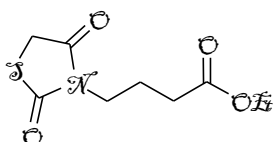


(R)-31a. (R)-methyl 2-benzyl-3-((5Z)-2,4-dioxo-5-((E)-3-phenylallylidene)thiazolidin-3-yl)propanoate

Same procedure used for **31a**.

$[\alpha]_D^{20}$ (c 1.0, MeOH) – 17.44.

Scheme 3.21



Ethyl 4-thiazolidinedionebutanoate

A 50 ml flame-dried round bottomed flask was charged with 20 ml of absolute ethanol and metallic Sodium (0.23g 10 mmol).

Meanwhile in another flame-dried round bottomed flask, thiazolidinedione (1.17g, 10 mmol) was dissolved in 30 ml of absolute ethanol. The ethanolic solution of sodium ethoxide was added to the thiazolidinedione solution and colour turned from yellow to grey-white.

After removal of ethanol at r.p. to residue, consisting in the sodic salt of thiazolidinedione, was dissolved in 5 ml of dry DMF, and ethyl 4-chloro butyrate (2,0 g, 12 mmol) was added.

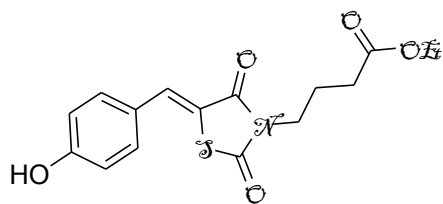
The reaction was leave on reflux for 2 h. The solvent was partially removed, ice was added and once melt the acqueous phase was extract with ethyl acetate (20 ml x 3).

The organic phase was dried over MgSO₄, filtered, and the solvent removed at r.p.

A yellow oil was obtained.

Purification through flash chromatography (P.E./AcOEt 6:4).afford a white to gray crystalline solid.

An analytical sample was stored at +4°C. ¹⁸



56. Ethyl 4-((Z)-5-(4-hydroxybenzylidene)-2,4-dioxothiazolidin-3-yl)butanoate.

Ethyl 4-thiazolidinedionebutanoate (300 mg, 1.30 mmol), 4-hydroxybenzaldehyde (158 mg, 1.30 mmol) and piperidine (1.30 mmol, 123 mg) were dissolved in 10 ml of Ethanol 7.5

ml/mmol compound). The mixture was stirred at room temperature for 18 h.

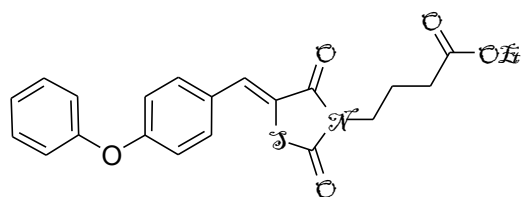
After removal of the solvent an orange oil was obtained. The compound was crystallized dissolving it in Glacial acetic acid and adding water to the obtained solution affording white needles.

Yield 37%

Melting Point 115-120°C

¹HNMR (DMSO-*d*₆) 10.20 (s, 1H, -OH), 7.80 (s, 1H, CH-), 7.49- 7.45 (d, 2H, J= 8, ArH), 6.92 – 6.88 (d, 2H, J= 8, ArH), 4.05 – 4.00 (q, 2H, OCH₂CH₃), 3.69 – 3.62 (t, 2H, NCH₂CH₂CH₂COOEt J_{min} = 8, J_{max} = 14 Hz,), 2.36 – 2.29 (t, 2H, NCH₂CH₂CH₂COOEt J_{min} = 8, J_{max} = 14), 1.85 – 1.77 (q, 2H, NCH₂CH₂CH₂COOEt).

Melting Point 115-120°C.



57. Ethyl 4-((Z)-5-(4-phenoxybenzylidene)-2,4-dioxothiazolidin-3-yl)butanoate.

In a flame dried round bottomed flask equipped with a calcium chloride tube, was sequentially charged with **56**

(150 mg, 0.45 mmol), phenylboronic acid (90 mg, 0.44 mmol), cupric acetate (90 mg, 0.44 mmol) and 10 ml of dry CH₂Cl₂.

the mixture was allowed to become homogeneous, then powdered activated Molecular sieves 4 A (0.3 g) and triethylamine (5 eq, 2.25 mmol, 228 mg) was added.

The reaction was stirred overnight, then filtered. The residue was washed with DCM (10 ml x 4), and the filtrate was concentrated at r.p.

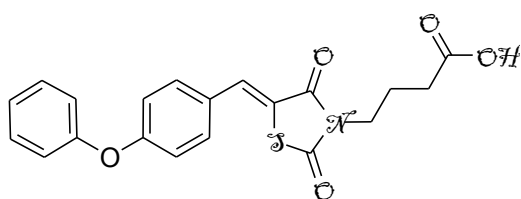
The residue was purified through flash chromatography (P.E. /AcOEt 8:2) affording a white oil that solidified on standing in a crystalline solid.¹⁹

Yield = 61% as a white solid.

Melting Point = 55-60°C

¹HNMR (DMSO-*d*₆) 7.90 (s, 1H, CH), 7.69 – 7.64 (d, 2H, J= 10, ArH), 7.48 – 7.43 (J_{min} = 7, J_{max} = 10 Hz, ArH), 7.29 – 7.21 (t, 1H, J_{min} = 7, J_{max} = 16 Hz, ArH), 7.14 – 7.10 (m, 4H, ArH), 4.12 (t, 2H, -COOCH₂CH₃), 3.72 – 3.65 (t, 2H, J_{min} = 6 J_{max} = 13 Hz NCH₂CH₂CH₂COOEt), 2.31 – 2.22 (t, 2H, J_{min} = 9 J_{max} = 18 NCH₂CH₂CH₂COOEt), 1.85 – 1.79 (q, 2H, NCH₂CH₂CH₂COOEt), 1.30 (t, 3H,

COOCH₂CH₃). ¹³CNMR 173.05, 166.77, 165.13, 158.58, 154.51, 131.81, 131.47, 129.69, 127.11, 123.94, 119.16, 117.64, 61.18, 30.26, 21.92, 14.17, 12.16.



58. 4-((Z)-5-(4-phenoxybenzylidene)-2,4-dioxothiazolidin-3-yl)butanoic acid

58 (100 mg, 0.26 mmol) was dissolved in glacial AcOH (4 ml/mmol) and HCl 37% acid (1 ml/mmol).

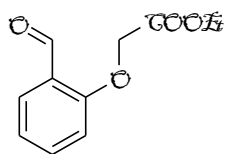
The mixture was then heated to 100°C obtaining after 4 h the carboxylic acid. The acid precipitate upon cooling was filtered on a Buchner funnel and recovered as mother-of-pearl flakes.

Yield = 34% as a white solid

Melting Point 138-142°C

¹HNMR (DMSO-*d*₆) 7.90 (s, 1H, CH), 7.69 – 7.64 (d, 2H, J = 10, ArH), 7.48 – 7.43 (J_{min} = 7, J_{max} = 10 Hz, ArH), 7.29 – 7.21 (t, 1H, J_{min} = 7, J_{max} = 16 Hz, ArH), 7.14 – 7.10 (m, 4H, ArH), 3.72 – 3.65 (t, 2H, J_{min} = 6 J_{max} = 13 Hz NCH₂CH₂CH₂COOEt), 2.31 – 2.22 (t, 2H, J_{min} = 9 J_{max} = 18 NCH₂CH₂CH₂COOEt), 1.85 – 1.79 (q, 2H, NCH₂CH₂CH₂COOEt). ¹³CNMR (DMSO-*d*₆) 173.05, 166.77, 165.13, 158.28, 154.46, 131.72, 131.45, 129.66, 127.06, 123.98, 119.17, 117.66, 30.26, 21.92, 12.16.

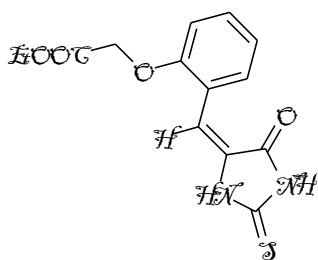
Scheme 3.22



59. Ethyl 2-(2-formylphenoxy)acetate. In a 250 ml round bottomed flask, salicylaldehyde (7.0 g, 42 mmol), ethyl bromoacetate (5.80 g 42 mmol), K₂CO₃ (42 mmol, 5.80 g) in anhydrous acetone (75 ml) were refluxed for 2

hours under an inert atmosphere. The suspension was filtered, and the filtrate was concentrated at r.p. The crude product was purified through flash chromatography (P.E./AcOEt 8:2).

Yield 88% as white needles.²⁰



59a. (E)-5-(2-(Ethyl O-acetoxy)benzylidene)-thiohydantoin.

Triethylamine (3.34 ml, 24 mmol) was added to a mixture of thiohydantoin (1.39 g, 12 mmol) and 2.50 g (12 mmol) of **59** in 15 ml of absolute ethanol under a nitrogen atmosphere.

The reaction was left under magnetical stirring for 24 hours, then the solvent was stripped at r.p. and the resulted residue was triturated with Et₂O, filtered on a Buchner funnel and washed with small portion of fresh ether until the colour turn from intense orange to a yellow powder.

Yield 73%

Melting Point 240°C

¹HNMR (DMSO-*d*₆) 9.94 (s, 1H, Ar-CH-Het), 7.76-7.01 (m, 4H), 6.79 (s, 1H), 4.93 (s, 2H), 4.15 (q, 2H, -CH₂CH₃), 3.38 (s, 1H), 1.22 (t, 3H, CH₃CH₂-).

General Procedure for N alkylation

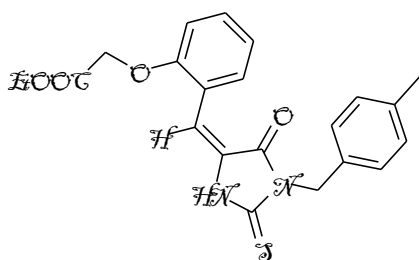
A three necked, flame-dried 50 ml round bottomed flask purged with nitrogen was charged with **59** and NaH (1 mmol, 40 mg 60% mineral oil dispersion).

After 30 minutes the evolution of hydrogen ceased and the sodium salt of **59** formed.

Then the appropriate benzyl bromide (2.5 eq, 2.5 mmol) dissolved in dry DMF (1 ml/mmol) was added drop wise over three hours at room temperature.

After the addition of the appropriate benzyl bromide, the reaction was refluxed overnight.

DMF was removed in vacuo and the residue purified through flash chromatography.



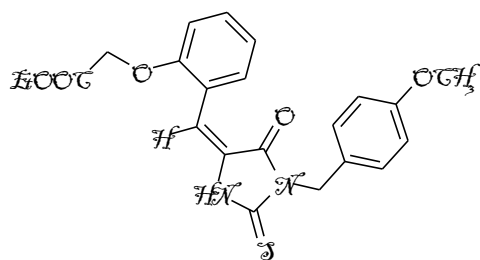
60. Ethyl (E)-5-(2-(O-acetoxy)benzylidene)-3-(4-methylbenzyl) thiohydantoin.

Flash chromatography eluent: PhMe/AcOEt 7:3

Yield 11%

MELTING POINT 148-153°C

¹HNMR (DMSO-*d*₆) 8.91 (s, 1H, NH), 7.39 (s, 1H, CH) 7.35- 7.09 (m, 7H, ArH), 6.76 (s,1H, CH), 6.81 – 6.77 (d, 1H, J= 8 Hz ArH), 4.74 (s, 2H, -CH₂COOEt), 4.56 (s, 2H, -CH₂C₄H₆CH₃), 4.31 (q, 2H, -COOCH₂CH₃), 2.35 (s, 3H, -C₆H₄CH₃), 1.32 (t, 3H, -COOCH₂CH₃)



61. Ethyl (E)-5-(2-(O-acetoxy)benzylidene)-3-(4-methoxybenzyl)thiohydantoin.

Flash chromatography eluent: PhMe/AcOEt 9:1

Yield 83%

Melting Point 135-140°C

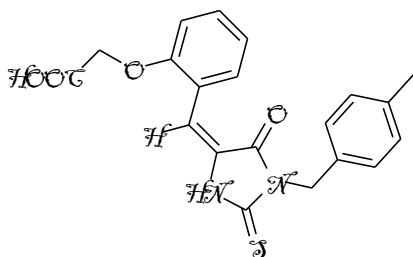
¹HNMR (DMSO-*d*₆) 8.91 (s, 1H, NH), 7.38 (s, 1H, CH), 7.35- 7.08 (m, 7H, ArH), 6.76 (s, 1H, CH), 6.81 – 6.77 (d, 1H, J= 8 Hz ArH), 4.74 (s, 2H, -CH₂COOEt), 4.56 (s, 2H, -CH₂C₄H₆ CH₃), 4.31 (q, 2H, -COOCH₂CH₃), 3.71 (s, 3H, -C₆H₄OCH₃), 1.32 (t, 3H, -COOCH₂CH₃).

General procedure for hydrolysis of ethyl ester

In a round bottomed flask, 0.15 mmol of the corresponding ester was dissolved in 4 ml of a mixture 3:1 MeOH/H₂O.

The solution obtained was then poured at 0°C under magnetical stirring and LiOH.H₂O (6 eq, 0.90 mmol) was added in one only portion.

The reaction was allowed to reach r.t. and stirred for 30 minutes, time after which the solution becomes clear. After conversion, the solvent was evaporated to r.p. and the residue was dissolved in 1 ml of water. The solution was cool to 0°C with an ice bath. Few drop of HCl 3% strength were added until a milky precipitate appear. The solid was filtered on a sintered funnel and dried. The product obtained was very pure and no crystallization was required.

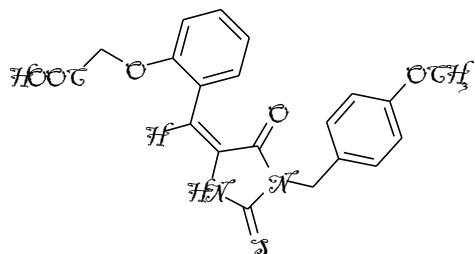


62. (E)-5-(2-(O-acetoxy)benzylidene)-3-(4-methylbenzyl)thiohydantoin

Yield 69%

Melting Point 150-155°C

¹HNMR (DMSO-*d*₆) 8.91 (s, 1H, NH), 7.39 (s, 1H, CH), 7.35- 7.09 (m, 7H, ArH), 6.76 (s, 1H, CH), 6.81 – 6.77 (d, 1H, J= 8 Hz ArH), 4.74 (s, 2H, -CH₂COOEt), 4.56 (s, 2H, -CH₂C₆H₄CH₃), 2.35 (s, 3H, -C₆H₄CH₃).



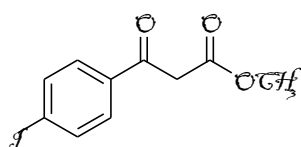
63. (E)-5-(2-(O-acetoxy)benzylidene)-3-(4-methoxybenzyl) thiohydantoin

Yield 73%

Melting Point 124-128°C

¹HNMR (DMSO-*d*₆) 8.91 (s, 1H, NH), 7.38 (s, 1H, CH), 7.35- 7.08 (m, 7H, ArH), 6.76 (s, 1H, CH), 6.81 – 6.77 (d, 1H, J= 8 Hz ArH), 4.74 (s, 2H, -CH₂COOEt), 4.56 (s, 2H, -CH₂C₆H₄CH₃), 3.71 (s, 3H, -C₆H₄OCH₃).

Scheme 3.24



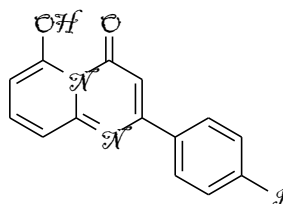
64. Methyl 3-(4-iodophenyl)-3-oxopropanoate.

4- iodoacetophenone (10.00 mmol, 2.45 g) was dissolved in 30 ml of dimethyl carbonate. NaH (440 mg 1.1 eq, 11 mmol 60% mineral oil) was slowly added and the mixture was refluxed for 2 hours.

Then solvent was removed in vacuo and residue crystallized from boiling P.E. ²¹

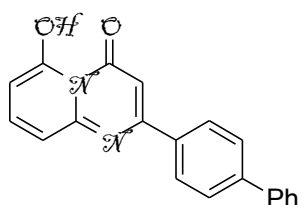
Yield 86%

¹HNMR 7.81 (d, 2H), 7.68 (d, 2H), 3.59 (s, 3H, -CH₃), 3.48 (s, 2H, CH₂).



65. 6-hydroxy-2-(4-iodophenyl)-4H-pyrido[1,2-a]pyrimidin-4-one.

A mixture of 2-aminopyridine (110 mg, 1.00 mmol) and **64** (456 mg, 1.50 mmol) in PPA (2.00 g) was heated at 100 °C for 1 h while stirring with a glass stick. The thick syrup thus obtained was slowly poured into crushed ice, and the resulting suspension was neutralized with 5% aqueous sodium hydroxide. The solid precipitate was collected by filtration, washed with water, and purified through flash chromatography (P.E./ AcOEt 8:2). ²² ¹HNMR 11.40 (s, 1H, -OH), 7.96-7.58 (m, 5H, ArH), 7.10 (d, 2H, ArH), 6.09 (s, 1H).



67a. 6-hydroxy-2-(4-biphenyl)-4H-pyrido[1,2-a]pyrimidin-4-one.

To 2 ml of toluene in a test tube with screw cap in inert atmosphere was added Pd(AcO)₂ (11.3 mg 0.05 mmol,), PPh₃ (52 mg, 0.2 mmol). The mixture was stirred for 15 minutes until the formation of complex occurred. Then add **64** (304 mg, 1.0 mmol), Phenylboronic acid (134 mg, 1.1 eq, 1.1 mmol) and 2 ml of Na₂CO₃ 2N.

The mixture was stirred for six hours, then reaction was dump in 30 ml of AcOEt and washed with brine (5 ml x 3). The organic layer was dried on MgSO₄, filtered, and concentrated in vacuo.

The residue was purified through flash chromatography (P.E./ AcOEt 5:5) and the product obtained further crystallized from AcOEt.²³

Yield= 7% as a yellow amorphous powder.

Melting Point 159- 163°C

¹HNMR 11.40 (s, 1H, -OH), 7.96-7.47 (m, 10H, ArH), 7.10 (d, 2H, ArH), 6.11 (s, 1H).

Bibliography

1. Einhorn, C.; Einhorn, J.; Marcadal-Abbadia C.; *Synthetic Communications: An International Journal for Rapid Communication of Synthetic Organic Chemistry* **2001**, 31, 741-748.
2. Goetz, F. J., Hirsch, J. A., Augustine R. L.; Ring-Chain Tautomerism in Anions Derived from Substituted (Arylideneamino)toluenes and (Arylideneamino)oxindoles; *J. Org. Chem.*, 1983, 48, 2468-2472.
3. S. Fliszár, R. F. Hudson and G. Salvadori *Helvetica chimica acta*, **1963**, 7, 1580-1589.
4. John W. Lyga, John A. Secrist III *J. Org. Chem.* **1983**, 48, 1982-1988
5. Alonso A. et al. Preparation of carboxybenzylalkanoates as stimulators of soluble guanylate cyclase. **2001** DE 19943636 A1 20010315.
6. Synthesis of β -hydroxy esters using highly active manganese Suh, Y. S.; Rieke, R. D; *Tetrahedron Letters* **2004** 451807–1809. Supp. Info.
7. *Org. Lett.*, **2010**, 12 (21), pp 4739–4741 supporting info.
8. Bruno G.; Costantino L.; Curinga L.; Maccari R.; Monforte F.; Nicolò F. et al. Synthesis and aldose reductase inhibitory activity of 5-Arylidene-2,4-thiazolidinediones. *Bioorganic & Medicinal Chemistry*. **2002**, 10, 1077-1084.
9. Hvidt, T.; Szarek, W. A.; Maclean, D. B.; Synthesis of enantiomerically pure β -amino- α -methylene- γ -butyrolactones by way of ozonolysis of aromatic α -amino acids, *Canadian Journal of Chemistry*, **1988**, 66 779-782.
10. Gage, J. R.; Evans, D. A.; (S)-4-Phenylmethyl-2-oxazolidone *Organic Syntheses*, **1990**, 68, 77.

11. Edmonds, M.K.; Abell, A.D.; Design and Synthesis of a Conformationally Restricted Trans Peptide Isostere Based on the Bioactive Conformations of Saquinavir and Nelfinavir *J. Org. Chemistry* **2001**, *66*, 3747-3752.
12. David A. Evans, Leester D. Wu, John J. M. Wiener, Jeffrey S. Johnson, David H. B. Ripin, and Jason S. Tedrow A General Method for the Synthesis of Enantiomerically Pure α -Substituted, α -Amino Acids through α -Substituted Succinic Acid Derivatives *J. Org. Chem.*, Vol. 64, No. 17, 1999 6411-6417.
13. Pandya, B.A.; Dandapani, S.; Duvall, J. R.; Rowley, A.; Mulrooney, C., A.; Practical asymmetric synthesis of α -hydroxy α -amino acids via complimentary aldol reactions *Tetrahedron* **2011** *67* 6131-6137
14. ¹HNMR data are report in Sheehan, M.; Spangler, R. J.; and Djerassi, C. J. *Org. Chem.* 1971,36, 3526.
Procedure and ¹³CNMR Szczepankiewicz, B. G.; Heathcock, C. H. A Novel Method for Suppression of the Abnormal Fischer Indole Synthesis *Tetrahedron*, **1997**, *53*, 8853-8870.
15. Lafontaine, J. A.; Provencal, D. P.; Gardelli, C.; Leahy, J. W.; The Enantioselective Total Synthesis of the Antitumor Macrolide Rhizoxin D (Supp. Info). *J. Org. Chem.* **2003**, *68*, 4215-4234.
16. Kolba, M.; Bartha, J.; A Convenient Preparation of Iodoalkyl Esters from Lactones *Synthetic Communications* **1981**, *11*, 763- 767.
17. Sepehr, S; Subrumanian, M.; Rhodanine derivatives as PPAR receptor modulators and their preparation, pharmaceutical compositions and use for treatment and prophylaxis of various diseases. WO **2006/041921** A2
18. Nuti, E.; Panelli, L.; Casalini, F.; Avramova, S., I.; Orlandini, E.; Santamaria, S.; Nencetti, S.; Tuccinardi, T.; Martinelli, A.; Design, Synthesis, Biological Evaluation, and NMR Studies of a New Series of Arylsulfones As Selective and Potent Matrix Metalloproteinase-12 Inhibitors *J.f Med. Chem.* **2009**, *52*, 6347-6361.
19. Mubammad A. et all. *J. Chem. Soc.: Perkin Trans.* (2) **2002**, pag 1662-1668

20. Oikawa, Y.; Sugano, K.; Yonemitsu, O. Meldrum's Acid in Organic Synthesis. 2. A General and Versatile Synthesis of α -Keto Esters. *J. Org. Chem.* **1978**, *43*, 2087-2088.
21. La Motta, C; Sartini, S.; Mugnaini, L.; Simorini, F.; Taliani, S.; Salerno, S.; Marini, A., M.; Da Settimo, F.; Lavecchia, A.; Pyrido[1,2-a]pyrimidin-4-one Derivatives as a Novel Class of Selective Aldose Reductase Inhibitors Exhibiting Antioxidant Activity *J. Med. Chem.* **2007**, *50*, 4917-4927.
22. S. Nerdinger, C. Kendall, X. Cai, R. Marchart, P. Riebel, M. R. Johnson, C.-F. Yin, Combined Directed ortho Metalation/Suzuki-Miyaura Cross-Coupling Strategies. Regiospecific Synthesis of *m*-Chlorodihydroxybiphenyls and Polychlorinated Biphenyls *J. Org. Chem.* **2007**, *72*, 5960-5967

CHAPTER 5

The ubiquitin–protein ligase system

The Ubiquitin-proteasome system.

The ubiquitin–protein ligase system (or ubiquitin protease system; UPS) was discovered in the early 1980. The presence of three enzymes was described and named as E1, E2 and E3. ¹ Ubiquitin is a small protein made by 76 aminoacids

Regulation of protein degradation is an essential aspect of cell signalling.

Cells must be able to respond immediately to environmental changes to maintain homeostasis or to undergo specified developmental decisions; Ubiquitin–proteasome system (UPS) is responsible for much of the regulated proteolysis in the cell. ²

The ubiquitin and ubiquitin-like pathways are integral to the normal function of eukaryotic cells. Protein turnover, trafficking, and the modulation of protein function have been ascribed to ubiquitination.

Ubiquitination of target proteins proceeds in a stepwise format involving E1, E2 and E3 enzymes.

The ubiquitin system is hierarchically structured and confers specificity for protein substrates through a multitude of E3 ubiquitin ligases. A few E1 ubiquitin-activating enzymes exist; however, at least 50 E2 ubiquitin-conjugating enzymes and about 500 E3 ubiquitin ligases are codified by human genome.

Ubiquitination occurs in three steps.

In the first:

- ubiquitin or ubiquitin-like proteins (Ubl) are activated through an ATP-dependent manner by the enzymes E1 which catalyzes the adenylation of the Ubl C-terminus. E1 enzyme forms a thioester between a conserved catalytic cysteine and the Ubl. Next, E1 is loaded with a second Ubl molecule, followed by its C-terminal adenylation.

In the second:

- The E1-Ubl thioester complex recruits a conjugating enzyme denoted as E2 to facilitate transfer of the thioester-linked Ubl to a conserved E2 cysteine (tranthioesterification).

And in the last:

- E2 enzyme interacts with a specific E3 ubiquitin-protein ligase resulting in the autoubiquitination of E3 or ubiquitination of target proteins on specific lysine residues. A schematic representation is depicted in Figure 4.1.

Target proteins can be ubiquitinated in a manner that their function, localization, or stability within the cell results altered. Generally, the addition of one to four ubiquitin molecules to a target protein leads to a change in its localization and/or function. The addition of many ubiquitin moieties

(polyubiquitination) leads to protein degradation by the 26S proteasome, a 2.5-MDa molecular machine built from approximately 31 different subunits, which catalyzes protein degradation.³

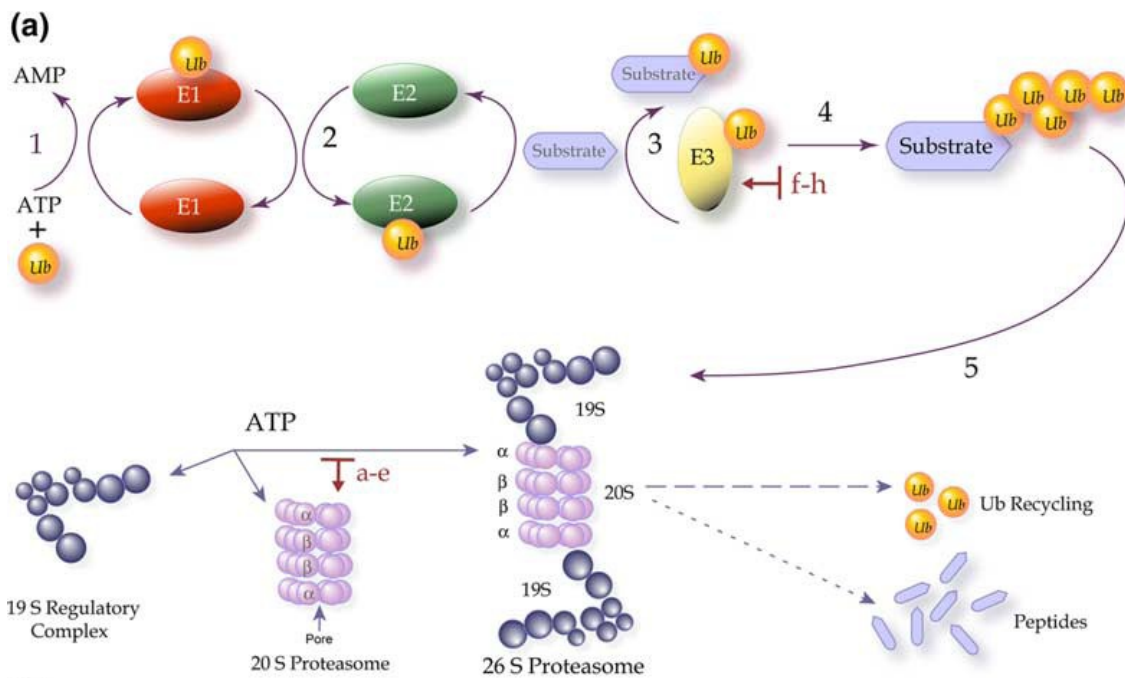


Figure 4.1. Schematic function of Ubiquitin- Proteasome system.¹

The 20S and 26S Proteasome Complexes

Proteasomes consist of a large proteinase complex with multiple catalytic domains that are located in the cytosol as well as the eukaryotic cell nucleus. The S26 proteasome is a multi-catalytic protease complex consisting of a S20 core, and S19 regulatory particle, or cap.

The 20S catalytic subunit contains six unique ATPdependent serine protease sites, divided equally between chymotrypsin, trypsin and caspase-like activities. The biological importance of the proteasome is defined by the observation that deletion of 13 out of 14 genes which make up the core S20 complex result in lethal phenotypes.⁴

The E1 enzymes

The Ub-E1 consists of four building blocks:

- the adenylation domains (hereafter, IAD and AAD, for “inactive” and “active” adenylation domain, respectively), the latter of which binds ATP and Ub;
- the catalytic cysteine half-domains, which contain the E1 active site cysteine (hereafter, FCCH and SCCH, for “first” and “second” catalytic cysteine half-domain, respectively) inserted into each of the adenylation domains;
- a four-helix bundle that represents a second insertion in the IAD and immediately follows the FCCH;
- the C-terminal ubiquitin-fold domain (UFD), which recruits specific E2s.⁵

Catalytic mechanisms of canonical E1s

The catalytic mechanism is best characterized for the ubiquitin E1, UBA1. After UBL C-terminal adenylation, the ubiquitin~AMP is attacked by the catalytic Cys of UBA1, producing a covalent thioester linkage between the Cys sulfhydryl of UBA1 and the C-terminus of ubiquitin. Subsequently, UBA1 catalyzes the adenylation of a second ubiquitin molecule. Thus, UBA1 becomes asymmetrically loaded with two ubiquitin molecules at distinct active sites: ubiquitin (T stand for thioester) is covalently linked to the E1’s Cys via a thioester bond; ubiquitin (A, stand for adenylation) is associated non-covalently at the adenylation active site. Ultimately, UBA1 physically associates with a cognate E2 conjugating enzyme, and a thioester transfer reaction ensues whereby the C terminus of ubiquitin (T) is transferred to the E2’s catalytic Cys. Individual steps of the E1 reaction are reversible. Progression of the cascade is driven by release of the small molecule products PPi and AMP in the first and second steps, respectively.

A curious feature of the E1-E2 cycle is the asymmetric double-loading of E1 with two ubiquitin molecules. Why double load? Although a previous study showed that a partially purified UBA1-ubiquitin complex containing only the single ubiquitin (T) is capable of transferring the ubiquitin to an E2, this transfer is accelerated by ubiquitin (A) adenylate. Also, UBA1 adenylation active site mutants generate an E2-Ub complex more efficiently than would be predicted based on their crippled adenylation of ubiquitin, further indicating cross-talk between the adenylation active site and E1-E2 thioester transfer. Coupling the second adenylation reaction with ubiquitin transfer to E2 might make the cascade energetically or conformationally favourable, or might prevent the E1 from

becoming trapped in an unfavourable conformation. A mechanism similar to the one of UBA1 has been confirmed for the heterodimeric E1 of NEDD8, NAE1-UBA3, through biochemical and structural studies. Thus, it is likely that mechanistic and structural studies of a subset of canonical E1s provide broad insights into this E1 class as a whole. ⁶

The E2 enzymes

E2 enzymes are easily recognized from their evolutionarily conserved 150 residue catalytic 'Ubc' domains. Ubc's have a compact structure shaped essentially like a prolate ellipsoid, comprised of four α -helices, a short 310 helix near the active site, and a four-stranded antiparallel β -sheet. On the "bottom", the active site Cys to which Ub (or Ubl) becomes conjugated is nestled in a catalytic groove surrounded by highly conserved amino acids that mediate both thioester formation (reception of Ub from the E1 Ub-activating enzyme) and substrate ubiquitination (isopeptide bond formation with a substrate lysine). Most notable is a trio of residues known as the 'HPN' motif, usually found ten residues to the N-terminal side of the active site Cys. The His is thought to play a structural role in forming the E2 active site, whereas the Asn residue is important for mediating the catalysis of an isopeptide between Ub and a substrate lysine. As the general mechanism for ubiquitination suggests, an E2 must interact with an E1 and an E3; both interactions use partly overlapping surfaces on one pole of the Ubc ellipsoid. The E1/E3 interaction site comprised the residues on the N-terminal helix, or helix 1 (H1), and loops 4 and 7 (L4 and L7; sometimes referred to as L1 and L2). The shared surface implies that an E2 must be free of the E3 before becoming re-loaded with Ub. Many E2s are characterized by additional segments located within and flanking the Ubc domain. For example, Cdc34 has a 12-residue acidic loop near the 310-helix of its Ubc that is important for catalyzing poly-Ub chain formation. More common are E2s that contain variable N- or C-terminal extensions appended to the Ubc domain. Thus historically, the E2 family has been divided into four classes according to the presence of these additional protein segments: Class I, Ubc domain only; Class II, Ubc domain plus a terminal extension; Class III, Ubc plus an N-terminal extension; Class IV, Ubc plus both N- and C-terminal extensions. However, while the topology of the Ubc domain is highly conserved, N- and C-terminal extensions are widely variable in both size and structure. Sizes of extensions vary from a ~50-residue C-terminal. Although a tidy way to group E2s, the classifications are not predictive for functionality, such as E3s with which a given E2 will interact, or whether an E2 transfers mono-Ub or is capable of building a poly-Ub chain. In a recent effort to classify E2s, a phylogenetic analysis of similarities within the Ubc domains yielded 17 different families of E2s. In this scheme, five of the ~45 Human E2s are assigned to the family

that includes the UbcH5 isoforms while other families have only one or two members. Assigning functional significance to each family may have limited utility when there are half as many families as E2s, and additional biochemical and functional characterization will be required to lend predictive value to this fine-grained classification.⁷

Rad6 E2 enzyme.

Rad6 and its human homologues, Rad6a/b, are particularly important E2 enzymes that have been shown to be involved in DNA damage tolerance (DDT), histone modification, and proteasomal degradation, a clear intrinsic ability to form ubiquitin chains, although other functions of Rad6 may exist. DDT has been extensively characterized as a two-step pathway. In the first step, Rad6/Rad18 monoubiquitinate PCNA on K164 at stalled replication forks to signal for recruitment of damage-tolerant polymerases. Next, Ubc13/MMS2/Rad5 can form K63-linked polyubiquitin chains on modified PCNA to initiate error-free DNA repair. In this process Rad6 monoubiquitinates only PCNA, even in vitro. Rad6a/b, with RNF20/40 (Bre1) as E3 ligase, will monoubiquitinate histone H2B in human cells on K120 as an essential step prior to H3 methylation by Set1 and Dot1. Finally, Rad6 together with Ubr1 is associated with ubiquitin chain formation within the N-rule pathway. In this role, Rad6 is essential for the formation of K48 ubiquitin chains on proteins bearing an N degron, which marks the target for proteasomal degradation. Interestingly, Rad18, Bre1, and Ubr1 all contain additional Rad6 recognition sites outside a canonical RING interface.⁸

UbcH5b E2 enzyme.

UbcH5b is one of the E2 enzymes that have been demonstrated to form polyubiquitin chains in cooperation with several E3 enzymes. UbcH5b has been postulated to gain access to various acceptor sites on the substrate in an efficient manner. Its structure has been recently elucidated.⁹

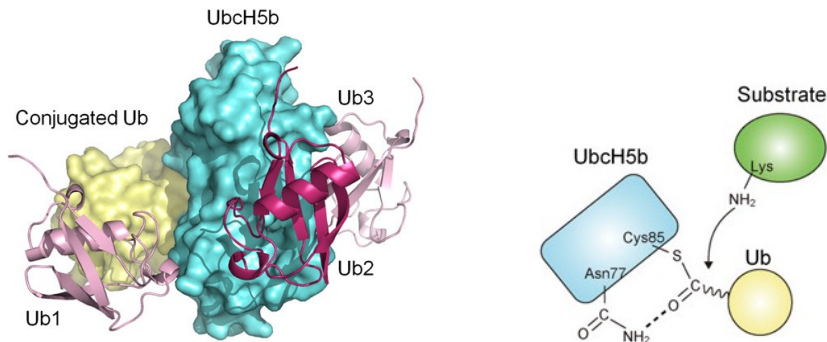


Figure 4.2. Model for catalytic reaction of nucleophilic attack on UbcH5b-Ub. ⁹

The E3 enzymes

Specificity in targeting proteins for ubiquitination lies mostly in the E3 enzyme.

There are two major classes of E3 enzymes:

- U- Box.
- The HECT (**H**omologous to the **E**6-**A**P **C**arboxyl **T**erminus) -type E3 ubiquitin ligases .
(These include Smurf1, Smurf2, AIP4, and Nedd4 among others).
- The RING finger domain proteins.

RING (**R**eally **I**nteresting **N**ew **G**ene) finger protein with ubiquitin E3 ligase activity implicates the presence of a double Zn^{2+} binding motif arranged in a cross-brace structure termed RING-finger, as being essential for ubiquitin E3 ligase catalytic activity.

The critical role of the Zn^{2+} containing RING domain of BCA2 has been demonstrated by point mutation of key zinc-binding cysteine residues leading to the complete loss of enzyme activity.

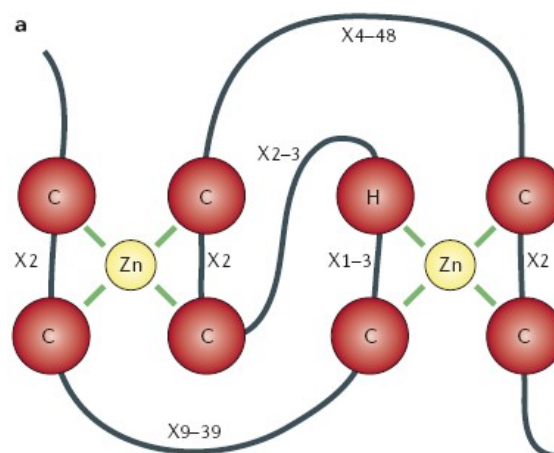


Figure 4.3. Most of the RING fingers contain two zinc atoms (yellow) coordinated with cysteine or cysteine/histidine-rich clusters (red).²

For example, ring finger proteins Mdm2, Efp and BRCA1/BARD have ubiquitin E3 ligase activity and have been shown to have a significant biological role in breast and other cancers.

A notable feature of RING E3 ubiquitin ligases is that the enzymatic activity of the E3 ligase can be monitored through autoubiquitination of the protein in vitro.

Autoubiquitination is the process by which the E3 enzymes catalyze the addition of polyubiquitin to themselves. This can result in the degradation or change of function of the E3 protein in vivo.¹⁰

The BCA2 E3 ubiquitin ligase.

Many of the known E3 ligases play a role in various diseases, including breast cancer development and progression. The Breast Cancer- associate protein 2 (BCA2) is one of this.

BCA2 is an E3 ubiquitin ligase that was isolated from an invasive breast cancer cell line, and has been shown to be highly expressed in 56% (530/945) of invasive breast cancers, but not in most normal tissues examined. Down-regulation of BCA2 has been shown to inhibit breast cancer cell growth and invasiveness. BCA2 is expressed in the cytoplasm and nucleus, and nuclear BCA2 correlates with positive estrogen receptor status ($p < 0.004$). The classification of BCA2 as a Really Interesting New Gene (RING)-finger protein with ubiquitin E3 ligase activity implicates the presence of a double Zn^{2+} β -binding motif arranged in a cross-brace structure, termed RING-finger, as being essential for ubiquitin E3 ligase catalytic activity. The critical role of the Zn^{2+} β containing RING domain of BCA2 has been demonstrated by point mutation of key zinc-binding cysteine residues leading to the complete loss of enzyme activity. BCA2 (also known as Rabring7) has been found to complex with a cytoplasmic binding partner Rab7, a small GTPase involved in cellular endocytosis and trafficking of oncogenic receptor tyrosine kinases (such as epidermal growth factor receptor (EGF-R)) for destruction in the lysosome. Hence, targeting BCA2 within breast cancer cells may allow Rab7 to fulfill its function in tyrosine kinase receptor degradation, preventing the receptor recycling and sustained mitogenic signaling known to contribute to the development of resistance to tyrosine kinase inhibitory therapeutics.

Taken together, the data outlined above suggest that BCA2 could prove an important therapeutic target within the E3 ubiquitin ligase class for the future treatment of breast cancer.

Given the crucial role of Zn^{2+} ions in the catalytic RING domain of BCA2, a series of “zinc-ejecting” compounds from the National Cancer Institute database have been screened for their

ability to inhibit BCA2 activity in BCA2-expressing breast cancer cell lines such as MCF-7. These studies have led to the identification of DSF (NSC25953) a registered drug for the treatment of alcoholism by virtue of additional ALDH1 activity, as a potent BCA2-inhibitory antitumor agent. In this paper, we describe the synthesis and antitumor evaluation of four series of novel “zinc-affinic” agents, in order to optimize selective activity against recombinant BCA2 and BCA2-expressing breast cancer cell lines. From this antitumor data, we derived SAR insight into BCA2-inhibitory pharmacophore requirements, leading to the identification of potent and selective BCA2-inhibitory antitumor agents without accompanying ADH-inhibitory activity.

By employing multitumor tissue microarray technology has been found that normal breast, colon, and head and neck tumors lack detectable BCA2 expression. Twenty of 20 breast cancers and 15 of 15 prostate cancers strongly expressed BCA2. Sixty percent of 17 renal cancers had strong BCA2 staining, and none of the clear cell renal tumors had detectable BCA2. Lower levels of BCA2 staining were seen in 57% of 16 colon cancers, in 65% of 22 pancreatic tumors, and in 73% of 17 bladder cancers. Weak expression of BCA2 was seen in 4 of 7 lung tumors and in 6 of 11 head and neck tumors.

A second larger tumor tissue microarray study examined BCA2 expression in 945 invasive breast cancers.

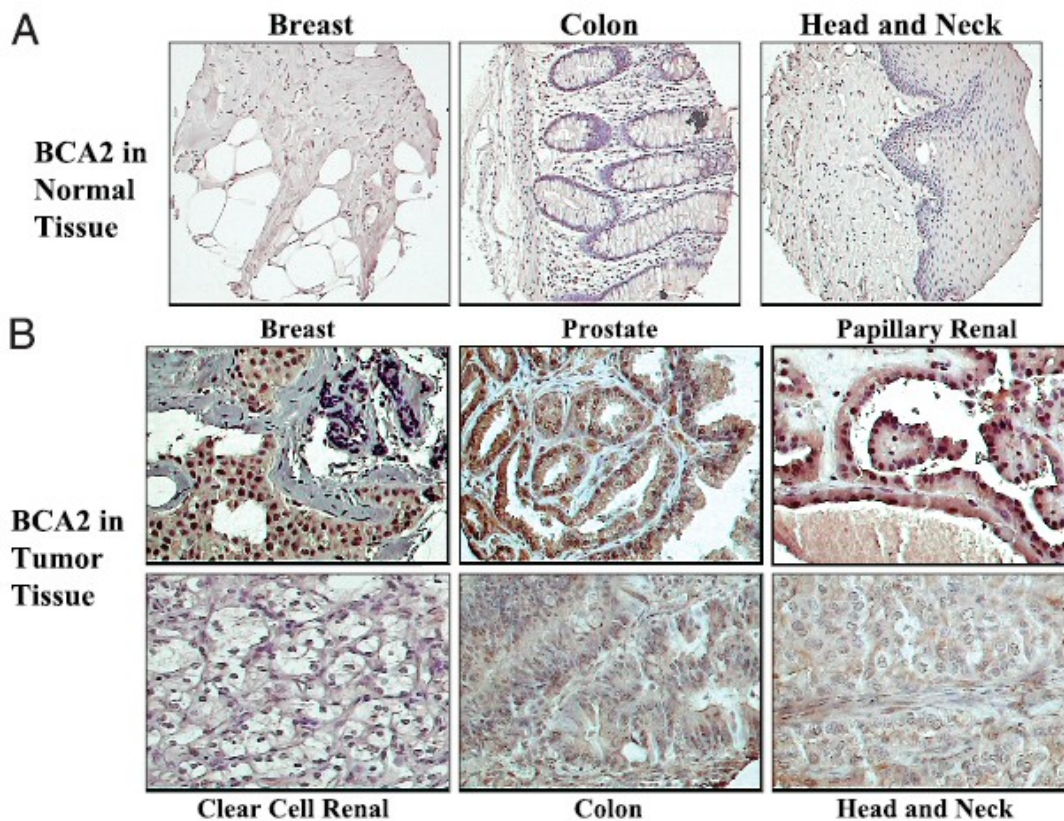


Figure 4.4. Expression of BCA2 protein in normal and tumor tissues. One hundred twenty-five tumor tissues and adjacent normal tissues from the same patient were assembled onto a tissue microarray slide, fixed, and probed for BCA2 expression by immunoperoxidase staining (positive reaction, brown). (A) The top panel shows representative cores (0.6 mm) of normal breast, colon and head and neck tissues stained for BCA2 protein expression. (B) The bottom panel shows strong nuclear and cytoplasmic expression of BCA2 in breast, prostate, and papillary renal cell cancers, but very weak staining in clear cell renal, colon, and head and neck carcinomas.

Comparison with patient data revealed that BCA2 expression correlates with clinical variables such as lymph node status, regional recurrence, and estrogen receptor expression pattern. Although BCA2 expression in the entire cohort did not correlate with overall survival, a subset of patients with regional recurrence history revealed that a higher BCA2 is linked with a significant 5-year survival benefit and that a low BCA2 is linked with lymph node metastasis. The correlation of BCA2 expression with estrogen receptor positivity indicates that BCA2 and estrogen receptor might be coregulated and cross-talked at the transcriptional level, perhaps in the nucleus.¹¹

Ubiquitination in cancer

Cancer can develop from stabilisation of oncoproteins or, alternatively, from destabilisation of tumour suppressor genes. Cancer-associated proteins that have been reported to be regulated by the ubiquitin–proteasome system include the tumour suppressors, p53 and p27, the cell surface receptors for growth factors, epidermal growth factor receptor (EGFR) or transforming growth factor- β Receptor (TGF- β R) complex, as well as cell cycle and oncogenic transcription regulators.

A recent study investigated the level of 20S catalytic proteasome core in plasma of healthy individuals versus that of patients plasma having various neoplastic diseases including acute myeloid leukaemia (AML), Hodgkins disease, chronic myeloproliferative syndromes and solid tumours. The results derived by comparing these individuals showed that the 20S catalytic proteasome core levels in plasma of the pathological states was markedly increased, and was, in fact, up to 1000-fold higher in patients with solid tumours compared with plasma of normal subjects. While the number of cancer-related proteins tagged with ubiquitin and destined for degradation in the proteasome as well as proteasome particles are manifold, little is known about the role of the individual components of the ubiquitin system in tumourigenesis. Only a limited number of the ubiquitin-conjugating enzymes and ligases have been examined for their expression pattern in a large number of human tumours.

A single E1 enzyme is responsible for the initial ubiquitin activation in mammalian cells. Although the deletion of the gene has been shown to be lethal, an involvement in cancer has not been described. An E2 conjugating enzyme (UbcH10) and few E3 ligases studied in relation to cancers, were shown to have high expression levels in malignancies. The E2 UbcH10, for which protein expression data are lacking, was found at extremely low RNA levels in normal tissues, while RNA expression was high in primary tumours such as lung, stomach, uterus and bladder cancers. The prototypic example of a protein that plays a pivotal role in many cancers and is regulated by substrate-specific E3 ubiquitin ligases is p53. The tumour suppressor protein p53 plays a crucial role in cell cycle control, DNA repair and apoptosis. Two E3 ligases, namely the RING-type E3 ligase Mdm2 and the HECT-type E3 ligase E6-AP can effect its degradation by the proteasome. Cervical cancers have been strongly associated with infections by the oncogenic human papilloma virus (HPV) forms 16 and 18. As a result, the E6 and E7 gene products of HPV are detected in these tumours. It is believed that p53 is present at very low levels in cervical cancer cells because it is associated with the E6/E6- AP E3 ligase complex, and is therefore rapidly degraded by ubiquitin-mediated proteolysis.

In the vast majority of tumours, Mdm2 regulates p53 by either inhibiting its transcriptional activity or targeting p53 for ubiquitination and proteasomal degradation.

Thus, overexpression of Mdm2 provides an alternative to p53 mutation and/or deletion leading to development of cancers. Mdm2 is recognised as the major ubiquitin ligase for p53 and has been found overexpressed in several human tumour types. While Mdm2 overexpression by means of gene amplification is mainly seen in soft tissue sarcomas and gliomas, transcriptional/translational overexpression has been found in acute lymphoblastic leukaemia (ALL), melanomas and breast carcinomas. Mdm2 overexpression was predictive for a poor outcome in sarcomas, gliomas and ALL, but was identified as a favourable prognostic marker in melanoma and breast cancer patients. Latter studies indicate that Mdm2 might have tissue-specific, p53-independent functions in cancers, for example as a regulator of cell proliferation by targeting tumour suppressor gene(s) as well as other key proteins governing cell growth (s).

Another HECT-type E3 ligase that has emerged as being important in certain cancers is Smad ubiquitination regulatory factor-2 (Smurf2). High-level expression of Smurf2 was shown to correlate with a poor prognosis in oesophageal squamous cell carcinoma. Smurf2 directs the ubiquitylation and proteasomal degradation of R-Smads, and the TGF- β receptor complex. TGF- β signalling molecules have been shown to play a crucial role in breast and other cancers and it is therefore likely that the Smurf2 HECT-type E3 ligase will also have functions in these tumour types. A RING-type E3 ligase with proven role in breast cancer is BRCA1. Germline mutations in

the RING finger of the tumour suppressor gene BRCA1 predispose women to early onset breast tumours. BRCA1 ubiquitin ligase activity is enhanced when it is dimerised with BRCA1-associated RING domain (BARD1) and has been implicated in p53-associated DNA damage response. Together, these findings indicate that cancer cells maintain a higher amount of proteolytic machinery that would likely enable them to cope with the normal cells proteomic “repair response” and either facilitate degradation of tumour suppressor proteins or activation of proto-oncogenes.

From this generalised perspective and after considering the fact that cancer remains a largely incurable disease with few long-term treatment options, the ubiquitin–proteasome system evolves tantalisingly with a multitude of opportunities for targeted therapeutic Interventions.¹

Many of the known E3 ligases play a role in various diseases, including breast cancer development and progression. Among the first RING proteins to be associated with ubiquitination and cancer were the multisubunit complex E3 ligases ROC1 and APC11.¹¹

Expanding understanding of the UPS and its role in human diseases has elicited significant interest in the development of small molecules that target specific components of the pathway. The role of the UPS in disease is really in its infancy, as only a small fraction (perhaps <20%) of the genes with potential links to the pathway based on known sequence motifs have been studied in any detail.

BCA2 and Estrogen Receptor Co-Expression in Invasive Breast Cancer

Estrogen regulates the proliferation and development of tissues expressing estrogen receptors and is a risk factor for breast cancer development. Ligand binding activates both estrogen receptor (ER)-dependent transcription and ER ubiquitination. ER ubiquitination and proteasome activity are intimately linked to ER-dependent transcriptional activation. Proteasome inhibitors and mutations that inhibit co-activator binding both abrogate ligand-mediated ER proteolysis and ERE transcriptional activity. Different ligands stimulate ER proteolysis to different degrees, and the ubiquitin ligases BRCA1, MDM2, and E6AP can all stimulate estrogen-induced transcriptional activity. The BCA2 protein is an ubiquitin ligase co-expressed with the ER in breast cancers. We have studied BCA2 protein expression in a large collection of over 1,000 invasive mammary carcinomas, termed the Henrietta Banting Breast Cancer Collection (HBBCC). This breast cancer tissue resource located at Sunnybrook Health Sciences Centre, Toronto, has been well characterized for established molecular markers such as ER, PR (progesterone receptor) and HER2/Neu, along with clinico-pathological variables and outcomes. By performing comparative BCA2 protein expression analysis on tissue microarrays of the HBBCC and by using the HBBCC database, we obtained clues about a potential function of the E3 ligase in invasive breast cancer. BCA2 is

expressed in the cytoplasm and nucleus of breast cancer tissues. Nuclear BCA2 expression however, was the predominant site of protein location in breast cancer cells (Figure 4.5). Nine hundred and forty-five invasive breast carcinomas of the HBBCC were evaluable for nuclear BCA2 expression, representative tissue sections are shown in (Figure 4.5a). Four hundred and fifteen cases or 43.9 % of the invasive breast cancer cohort had low nuclear BCA2 levels (BCA2 intensity score ≤ 1), 530 patient tissues or 56.1% of the study cohort were found to overexpress BCA2 (BCA2 score >1). Some normal breast tissues also expressed low amounts of nuclear BCA2 protein (score ≤ 1). Sixty-seven percent (635) of the HBBCC breast cancers were estrogen receptor positive.

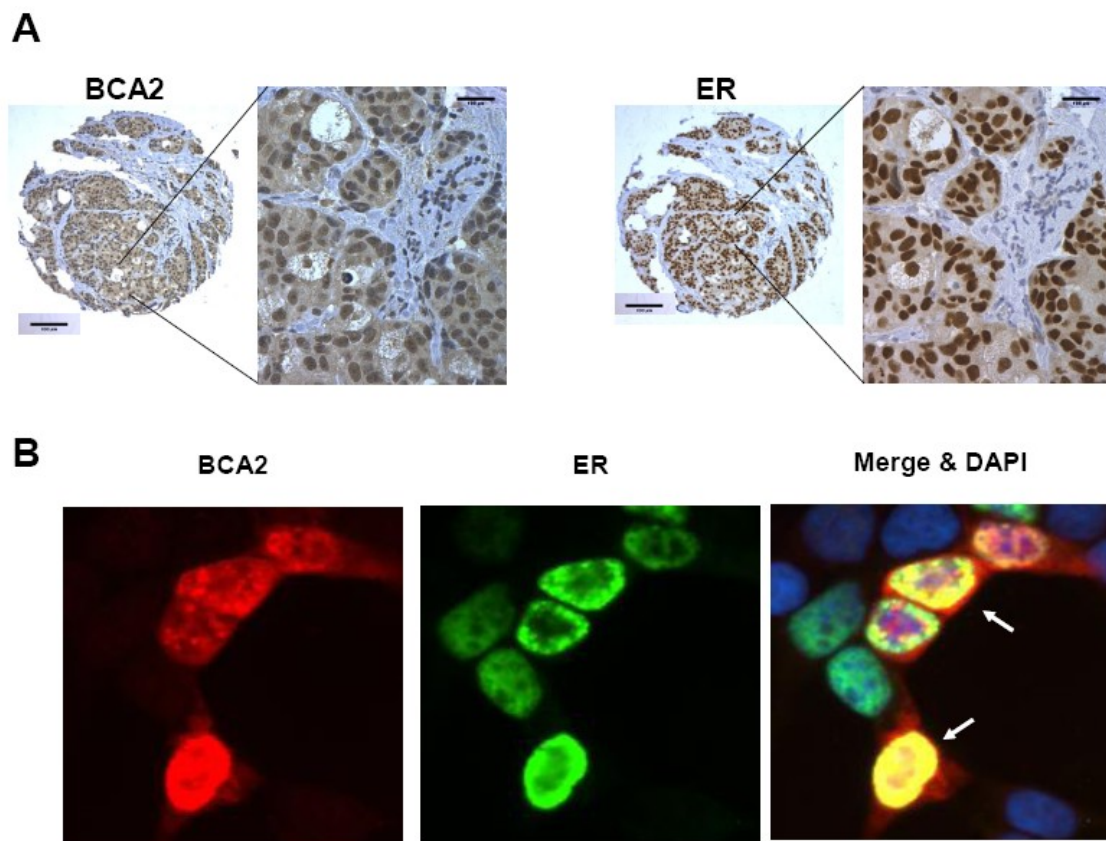


Figure 4.5. (a) Comparison of BCA2 and ER expression by immunoperoxidase staining in a representative case of invasive breast cancer. The data reveal co-expression of ER and BCA2 in the nuclei of cells staining positive for the antigens (brown color: diaminobenzidine). Overall, 67% of the 945 invasive breast cancer cases were positive for ER and of those 74% were positive for both, ER and BCA2. (b) Colocalization of ER (green, FITC-labeled anti-mouse antibody) and BCA2 (red, TRITC-labeled anti-rabbit antibody) in the nuclei (merge: yellow, white arrows; nuclei were counterstained with DAPI = blue) of HEK293T cells.

The statistical analysis of the HBBCC nuclear BCA2 protein expression study revealed that three variables yield significant results: first, patients with low BCA2 (57.7% of 213), were more likely to have lymph node metastasis at presentation than those with higher BCA2 levels (49.9% of 229, $p=0.02$). Second, women with invasive breast cancers with low BCA2 (8.6 % of 415) were more likely to experience regional re-occurrence than those with higher BCA2 (5.3 % of 530) ($p = 0.05$). The third significant correlation was very strong: *nuclear BCA2* expression was correlated with a *positive estrogen receptor* status (figure 4.5a).

67.1 % of all 945 invasive HBBCC cases stained positive for ER expression. 74% of breast cancers that were ER-positive had also nuclear $BCA2 > 1$ ($p = 0.004$). Because of the significant statistical correlation found between invasive breast cancers expressing ER and BCA2, we compared the pattern of expression of these two proteins. Core by core analysis of consecutive tissue sections indicated that BCA2 and ER are mostly co-expressed (odds ratio = 1.5) (Figure 4.5a), cells strongly positive for BCA2 were positive for ER. It is important to note that high expression of BCA2 is not beneficial at the cellular level for inhibiting cancer progression and may be a contributing factor in metastasis. However the high correlation of co-expression with ER makes higher expression of BCA2 a marker for good prognosis in breast cancer due to the availability of highly effective treatment options.¹²

The MDM2-p53 path and its inhibitors.

The p53 tumor suppressor protein is required for the cytostatic and cytotoxic effects of many anticancer agents with loss of p53 function correlating with a decrease in sensitivity to these agents. Adjuvant therapies that augment p53 function are predicted to sensitize cells to cancer therapies that rely upon p53 for their efficacy. The p53 proximal regulator, MDM2, is an ubiquitin ligase that binds to and negatively regulates p53 stability and function. Pharmacological agents that block the MDM2-p53 interaction or that selectively inhibit MDM2-mediated proteolytic degradation of p53 can potentiate the anti-proliferative properties of p53 in cultured tumor cells and in xenograft models, suggesting that MDM2 antagonists may have high therapeutic potential.¹³

The first small-molecule capable to inhibit MDM2 is Nutlins (cis-imidazoline derivatives) which were identified in a chemical library screen for small molecules able to block the interaction between p53 and MDM2. Based on their structural, biochemical and pharmacodynamical parameters, Nutlins mimic the spatial conformation of the crucial MDM2-interacting residues on p53 and therefore are able to occupy the p53-binding pocket and displace p53 from it.

As expected, Nutlins activate p53-dependent cell-cycle arrest and apoptosis in cancer cell lines. Importantly, Nutlins are effective in vivo upon oral administration: they halt the growth of nude mouse tumour xenografts without noticeable toxicity to healthy tissues. These findings indicate reasonable bioavailability of these small-molecule MDM2 inhibitors.

Another p53-stabilizing small molecule (RITA; 2,5-bis(5-hydroxymethyl-2-thienyl)furan) was initially found to have anticancer activity in the National Cancer Institute Anticancer Drug Screen and recently scored as a hit in another functional chemical library screen designed to identify compounds that specifically arrest growth of a p53-positive cancer cell line.

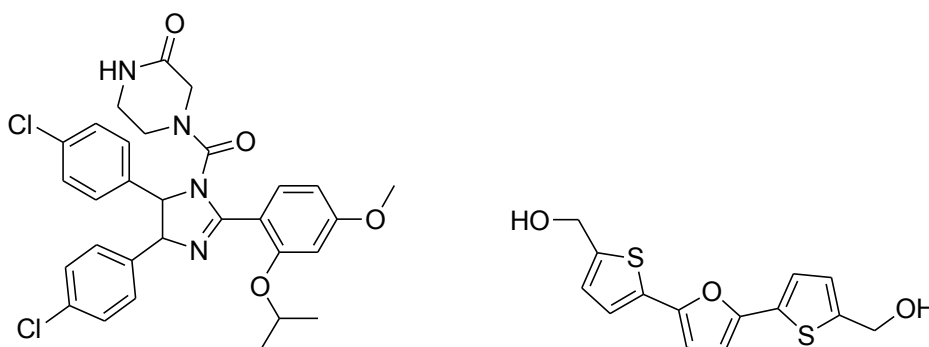


Figure 4.6. Nutlin 3 and RITA.

RITA is unrelated to the Nutlins both structurally and functionally. In contrast to the Nutlins, RITA does not seem to bind MDM2. Instead, it binds the N terminus of p53 and, although no definitive structural data are currently available, it seems to either prevent the recognition of p53 by MDM2, stabilize the N-terminal α -helix domain of p53 in the MDM2 groove, or both⁷⁵. Interestingly, RITA seems to prevent p53 from interacting with other regulatory proteins⁷⁵, such as p53-associated parkin-like cytoplasmic protein (PARC, the p53 cytoplasmic anchor) and p300, which, in addition to acetylating p53 can promote p53 polyubiquitylation by MDM2 as p53's 'E4'. The RITA-stabilized p53 is transcriptionally active as it can promote expression of endogenous p53-target genes.

Most excitingly, RITA slows down the growth of mice tumour xenografts in a dose-dependent manner.²

Bibliography

1. Burger, A., M.; Seth, A., K.; The ubiquitin-mediated protein degradation pathway in cancer: therapeutic implications. *European Journal of Cancer* **2004** *40* 2217–2229)
2. Nalepa, G.; Rolfe, M.; Harper, J. W. Drug discovery in the ubiquitin- proteasome system. *Nat. Rev. Drug Discovery* **2006**, *5*, 596–613.
3. Voges, D.; Zwickl, P.; Baumeister W.; The 26S proteasome: a molecular machine designed for controlled proteolysis. *Annu Rev Biochem.* **1999**; *68* ,1015-68.
4. Thompson, S. J.; Loftus, L. T.; Ashley, M. D.; Meller R.; Ubiquitin-proteasome system as a modulator of cell fate. *Current Opinion in Pharmacology* **2008**, *8*, 90–95.
5. Lee, I.; Schindelin, H.; Structural Insights into E1-Catalyzed Ubiquitin Activation and Transfer to Conjugating Enzymes *Cell* **2008**, *134*, 268–278.
6. Schulman, B. A.; Wade Harper, J.; Ubiquitin-like protein activation by E1 enzymes: the apex for downstream signalling pathways. *Nat Rev Mol Cell Biol.* **2009** *5* 319–331.
7. Wenzel, D. M.; Stoll, K., E.; Klevit, R. E.; E2s: Structurally Economical and Functionally Replete. *Biochem J.* **2010** *1* 31–42.
8. Hibbert R., G.; Huang, A.; Boelens, R.; Sixma T., K.; E3 ligase Rad18 promotes monoubiquitination rather than ubiquitin chain formation by E2 enzyme Rad6. *Proc. Natl. Acad. Sci.* **2011** *108* 5590-5.
9. Sakata, E.; Satoh, T.; Yamamoto, S.; Yamaguchi, Y.; Yagi-Utsumi, M.; Kurimoto, E.; Tanaka, K.; Wakatsuki, S.; Kato, K.; Crystal Structure of UbcH5b-Ubiquitin Intermediate: Insight into the Formation of the Self-Assembled E2-Ub Conjugates *Structure* **2010** *18* 138–147.
10. Amemiya, Y.; Azmi, P.; Seth, A.; Crystal structure of UbcH5b~ubiquitin intermediate: insight into the formation of the self-assembled E2~Ub conjugates. *Mol Cancer Res* **2008** *6* 1385-1396

11. Burger, A.; Amemiya, Y.; Kitching, R.; Seth, A., K.; Novel RING E3 ubiquitin ligases in breast cancer *Neoplasia* **2006** *8* 689-695.
12. Burger, A.; Kona, F.; Amemiya, Y.; Gao, Y.; Bacopulos, S.; Seth, A., K.; Role of the BCA2 ubiquitin E3 ligase in hormone responsive breast cancer. *The Open Cancer Journal*, **2010** *3* 116-123.
13. Ghassemifar, S.; Mendrysa, SM.; MDM2 antagonism by nutlin-3 induces death in human medulloblastoma cells *Neurosci Lett.* **2012** in press.

CHAPTER 6

Inhibitors of E2, E3 enzymes

Carbamo(dithioperoxo)thioates derivatives as BCA2 inhibitors.

BCA-2 is an enzyme over-expressed in more than 57% of aggressive breast cancer carcinomas cell line.

Westwell et al. From the Cardiff University, have identified compounds capable to inhibit BCA2. A precise rationale was follow for the identification of inhibitors of BCA2. ¹

1. Exploring the Structural Requirements for Inhibition of the Ubiquitin E3 Ligase Breast Cancer Associated Protein 2 (BCA2) as a Treatment for Breast Cancer

A series of molecule with a zinc- binding core capable to remove Zn^{2+} from the RING domain of BCA2 was synthesized taking as model Disulfiram (DSF), a well know compound used for fight alcoholism which have a zinc binding group moiety recognized in literature. ^{2,3}

As a matter of fact, DSF dramatically decrease the conversion of acetaldehyde to acetic acid after ingestion of alcohol through inhibition of human mitochondrial aldose.

Inhibition of BCA2 by DSF is not correlated to its zinc-chelating property, but to its capacity in the modification of active site, as a matter, for DSF, the zinc-ejection appear to be favourite respect chelation mechanism.

In order to elucidate the structure-activity relationship, Brahemi et al., have synthesize disulfiram analogues, dithiocarbamates, benzisothiazolones and finally carbamo(dithioperoxo)thioate (Figure 5.1).

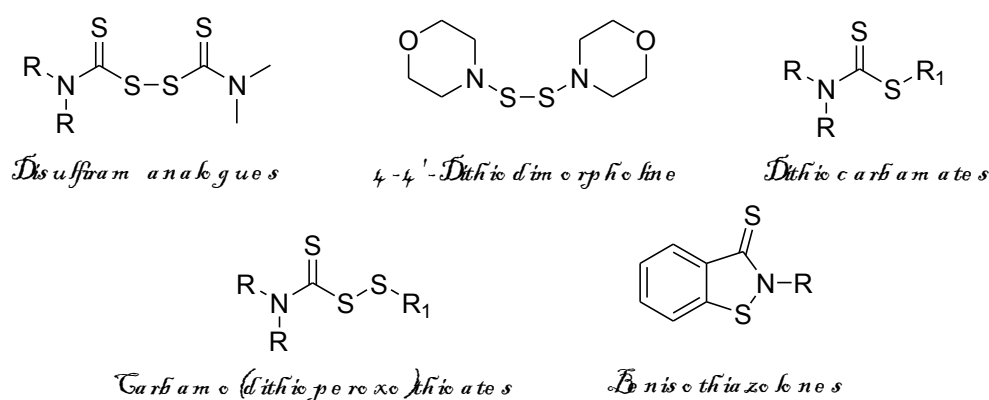
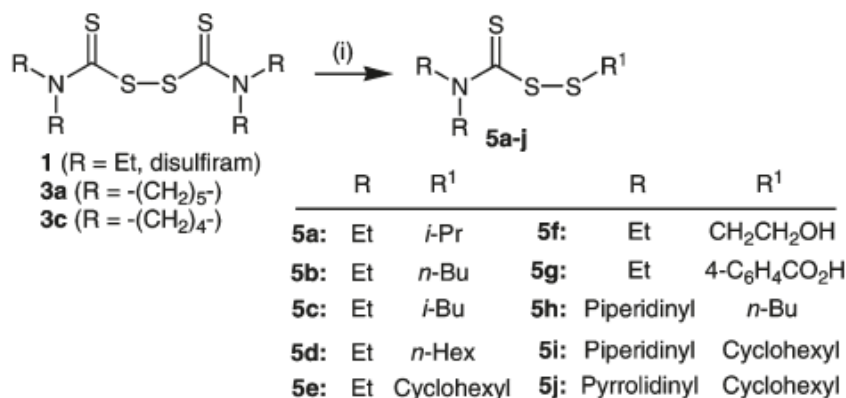


Figure 5.1 Sulphur based inhibitors synthesized by Brahemi et al. as BCA2 inhibitors.¹

Carbamo(dithioperoxo)thioates were synthesized refluxing the corresponding symmetrical Disulfiram analogue in ethanol with the appropriate thiol. ¹



^a Reagents: (i) R¹SH, EtOH, reflux, 16 h.

compound	mean IC ₅₀ ± SD (μM) ^b in cell lines ^c				
	MCF-7	MDA-MB-231	MDA-MB-231/ER	T47D	MCF10A
1 (DSF)	0.1 ± 0.01	> 10	0.32 ± 0.14	0.17 ± 0.03	10 ± 0.2
5a	0.39 ± 0.28	0.96 ± 0.03	0.25 ± 0.1	0.23 ± 0.01	> 10
5b	0.4 ± 0.3	7.4 ± 2.6	0.3 ± 0.13	0.15 ± 0.02	> 10
5c	0.45 ± 0.25	6.0 ± 2.8	2.1 ± 0.43	0.20 ± 0.02	> 10
5d	0.43 ± 0.1	> 10	0.35 ± 0.28	0.23 ± 0.02	> 10
5e	0.3 ± 0.28	0.96 ± 0.01	0.28 ± 0.17	0.18 ± 0.02	> 10
5f	0.5 ± 0.24	> 10	2.75 ± 0.17	0.30 ± 0.03	> 10
5g	0.5 ± 0.2	6.3 ± 2.6	0.55 ± 0.12	0.15 ± 0.01	> 10
5h	0.65 ± 1.2	8 ± 1.6	0.39 ± 0.17	0.35 ± 0.03	> 10
5i	0.6 ± 0.1	6.7 ± 2.5	2.3 ± 0.22	0.25 ± 0.03	> 10
5j	1.4 ± 1.8	4.7 ± 3.9	0.25 ± 0.08	1.35 ± 0.02	> 10

Scheme 5.2 Synthetic pathway for the synthesis of carbamo(dithioperoxo)thioates, product synthesized and inhibitory activity over cancer cell lines.¹

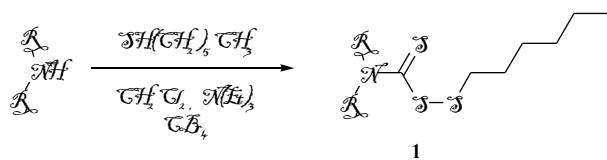
During the time i spent in Cardiff University under the supervision of Prof. Andrew D. Westwell, i synthesized novel carbamo(dithioperoxo)thioates with various secondary amines.

Procedure used is depicted in scheme 5.3, the substituted secondary amines employed for the synthesis of the title compounds are report in the adjacent chart.

Tetrabromomethane was used stechiometrically in the reaction for promote the formation of carbamodithioperoxo bond⁴.

Hexanethiole was used as common reagent for the introduction of the alkyl chain in all the reactions. Almost all the reactions were carried out at room temperature using dichloromethane as solvent except for synthesise compound **1c**, temperature was kept at 0 °C and amine was added very slowly because of reaction exothermicity.

Biological evaluations are ongoing.



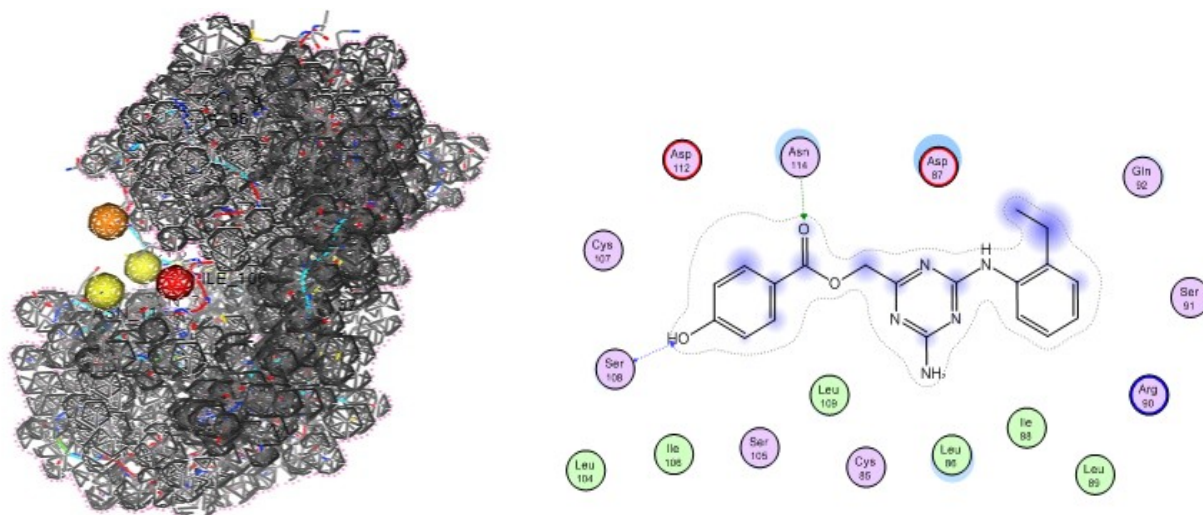
Comp.	R	R ₁
1a	-(CH ₂) ₅ -	
1b	-(CH ₂) ₂ O(CH ₂) ₂ -	
1c	(CH ₂) ₂ NCH ₃ (CH ₂) ₂	
1d	-(CH ₂) ₄ -	

Scheme 5.3. More efficient synthetic route to carbamo(dithioperoxo)thioates.

Triazinic derivatives as Rad6, UbcH5b.

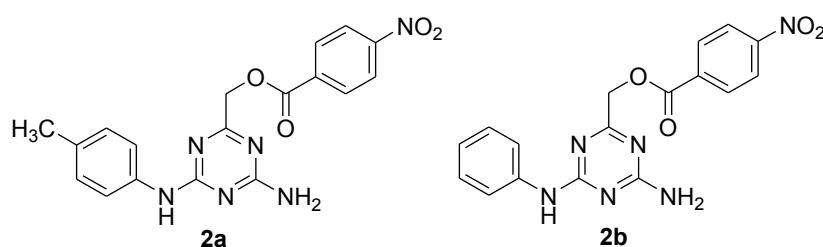
A good amount of triazine-based scaffold BCA2 inhibitors was synthesized by previous PhD student Brahemi G.

He was looking for a pharmacophore capable to inhibit the binding between Ubiquitin and E2 enzyme UbcH5b and his research culminated in the discover of a triazinic based scaffold.



Scheme 5.4 Pharmacophore generation and interaction with aminoacidic residues taken from Brahemi's thesis.

As a matter, the library of triazines was screened in order to obtain the inhibition value on BCA2, an overall negative IC₅₀ values were obtained, but two compounds shown pretty good activity (figure 1.5).



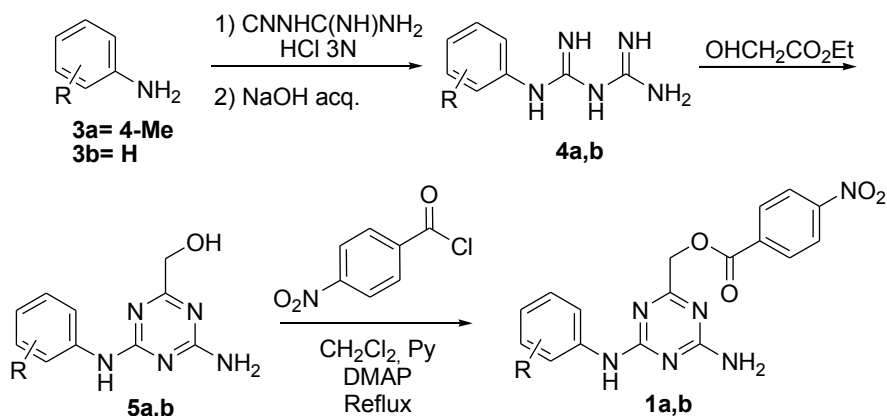
Compound	Rad6 IC ₅₀ (mM)	UbcH5b IC ₅₀ (mM)
2a	0.25	0.65
2b	1	inactive

Figure 5.4 Active compounds **1a** and **1b**.

The classical pathway started with the synthesis of biguanidine **4a** and **4b** from aniline or *para*-toluidine and dicyanamide which were refluxed in aqueous hydrochloric acid.

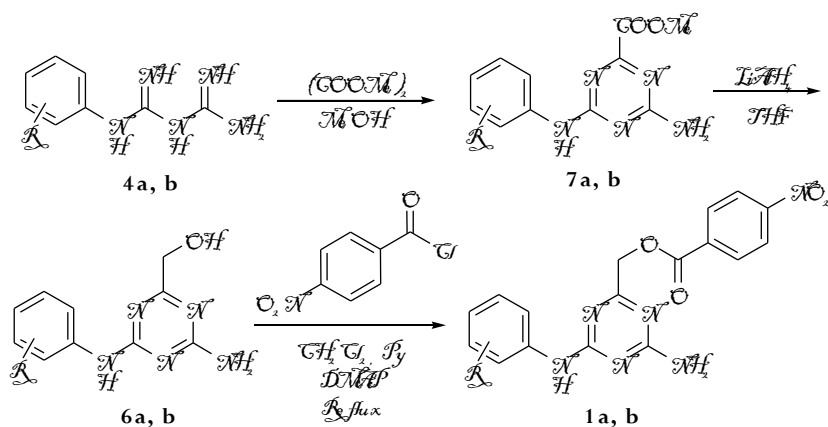
The biguanidine free-base **4a, b** were obtained from the corresponding hydrochloride by treatment with aqueous sodium hydroxide, then cyclized to triazine **5a, b** with ethyl glycolate and esterified with 4-nitrobenzoylchloride affording **1a,b**.

Actually, the cyclization step of biguanidine with ethyl glycolate turned out rather ineffective, as it afforded the corresponding alcohol in low yields. This is why we developed another system for the obtainment of **1.6**.



Scheme 5.5 Brahemi's route to substituted triazines.

The biguanidine was cyclized with dimethyl oxalate instead of ethyl glycolate and the corresponding ester **7a, b** was reduced with Lithium aluminium hydride in dry THF to afford with moderate yield the alcohol **6a, b** (scheme 5.6).

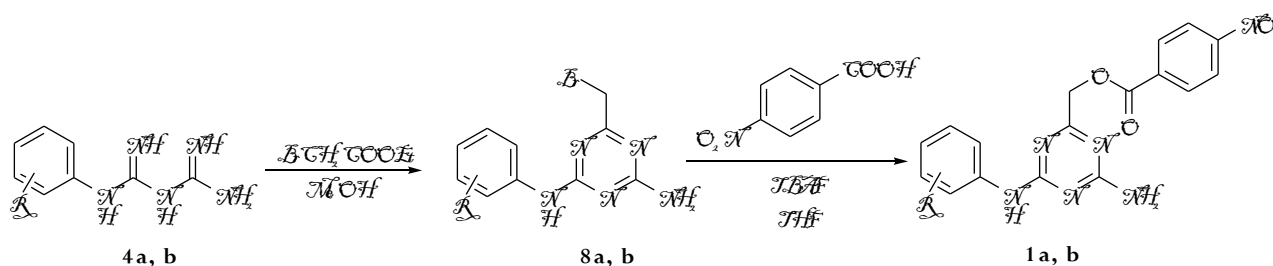


Scheme 5.6 Cyclization with dimethyloxalate and successive reduction.

But another synthetic protocol was adopted for manufacture of title compounds for further raise the yields. Avoiding reducing agents and dry solvents were primary objectives.

We performed a cyclization with ethyl bromoacetate and the bromo derivative 8a and 8b were obtained in good yield. Once opportunely purified through flash chromatography, they were made react with 4-nitrobenzoic acid and TBAF in THF to give the title compound in almost quantitative yields (scheme 5.7).

TBAF performed as a mild base which favours ester formation.⁵

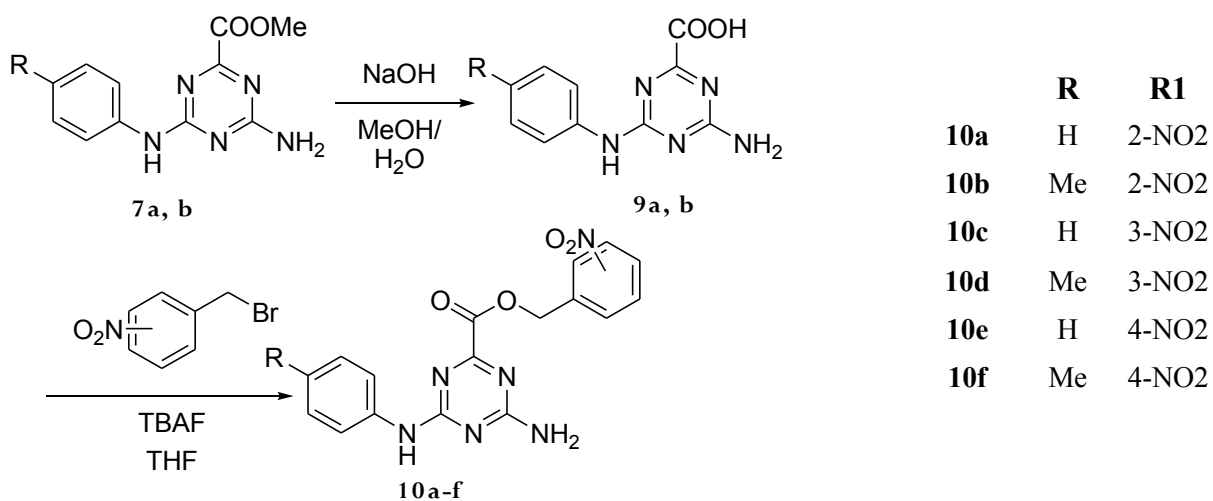


Scheme 5.7 Cyclization with ethyl bromoacetate and treatment with TBAF and 4-nitrobenzoic acid.

Title compounds were obtained in very good yields. Washing organic phase with water and extracting the excess of carboxylic acid with an alkaline solution left final product almost pure. Purification through flash chromatography or crystallization however was necessary for high purity. Exploiting this method, we were able to synthesize the inverse esters of title compounds depicted below (scheme 5.8).

These molecules were made for a better understanding of structure - activity relationship, and for a better knowledge of the esteric function in the inhibition of BCA2.

Synthesis started from methyl ester 7a, b. Subsequent basic hydrolysis and acidification afforded the carboxylic acid 9a, b which reacted with 4-nitrobenzylbromide and TBAF in acetonitrile, afforded the title compound as a precipitate in the reaction environment. The powder was then washed with fresh acetonitrile, on Buchner funnel, and no further purification occurred.



Scheme 5.8 Synthesis of compounds with inversed esteric moiety.

Biological results are expected within few months.

Bibliography

1. Brahem, G.; Kona, F., R.; Fiasella, A.; Buac, D.; Soukupova, J.;Brancale, A.; Burger, A. M.; Westwell, A. D.; Exploring the Structural Requirements for Inhibition of the Ubiquitin E3 Ligase Breast Cancer Associated Protein 2 (BCA2) as a Treatment for Breast Cancer *J. Med. Chem.* **2010** *53* 2757–2765.
2. Bond, A. M.; Hollenkamp, A. F.; Exchange and other reactions associated with zinc(II) dithiocarbamate oxidation and reduction processes observed at mercury and platinum electrodes in dichloromethane. *Inorg. Chem.* **1990**, *29*, 284–289.
3. Saravanan, M.; Prakasam, B. A.; Ramalingam, K.; Bocelli, G.; Cantoni, A. M(S)2(I)2 (M=Zn, Cd) and Hg(S)3I coordination environment of transition metal complexes - synthesis, spectral, and single crystal X-ray structural investigations. *Z. Anorg. Allg. Chem.* **2005**, *631*, 1688–1692.
4. Liang, F.; Tan, J.; Piao, C.; Liu, Q.; Carbon Tetrabromide Promoted Reaction of Amines with Carbon Disulfide: Facile and Efficient Synthesis of Thioureas and Thiuram Disulfides Hexanethiole *Synthesis* **2008** *22* 3579-3584.
5. Wu, Chung-Yi, W.; Ashraf, B.; Sheng-Kai, W.; Chen, Y.;Tetrabutylammonium fluoride-mediated rapid alkylation reaction in microtiter plates for the discovery of enzyme inhibitors in situ. *ChemBioChem* **2005**, *6*, 2176-2180.

CHAPTER 7

Experimental Section

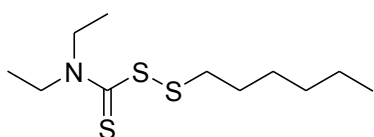
General

Melting points were measured on a Griffin apparatus and are uncorrected. Mass spectra were recorded on a Bruker MicroTOF LC instrument or at the EPSRC National Mass Spectrometry Centre (Swansea, U.K.). NMR spectra were recorded on a Bruker AVANCE 500 MHz instrument; coupling constants (*J* values) are in Hz. Merck silica gel 60 (40-60 μm) was used for column chromatography. All commercially available starting materials were used without further purification.

Scheme 5.3

General procedure for the obtainment of disulfiram analogue (Except for *N*-methylpiperazine-*N,N*-diethyltrithioperoxocarbamate)

Carbon disulphide (6 mmol, 0.36 ml) was added to a mixture of the appropriate secondary amine (7.2 mmol) and thiol (7.2 mmol) in DCM (12 ml). Colour change from transparent to pale yellow. The mixture was cooled to 0°C in an ice bath for 5 minutes, then NEt₃ (6 mmol, 0.63 ml) was added and the colour change from pale to bright yellow. CBr₄ (6 mmol) was added and colour turn to brown. After two hours of stirring the reaction was partitioned between water and DCM. Water phase was discarded and washed with 10x3 ml of DCM. The organic phases were reunited and dried on MgSO₄ and filtered. Solvent was removed with the aim of reduced pressure and the oily residue was purified through flash chromatography.¹



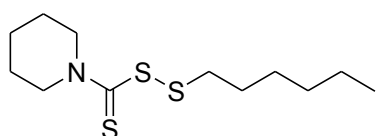
1a. Hexyl *N,N*-diethyltrithioperoxocarbamate.

Flash chromatography Hexanes/AcOEt 95:5

Yield 48% as a yellow oil.

¹H NMR (CDCl₃) \square 0.90- 0.93 (3H, t, *J* = 6.50, CH₃CH₂CH₂), 1.10-1.35 (10H, m, 2 x CH₂, CH₃CH₂CH₂), 1.40 (2H, m, SCH₂CH₂CH₂), 1.60 (2H, m, SCH₂CH₂), 2.80 (2H, t, *J* = 6.9, SCH₂), 3.8 (2H, q, *J* = 6.8, NCH₂), 4.0 (2H, q, *J* = 6.8, NCH₂)

³C NMR (CDCl₃) \square 11.15, 12.93, 13.80, 21.97, 27.47, 27.83, 30.82, 38.00, 46.78, 51.08, 193.96



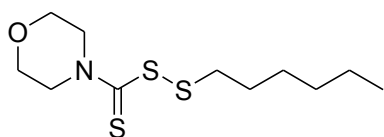
1b. Piperidine *N,N*-diethyltrithioperoxocarbamate.

Flash chromatography Hexanes/AcOEt 95:5

Yield 40% as a yellow oil.

$^1\text{H NMR}$ (CDCl_3) \square 0.90- 0.93 (3H, t, $J = 6.50$, CH_3 (CH_2) $_5$ -), 1.32 (4H, m, $-(\text{CH}_2)_3\text{-CH}_2\text{-CH}_2\text{-CH}_3$), 1.40 – 1.46 (2H, m, $\text{SCH}_2\text{CH}_2\text{CH}_2$), 1.66 – 1.75 (8H, m, $-\text{CH}_2\text{CH}_2\text{CH}_2\text{NCH}_2\text{CH}_2\text{CH}_2-$, $-\text{SCH}_2\text{CH}_2-$), 2.87 – 2.90 (2H, t, $J = 7.7$, SCH_2), 4.01 (2H, s, $-\text{NCH}_2$), 4.33 (2H, s, $-\text{NCH}_2$). $^{13}\text{C NMR}$ (CDCl_3) \square 14.01, 22.50, 24.18, 28.25, 28.55, 31.39, 38.83, 198.20.

1c. Morpholine *N,N*-diethyltrithioperoxocarbamate

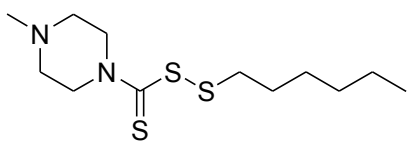


Flash chromatography Hexanes/AcOEt 95:5

Yield 52% as a yellow oil.

$^1\text{H NMR}$ (CDCl_3) \square 0.90- 0.93 (3H, t, $J = 6.50$, CH_3 (CH_2) $_5$ -), 1.33 (4H, m, $-(\text{CH}_2)_3\text{-CH}_2\text{-CH}_2\text{-CH}_3$), 1.40 – 1.46 (2H, m, $\text{SCH}_2\text{CH}_2\text{CH}_2$), 1.66 – 1.72 (2H, m,), 2.87 – 2.90 (2H, t, $J = 7.7$, SCH_2), 3.81 (4H, s, $-\text{OCH}_2\text{CH}_2\text{NCH}_2\text{CH}_2-$), 4.24 (4H, s, $-\text{OCH}_2\text{CH}_2\text{NCH}_2\text{CH}_2-$).

$^{13}\text{C NMR}$ (CDCl_3) \square 14.01, 22.50, 28.22, 28.59, 31.37, 38.77, 39.23, 60.30, 60.36, 198.20.



1d. *N*-methylpiperazine-*N,N*-diethyltrithioperoxocarbamate

Carbon disulphide (6 mmol, 0.36 ml) was added to a mixture of the appropriate secondary amine (7.2 mmol) and thiol (7.2 mmol) in

DCM (12 ml).

Colour change from transparent to yellow.

The mixture was cooled to 0°C in an ice bath for 5 minutes, then NEt_3 (6 mmol, 0.63 ml) was added and the colour change to bright yellow.

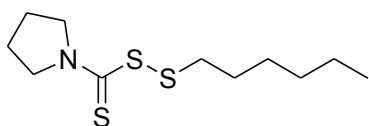
CBr_4 must be dissolved in DCM (12 ml) and added dropwise to the reaction mixture efficiently cooled to 0°C. A yellow precipitate formed.

Quench the reaction with few drops of water and filter the mixture for remove the solid. The solvent was removed under vacuum.

Flash chromatography AcOEt/MeOH/ NEt_3 95:4:1.

Yield 52% as a yellow oil.

$^1\text{H NMR}$ (CDCl_3) \square 0.90- 0.93 (3H, t, $J = 6.50$, CH_3 (CH_2)₅), 1.33 (4H, m, $-(\text{CH}_2)_3-\text{CH}_2-\text{CH}_2-\text{CH}_3$), 1.40 – 1.46 (2H, m, $\text{SCH}_2\text{CH}_2\text{CH}_2$), 1.66 – 1.71 (2H, m,), 2.36 (3H, s,), 2.53 – 2.55 (4H, t,), 2.87 – 2.90 (2H, t,), 4.09 (2H, s,), 4.39 (2H, s,). $^{13}\text{C NMR}$ (CDCl_3) \square 14.01, 22.50, 28.23, 28.60, 31.37, 38.79, 45.39, 54.40, 197.67.



1e. Pyrrolidine *N,N*-diethyltrithioperoxocarbamate.

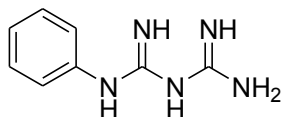
Flash chromatography Hexanes/AcOEt 95:5

Yield 63 % as a yellow oil.

$^1\text{H NMR}$ (CDCl_3) \square 0.90- 0.93 (3H, t, $J = 6.50$, CH_3 (CH_2)₅), 1.32 (4H, m, $-(\text{CH}_2)_3-\text{CH}_2-\text{CH}_2-\text{CH}_3$), 1.41 – 1.44 (2H, t, $\text{SCH}_2\text{CH}_2\text{CH}_2$), 1.66 – 1.72 (2H, m,), 1.99 – 2.05 (2H, t, $J =$), 2.11 – 2.16 (2H, t), 2.87 – 2.90 (2H, t, $J = 7.3$), 3.75 – 3.78 (2H, t, $J = 6.8$), 3.98 – 4.00 (2H, t, $J = 6.8$).

$^{13}\text{C NMR}$ (CDCl_3) \square 14.01, 22.51, 24.19, 26.30, 26.51, 28.24, 28.60, 31.39, 38.72, 50.53, 56.62, 192.99.

Synthesis of biguanidine.



4b. Phenylbiguanidine.

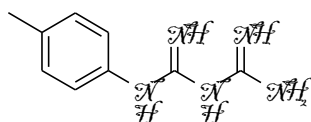
Aniline and dicyanamide were dissolved in an acidic mixture of HCl 3 N and refluxed for 4 hours until all the aniline reacted.

Let the reaction reach r.t. The resulting crystalline solid was collected on a Buchner funnel and washed with cold water.

The hydrochloride obtained was then dissolved in hot water, and NaOH 1 N was added until pH reach 10-11. The crystalline free base was collected again with filtration by suction and crystallized dissolving it in the minimum amount of hot ethyl acetate, filtered and precipitated with Hexanes.

$^1\text{HNMR}$ ($\text{DMSO}-d_6$) \square 7.12 (1H, t, $J = 7.2$, H-4), 7.21 (2H, d, $J = 7.4$, H-2, H-6), 7.30 (2H, t, $J = 8.6$, H-3, H-5), 7.45 (5H, bs, NH_2 3 x NH), 10.01 (1H, bs, NH) $^{13}\text{CNMR}$ ($\text{DMSO}-d_6$) \square 120.41, 120.71, 123.21, 128.33, 128.57, 138.66, 155.25, 161.15

Yield = 89%



4a. 4-methylphenylbiguanidine.

Para-toluidine hydrochloride and dicyanamide were dissolved in water and refluxed for 3-4 hours. Until all the toluidine reacted.

No Hydrochloric acid has been used.

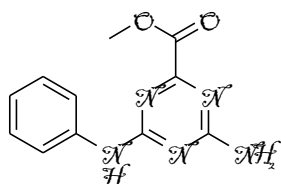
$^1\text{H NMR}$ ($\text{DMSO-}d_6$) \square 2.29 (3H, s, PhCH_3), 7.10 (2H, d, $J = 8.4$, H-2 H-6), 7.15 (1H, bs, NH), 7.25 (2H, d, $J = 8.4$, H-3 H-5), 7.35 (4H, m, NH_2 NH NH), 9.8 (1H, s, NH) $^{13}\text{C NMR}$ ($\text{DMSO-}d_6$) \square 20.38(CH_3), 121.05, 129.00, 132.41, 135.96, 155.52, 160.96.

Yield 93%.

Scheme 5.6

General method for cyclization of biguanidines.

4a or **4b** (2.0 mmol) and dimethyl oxalate (118 mg, 3 eq, 6.0 mmol) was dissolved in 20 ml of dry methanol and stirred at r.t. under nitrogen for about 2 hours. A yellowish precipitate formed. The mixture was refluxed for about four hours. Purification of crude reaction product over a short pad of silica gel afford a crystalline product. ²



7b. methyl 4-amino-6-(phenylamino)-1,3,5-triazine-2-carboxylate.

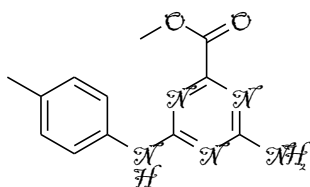
Flash chromatography Dichloromethane/ Methanol 95:5.

Obtained 400 mg of product as white crystalline powder.

Yield 81%

$^1\text{H NMR}$ ($\text{DMSO-}d_6$) \square 3.78 (3H, s, COOCH_3), 7.02 (1H, t, $J = 7.1$, H-4'), 7.05 (2H, bs, NH_2), 7.32 (2H, t, $J = 7.8$, H-3', H-5'), 7.80 (2H, d, $J = 7.7$, H-2', H-6'), 9.79 (1H, bs, NH).

$^{13}\text{C NMR}$ ($\text{DMSO-}d_6$) \square 52.31, 120.09, 122.42, 128.79, 136.03, 163.78, 164.39, 165.34, 167.10.



7a. methyl 4-(p-tolylamino)-6-amino-1,3,5-triazine-2-carboxylate.

Obtained White crystalline powder.

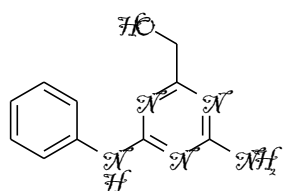
Obtained 410 mg of product as white crystalline powder.

Yield 79%

$^1\text{H NMR}$ ($\text{DMSO-}d_6$) \square 2.24 (3H, s, $-\text{CH}_3$), 3.81 (3H, s, COOCH_3), 7.07-7.09 (2H, d, 2,6-H, $J = 10$), 7.39 (1H, s, $-\text{NH}_2$), 7.51 (1H, s, $-\text{NH}_2$), 7.64-7.66 (2H, d, 3,5-H), 9.86 (1H, s, $-\text{NH}-$). $^{13}\text{C NMR}$ ($\text{DMSO-}d_6$) \square 20.38, 52.37, 120.16, 128.85, 131.46, 136.74, 163.93, 164.23, 165.28, 167.10.

General method for reduction of methyl esters to alcohols

A solution of the appropriate Triazine **4a** or **b** (1.0 mmol) in dry THF (10 ml) was added dropwise to a suspension of LiAlH₄ (114 mg, 3 eq, 3 mmol) in 6 ml of dry THF (2ml/mmol LiAlH₄). Mixture was stirred at r.t. for about two hours, until all the starting material consumed (TLC). Reaction was quenched with wet THF, and a 1 N solution of NaOH was added dropwise in order to destroy LiAlH₄ and dissolve alluminates. Mixture was partitioned between AcOEt and brine. Aqueous Layer was extracted twice with AcOEt (20 ml x 2). Organic extracts are reunited, dried over MgSO₄, filtered and solvent was removed at r.p. The residue was purified through flash chromatography.

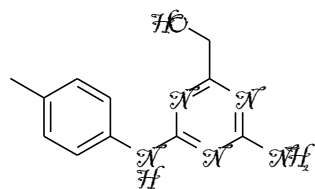


6b. (4-amino-6-(phenylamino)-1,3,5-triazin-2-yl)methanol.

Flash chromatography (DCM/MeOH 9:1).

Obtained 65 mg of product (yield 39%).

¹HNMR (DMSO-*d*₆) □ 4,31 (2H, J= 5,6) 4,8 (1H, t, J = 5,6 OH), 7.02 (1H J=7.1, H-41), 7.05 (2H, bs) 7.32 (2H, t, J = 7.8), 7.80 (2H, d, J= 7.7), 9.51 (1H, s, NH).
¹³CNMR (DMSO-*d*₆) □ 63.71, 119.79, 121.89, 128.32, 139.86, 164.09, 166.61, 176.90.



6a. (4-(p-tolylamino)-6-amino-1,3,5-triazin-2-yl)methanol.

Flash chromatography (DCM/MeOH 9:1) afford 65 mg of product.

Yield 8%

Melting point: 227-228 °C

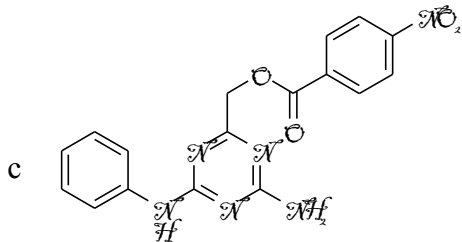
¹HNMR (DMSO-*d*₆) □ 2.20 (3H, s, PhCH₃), 3.41 (1H, bs, OH), 4.40 (2H s, CH₂OH), 5.10 (2H, s, NH₂), 6.91 (1H, s, NH), 7.09 (2H, t, J = 8.5, H-2' H-6'), 7.31 (2H, d, J = 8.5, H-3' H-5')

¹³CNMR (DMSO-*d*₆) □ 20.68, 63.79, 120.09, 122.42, 128.79, 136.03, 163.78, 164.39, 167.10.

General procedure for esterification.

A mixture of **6a** or **6b** (1.0 mmol), NEt₃ (1.1 eq., 1.1 mmol) and DMAP (5 mol%) was dissolved in dry DCM (20 ml/mmol alcohol). 4-nitrobenzoyl chloride (279 mg, 1.5 eq, 1.5 mmol) in dry DCM (10 ml/mmol acyl chloride) was added dropwise.

The mixture was left on stirring at r.t. overnight, then brine (5 ml) was added to the reaction and the organic layer separated, washed with NaHCO₃ 10% solution, dried over MgSO₄, filtered and solvent evaporated in vacuo.



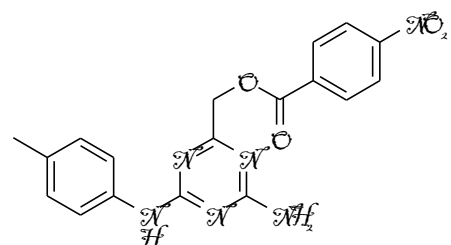
1b. (4-amino-6-(phenylamino)-1,3,5-triazin-2-yl)methyl 4-nitrobenzoate.

Flash chromatography (AcOEt/Hexane 5:5) afforded title compound

Yield 50%.

Melting point: 168-169 °C

¹HNMR (DMSO-*d*₆) □ 5.18 (2H, s, CH₂O), 6.80 (1H, m, H-4'), 7.15 (4H, m, NH₂ H-2' H-6'), 7.62 (2H, m, H-3' H-5'), 8.25 (2H d, *J* = 8.9, H-2'' H-6''), 8.40 (2H, d, *J* = 8.8, H-3'' H-5''), 9.48 (1H, s, NH) ¹³CNMR (DMSO-*d*₆) □ 65.48, 119.89, 122.05, 123.67, 128.16, 130.65, 134.90, 139.53, 150.38, 159.00, 164.05, 166.51, 172.11



1a. (4-(p-tolylamino)-6-amino-1,3,5-triazin-2-yl)methyl 4-nitrobenzoate.

Flash chromatography (AcOEt/Hexane 5:5) afforded title compound.

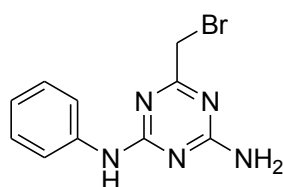
Yield 70%.

¹HNMR (DMSO-*d*₆) □ 2.18 (3H, s, PhCH₃), 5.17 (2H, s, CH₂O), 6.96 (2H, bs, NH₂), 7.01 (2H, m, H-2' H-6'), 7.50 (2H, m, H-3' H-5'), 8.21 (2H, d, *J* = 8.7, H-2'' H-6''), 8.2 (2H, d, *J* = 8.7, H-3'' H-5'') ¹³CNMR (DMSO-*d*₆) □ 20.26, 59.71, 120.13, 123.89, 128.54, 130.93, 134.94, 136.87, 138.00, 150.36, 163.94, 164.05, 166.50, 171.98

Scheme 5.7

General procedure for the obtainment of 8a 8b.

4a or **4b** (5.21 mmol) was dissolved in methanol (1ml/mmol) then, under stirring, ethyl bromoacetate (865 mg, 5.21 mmol) was added dropwise. The reaction mixture was allowed to stir at room temperature overnight. The solvent was then removed with the aim of reduced pressure. The brownish residue was purified through flash chromatography affording the product.

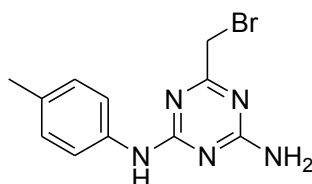


8b. 6-(bromomethyl)-N2-phenyl-1,3,5-triazine-2,4-diamine.

Flash chromatography (Hex/ AcOEt 6:4)

Yield 43%

$^1\text{H NMR}$ (DMSO- d_6) \square 4.18 (2H, s, BrCH₂-), 7.02 (1H, t, $J = 7.1$, H-4'), 7.05 (2H, s, NH₂), 7.32 (2H, t, $J = 7.8$, H-3', H-5'), 7.80 (2H, d, $J = 7.7$, H-2', H-6'), 9.51 (1H, s, NH). $^{13}\text{C NMR}$ (DMSO- d_6) \square 33.89, 119.89, 121.92, 128.32, 137.06, 164.09, 164.61, 172.90



8a. 6-(bromomethyl)-N2-p-tolyl-1,3,5-triazine-2,4-diamine

Flash chromatography (Hex/ AcOEt 6:4)

Yield 39%

Melting Point 170°C (Dec.)

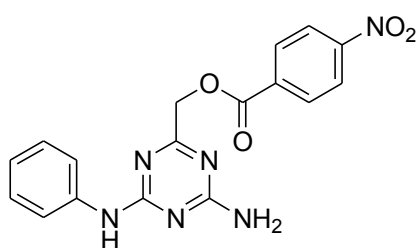
$^1\text{H NMR}$ (DMSO- d_6) \square 2.24 (3H, s, PhCH₃), 4.18 (2H, s, BrCH₂-), 7.07-7.10 (2H, d, 2,6-H), 7.19 (2H, s, -NH₂), 7.62-7.65 (2H, d, 3,5-H), 9.52 (1H, s, NH). $^{13}\text{C NMR}$ (DMSO- d_6) \square 20.36, 33.91, 120.08, 128.85, 131.19, 136.92, 164.37, 167.05, 172.95.

Scheme 5.6, 5.7.

General method for the synthesis of title compounds 1a, 1b.

In a round bottomed flask **8a** or **8b** (0.34 mmol) and 4-nitrobenzoic acid (120 mg, 0.68 mmol, 2eq) was dissolved in THF (12 ml). TBAF (1.4 ml, 2 eq, 1.4 mmol, 1M sol in THF) was added dropwise.

Reaction mixture was heated to reflux until completion (2 hours). THF was then removed in vacuo, and the highly viscous residue was partitioned between AcOEt (50 ml) and water (10 ml x 2), then with a saturated solution of NaHCO₃ (10 x 3) until neutral to litmus paper. The organic phase was dried over MgSO₄ and filtered. AcOEt was removed in vacuo. The yellowish residue was purified through flash chromatography (CH₂Cl₂/ MeOH 98:2). An analytical sample can be obtained through crystallization from acetonitrile affording very small yellow crystals. ³



1b. (4-amino-6-(phenylamino)-1,3,5-triazin-2-yl)methyl 4-nitrobenzoate.

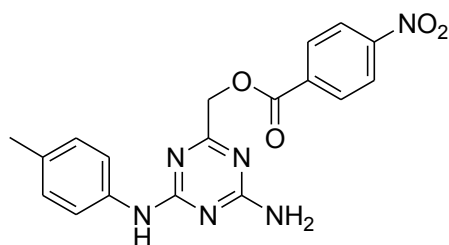
Yield 86%

Melting Point 148-150 °C

¹HNMR (DMSO-*d*₆) □ 5.22 (2H, s, CH₂O), 6.90 (1H, s, NH),

7.09 (3H, m, H-2', H-4', H-6'), 7.61 (2H, t, *J* = 7.9, H-3', H-5'), 7.72 (3H, m, H-3'', H-4'', H-5''), 8.13 (2H, d, *J* = 7.2, H-2'', H-6''), 9.01 (1H, bs, NH)

¹³CNMR (CDCl₃) □ 64.89, 119.80, 121.91, 128.13, 128.77, 129.31, 129.54, 133.45, 139.61, 164.02, 165.45, 166.51, 172.56.



1a. (4-(*p*-tolylamino)-6-amino-1,3,5-triazin-2-yl)methyl 4-nitrobenzoate.

Yield 79%

Melting Point 172-173 °C

¹HNMR (DMSO-*d*₆) □ 2.18 (3H, s, -CH₃), 5.15 (2H, s,

-CH₂Br), 7.04 (4H, s -NH₂, 2,6-H), 7.52 (2H, s, 3,5-H), 8.27-8.29 (2H, 2,6-H), 8.39-8.41 (2H, 3,5-H), 9.38 (1H, -NH-). ¹³CNMR (CDCl₃) □ 19.81, 65.36, 120.04, 120.14, 123.29, 128.48, 130.83, 131.31, 135.75, 137.22, 150.78, 163.77, 164.68, 167.47.

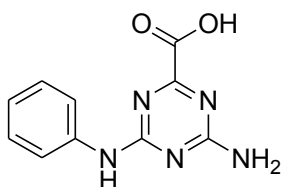
Scheme 5.8

General procedure for the obtainment of carboxylic acid 9a, 9b.

9a or **9b** (1.00 mmol) was dissolved in 50 ml of ethanol, 10 ml of 1 N solution of NaOH was added. The mixture was refluxed for three hours until consumption of starting material.

The reaction was left cool to r.t. and the solvents removed in vacuo.

The residue was acidified with HCl 1 N (about 10 ml) until the solution reach a strong acidic pH (1-2). Filter the precipitate on a buchner funnel, wash it with plenty of water and 10 ml x 2 AcOEt. Then let it air dry.

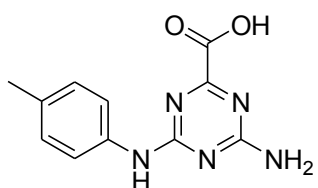


9b. 4-amino-6-(phenylamino)-1,3,5-triazine-2-carboxylic acid.

Melting Point > 250°C

Yield 94 % as a white to yellowish solid.

¹HNMR (DMSO-*d*₆) 9.85 (s, 1H), 7.65- 7.63 (d, 2H, J= 10 Hz), 7.41 (s, 2H), 7.10 – 7.08 (d, 2H, J= 10 Hz). ¹³CNMR (DMSO-*d*₆) 166.81, 165.25, 164.97, 164.15, 136.72, 131.45, 128.88, 120.15.



9a. 4-(p-tolylamino)-6-amino-1,3,5-triazine-2-carboxylic acid.

Melting Point > 250°C

Yield 91 % as a white to yellowish solid.

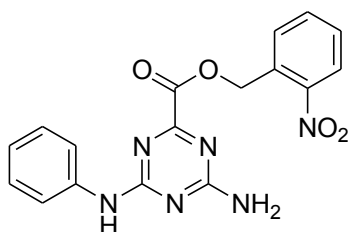
¹HNMR (DMSO-*d*₆) 9.80 (s, 1H), 7.66- 7.64 (d, 2H, J= 10 Hz), 7.40 (s, 2H), 7.10 – 7.08 (d, 2H, J= 10 Hz), 2.26 (s, 3H). ¹³CNMR (DMSO-*d*₆) 166.78, 165.28, 164.97, 164.18, 136.74, 131.46, 128.85, 120.16, 20.37.

Scheme 5.8.

General method for the synthesis of title compounds 10a-10f.

In a round bottomed flask **9a** or **9b** (1.00 mmol) and the appropriated mono nitrobenzoyl chloride (237 mg 1.1 mmol, 1.1 eq) was dissolved in acetonitrile (14 ml). TBAF (1.4 ml, 2 eq, 1.4 mmol, 1M sol in THF) was added dropwise. Reaction mixture was stirred overnight.

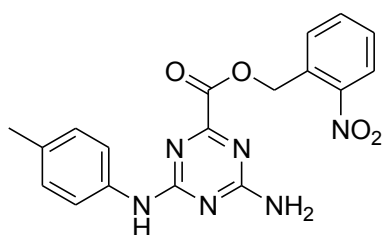
A yellowish precipitate formed. Collect the stuff on a buchner funnel and triturated the compound with fresh acetonitrile. An analytical sample can be obtained through cristallization from acetonitrile affording very small crystals. ³



10a. 2-nitrobenzyl 4-amino-6-(phenylamino)-1,3,5-triazine-2-carboxylate.

Yield = 93%

$^1\text{HNMR}$ ($\text{DMSO-}d_6$) 9.94 (s, 1H), 8.20 – 8.18, 7.84 – 7.79 (m, 4H), 7.69 – 7.66 (t) 7.61 (s, 1H) 7.46 (s, 1H), 7.31- 7.28 (t), 7.04 – 7.01 (t), 5.69 (s, 2H). $^{13}\text{CNMR}$ ($\text{DMSO-}d_6$) 166.01, 163.21, 162.59, 161.78, 146.23, 138.17, 133.16, 129.83, 128.45, 127.30, 123.90, 121.44, 119.01, 62.45.

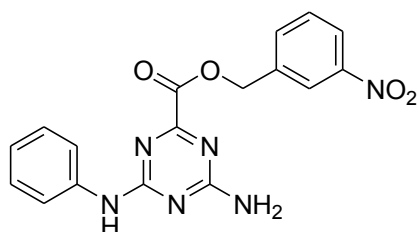


10b. 2-nitrobenzyl 4-(p-tolylamino)-6-amino-1,3,5-triazine-2-carboxylate.

Yield = 82%

Melting Point 203 – 204°C

$^1\text{HNMR}$ ($\text{DMSO-}d_6$) 9.86 (s, 1H) 8.20 – 8.18 (d, 1H, $J=10$ Hz), 8.18 – 7.79 (t, 2H), 7.69 – 7.65 (m, 3H), 7.56 (s, 1H, NH), 7.43 (s, 1H, NH), 7.10 – 7.09 (d, 2H, $J=5$ Hz), 5.69 (s, 2H), 2.26 (s, 3H). $^{13}\text{CNMR}$ ($\text{DMSO-}d_6$) 167.11, 163.67, 162.94, 136.69, 134.28, 131.53, 130.97, 129.57, 128.84, 125.01, 120.22, 63.53, 20.39.

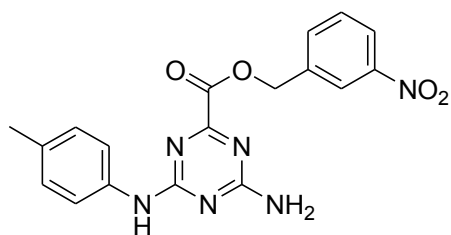


10c. 3-nitrobenzyl 4-amino-6-(phenylamino)-1,3,5-triazine-2-carboxylate.

Yield = 62.4 %

Melting Point 189°C

$^1\text{HNMR}$ ($\text{DMSO-}d_6$) 9.92 (s, 1H, NH), 8.35 (s, 1H,) 8.25- 8.23 (d, 1H, $J=10$ Hz) 7.94- 7.93 (d, 1H, $J=5$), 7.80- 7.80- 7.78 (d, 1H) 7.75- 7.72 (t, 1H, $J_{\text{min}}=10$, $J_{\text{max}}=15$) 7.59 (s, 1H, -NH $_2$), 7.44(s, 1H, -NH $_2$) 7.30- 7.26 (t, 2H, $J_{\text{min}}=10$ $J_{\text{max}}=20$ Hz) 7.03- 7.00 (t, 1H, $J_{\text{min}}=10$, $J_{\text{max}}=15$ Hz) 5.48 (s, 2H). $^{13}\text{CNMR}$ ($\text{DMSO-}d_6$) 167.09 164.28 163.86 163.13 147.81 139.29 137.73 134.94 130.16 128.41 123.23 123.01 122.53 120.07 65.65.



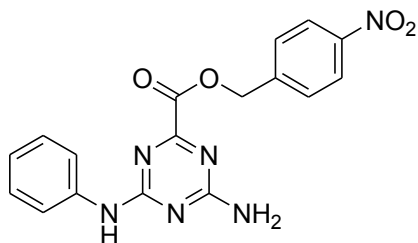
10d. 3-nitrobenzyl 4-(p-tolylamino)-6-amino-1,3,5-triazine-2-carboxylate.

Yield = 72%

Melting Point 207-209°C

$^1\text{HNMR}$ ($\text{DMSO-}d_6$) 9.84 (s, 1H, NH), 8.34 (s, 1H,) 8.25 (s, 1H) 7.94- 7.92 (d, 1H, $J=10$), 7.80- 7.78 (d, 1H) 7.75- 7.72 (t, 1H, $J_{\text{min}}=10$, $J_{\text{max}}=15$) 7.66 (d, 2H, -NH $_2$), 7.54 (s, 1H, -NH $_2$) 7.42 (s, 1H, -NH $_2$) 7.10 (s, 2H, $J_{\text{min}}=10$ $J_{\text{max}}=20$ Hz) 5.48 (s,

2H), 2.25 (s, 3H). ¹³CNMR (DMSO-*d*₆) 167.08, 164.19, 163.81, 163.17, 147.80, 137.75, 136.70, 134.94, 131.50, 130.16, 128.82, 123.23, 123.01, 120.19, 65.61, 20.38.

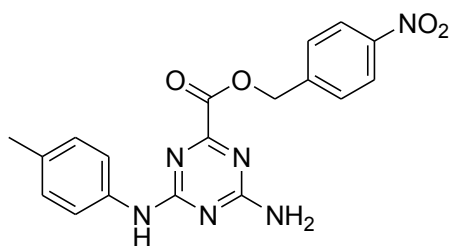


10e. 4-nitrobenzyl 4-amino-6-(phenylamino)-1,3,5-triazine-2-carboxylate.

Yield = 67%

Melting Point 218°C

¹HNMR (DMSO-*d*₆) 9.93 (s, 1H, NH) 8.28- 8.27 (d, 2H, ArH, J= 8.75 Hz) 7.80- 7.79 (d, 2H, ArH, J= 10) 7.74- 7.72 (d, 2H, ArH, J= 10) 7.60 (s, 1H, -NH₂) 7.45 (s, 1H, -NH₂) 7.30 - 7.27 (t, 2H, J min = 10, Jmax = 16 Hz) 7.03- 7.00 (t, 1H,) 5.50 (s, 2H, ArCH₂-). ¹³CNMR (DMSO-*d*₆) 167.10 164.29 163.83 163.08 147.29 143.17 139.29 128.96 128.41 123.62 122.55 120.10 65.54.



10f. 4-nitrobenzyl 4-(p-tolylamino)-6-amino-1,3,5-triazine-2-carboxylate.

Yield = 55 %

Melting Point 246-248°C

¹HNMR (DMSO-*d*₆) 9.85 (s, 1H, NH), 8.28 – 8.27 (d, 2H, J= 5 Hz), 7.73 – 7.71 (d, 2H, J= 10 Hz), 7.66 – 7.65 (d, 2H, J= 5 Hz), 7.55 (s, 1H, NH) 7.42 (s, 1H, NH), 7.10 – 7.08 (d, 2H, J= 10 Hz), 5.49 (s, 2H), 2.26 (s, 3H). ¹³CNMR (DMSO-*d*₆) 167.10, 164.22, 163.79, 163.12, 147.28, 143.18, 136.69, 131.53, 128.94, 128.83, 123.61, 120.22, 65.499, 20.37.

Bibliography

1. Liang, F.; Tan, J.; Piao, C.; Liu, Q.; Carbon Tetrabromide Promoted Reaction of Amines with Carbon Disulfide: Facile and Efficient Synthesis of Thioureas and Thiuram Disulfides Hexanethiole *Synthesis* **2008** 22 3579-3584.
2. Lebel, O.; Perron, M.-E.; A New Class of Selective Low-Molecular-Weight Gelators Based on Salts of Diaminotriazinecarboxylic Acids *Chem. Mater.*, **2006**, 18, 3616–3626
3. Wu, Chung-Yi, W.; Ashraf, B.; Sheng-Kai, W.; Chen, Y.; Tetrabutylammonium fluoride-mediated rapid alkylation reaction in microtiter plates for the discovery of enzyme inhibitors in situ. *ChemBioChem* **2005**, 6, 2176-2180.